JPRS-CST-85-039

13 November 1985

China Report

SCIENCE AND TECHNOLOGY

FBIS FOREIGN BROADCAST INFORMATION SERVICE

NOTE

JPRS publications contain information primarily from foreign newspapers, periodicals and books, but also from news agency transmissions and broadcasts. Materials from foreign-language sources are translated; those from English-language sources are transcribed or reprinted, with the original phrasing and other characteristics retained.

Headlines, editorial reports, and material enclosed in brackets [] are supplied by JPRS. Processing indicators such as [Text] or [Excerpt] in the first line of each item, or following the last line of a brief, indicate how the original information was processed. Where no processing indicator is given, the information was summarized or extracted.

Unfamiliar names rendered phonetically or transliterated are enclosed in parentheses. Words or names preceded by a question mark and enclosed in parentheses were not clear in the original but have been supplied as appropriate in context. Other unattributed parenthetical notes within the body of an item originate with the source. Times within items are as given by source.

The contents of this publication in no way represent the policies, views or attitudes of the U.S. Government.

PROCUREMENT OF PUBLICATIONS

JPRS publications may be ordered from the National Technical Information Service, Springfield, Virginia 22161. In ordering, it is recommended that the JPRS number, title, date and author, if applicable, of publication be cited.

Current JPRS publications are announced in Government Reports Announcements issued semi-monthly by the National Technical Information Service, and are listed in the Monthly Catalog of U.S. Government Publications issued by the Superintendent of Documents, U.S. Government Printing Office, Washington, D.C. 20402.

Correspondence pertaining to matters other than procurement may be addressed to Joint Publications Research Service, 1000 North Glebe Road, Arlington, Virginia 22201.

JPRS-CST-85-039

13 November 1985

CHINA REPORT
SCIENCE AND TECHNOLOGY

CONTENTS

PEOPLE'S REPUBLIC OF CHINA

NATIONAL DEVELOPMENTS

ABSTRACTS

PHYSICAL CHEMISTRY

PHYSICS

NATIONAL DEVELOPMENTS

SONG JIAN SPEAKS AT BEIJING TECHNOLOGY SYMPOSIUM

OW041256 Beijing XINHUA in English 1034 GMT 4 Oct 85

/Text/ Beijing, 4 October (XINHUA)--A China-European Communities symposium on new technology revolution, marking the 10th anniversary of the establishment of diplomatic relations between China and the Communities, opened here today.

During the 4-day meeting, 39 Chinese and foreign experts will present papers on such subjects as the impact of the revolution in technology on economic and social development, the relationship between new technologies and traditional industries, information technology and biotechnology, the principles and measures to promote new technological industries, and scientific policy and management.

Addressing the opening ceremony, Song Jian, minister of China's State Science and Technology Commission, said that over the past 10 years, there have been major developments in cooperation in politics, economics, science and technology between China and the European Communities. In science and technology, many important cooperative projects involving energy, transport, materials, agriculture, medicine, bioengineering, space technology, remote sensing, communications and information technology have been agreed upon between the two sides.

Song said, "Such cooperation has brought benefits to both sides and represents a positive contribution to world development and support for China's modernization program." He noted that since the policy of opening to the outside world was adopted China has opened more channels of cooperation with other countries and introduced advanced foreign technology and capital to promote the country's modernization drive. China will double efforts to strengthen and develop the cooperative relationship with the communities and promote world peace, stability and prosperity, he added.

K. H. Narjes, vice president of the European Communities Commission, reviewed the long history of technical cooperation between Europe and China and expressed his satisfaction with the cooperation between the two sides over the past 10 years. He hoped that such cooperation would be further expanded and diversified. There are good prospects for cooperation in information, telecommunications and biological sciences between the Communities and China, Narjes said.

CSO: 4010/2002

NATIONAL DEVELOPMENTS

S&T SUPPORT TO CIVILIANS BY DEFENSE INDUSTRIES REPORTED

Beijing GUANGMING RIBAO in Chinese 1 Aug 85 p 2

[Report by Zhang Bingqi [1728 3521 6386] and Yu Qingtian [0060 1987 3944]: "Take Advantage of Our Intellectual Resources, Give Further S&T Support to Civilians: National Defense Science, Technology and Industry Commission Gives S&T Support to Civilians In Over 360 Projects"]

[Text] In the movement to build socialist spiritual and material cultures jointly by the army and the people, units of the National Defense Science, Technology and Industry Commission stress taking advantage of the abundant intellectual resources and strong technological capability and giving active scientific and technical [S&T] support to the people. By the eve of August 1st, this year, the number of projects with S&T support to civilians has reached 362, which is 260 more than last year, and economic benefits have also increased more than six-fold over those of last year. Of the more than 400 joint military and civilian construction projects, 85 have already been cited by the government above the county level.

Take Part in Local S&T and Economic Organizations, Make Direct Suggestions To Develop the National Economy and S&T Undertakings

Some test bases and research institutes have released large numbers of S&T staff members to join local S&T societies and organizations and to attend local discussion conferences and debates on economic revitalization to give counsel on developing local resources. The National Defense Science and Technology College has sent professors and assistant professors on several occasions to become involved in Liuyang and to conduct on-the-spot investigations. Using the principles of system engineering, they helped Liuyang formulate a comprehensive development plan which relatively conforms to reality and has been welcomed by local government and the masses of people. The National Defense Science and Technology University has also been engaged in supporting more than 40 local construction projects whose economic benefits are expected to be as high as over 6 million yuan.

Training All Types of Local Technicians

In accordance with their own business capability and local needs, the various bases, schools and research institutes have successively operated key

technical training classes in more than 10 specialities including computers, agricultural systen engineering, construction industrial design, microcomputers and automobile driving. In the first half of the year alone, almost 1,000 qualified local persons have been trained in various specialities. The local masses have called S&T support to civilians their "best support." A certain nuclear test base has not only helped the Xinjiang No 1 Textile Mill with a full automation system and one construction engineering corporation in Hami in microcomputer management, it has also helped to train technicians so that they become skilled in operational techniques.

Transferring Technical Achievements

Since the beginning of this year, various units of the National Defense Science, Technology and Industry Commission have proceeded from developing the overall national economy and transferred over 50 different technical achievements. The headquarters clinic of the Commission has transferred the technology of the "small emergency kit" to the Shanghai Jinhua Experimental Machinery Plant so that this small plant which was on the verge of bankruptcy became able to make up deficits and generate profits.

Giving Economic and Technical Support Without Compensation

Many of the test units of the National Defense Science, Technology and Industry Commission are stationed in the frontiers, plateaus and deserts where the local S&T and economies are relatively backward. In recent years, the commission annually releases a certain amount of technical force by investing human, material and financial resources to support economic construction in minority nationality regions without compensation. A certain satellite launch base transferred a large portion of its technical resources and construction staff and invested 170,000 yuan to help railroad construction in minority nationality regions. Another base helped a local secondary school to build a printing plant by investing 150,000 yuan and transferring technical and management personnel. Business has been prosperous since it started, making a profit of almost 20,000 yuan and changing the face of the "impoverished school" in one stroke.

9586
CSO: 4008/2027

NATIONAL DEVELOPMENTS

PRC'S CHARACTER-FORM COMPUTER CODING PATENT PURCHASED

HK270149 Beijing ZHONGGUO XINWEN SHE in Chinese 0802 GMT 24 Sep 85

[Report: "Four Foreign Companies Have Bought the Patent for the Character-Form Computer Coding Method Invented by Li Jinkai"]

[Text] Beijing, 24 Sep (ZHONGGUO XINWEN SHE)--Four foreign and Hong Kong companies have recently bought the patent of the character-form computer coding method invented by Li Jinkai, famous Chinese specialist in computer coding.

These four companies are: Japan's (Jia Eng 0163 5174?) Company, Ltd; Mankwan Computer Company, a U.S.-Hong Kong joint venture; Fareast United Electronic, Ltd; and Rensful International, Ltd.

Li Jinkai is a lecturer at Beijing Teachers' University, and concurrently director of the China Information Research Institute. His invention of the character-form computer coding method has been evaluated highly by Chinese and foreign specialists. Not long ago, Li Jinkai succeeded in developing a multifunction, multilanguage computer system based on the latest results of his scientific research. The application of this new type of computer system has made possible the input of all kinds of languages. Words can be processed by those who do not know the foreign language based on the character form. While applying the character-form method, words can also be processed in Pinyin, and any Han character can be processed with an average of 2.25 key strokes, saving more than half the time [as published] than the 4-digit standard telegraphic code. Guided by the display panel of this computer system, human brain work can be lightened. The system has displayed good artificial intelligence.

It is learned that the China Information Research Institute has created more than $100,000 worth of foreign exchange through transfer of the patented technology abroad.

/9599
CSO: 4010/1014

NATIONAL DEVELOPMENTS

LANZHOU LABORATORY OPENS TO FOREIGN SCIENTISTS

OW090907 Beijing XINHUA in English 0802 GMT 9 Oct 85

/Text/ Lanzhou, 9 October (XINHUA)--A research laboratory in Lanzhou, capital of Gansu Province, has opened its doors to foreign scientists.

The biology- and gas-geochemistry laboratory at Lanzhou Geology Institute is the 18th in China to be opened up for use by overseas scientists, but the first in the economically-underdeveloped northwest.

The move is aimed at doing away with the former practice of closed-door research, and promoting exchange and cooperation between Chinese and foreign scientists, said an official of the institute, which is attached to the Chinese Academy of Sciences.

The laboratory offers all necessary equipment for analyses of rare gas isotopes. Scientists can also determine the abundance ratio of isotopes of carbon, hydrogen, oxygen, nitrogen and sulphur, and study oil and gas formation and trace elements.

The official said foreign scientists wishing to work on research programs could apply to the laboratory's academic committee.

The institute would provide funds, facilities and allowances for foreign applicants, who would undertake research work chosen by the committee. Those wishing to puruse their own research would have to pay a fee.

Research programs over the next 3 years include "The Impact of Organisms on Pneumatogenic Mineral Formation," "The Influence of the Climate and Environment on Oil and Gas Formation," "The Cause of Mineral Formation" and "The Cycle of Carbon Dioxide and its Effect on the Environment and the Climate."

The Chinese Academy of Sciences opened two research institutes to foreign scientists earlier this year as well as another 17 laboratories.

They include the Beijing-based Theoretical Physics Institute and the Institute of Mathematics, the Structural Chemistry Laboratory of Fuzhou, the Vacuum Physics Laboratory in Beijing, the Ion and Infrared Physics Laboratory in Shanghai and the Laser Spectrum Laboratory in Hefei.

CSO: 4010/2002

NATIONAL DEVELOPMENTS

RESTRUCTURING OF GUANGDONG'S S&T SYSTEM REPORTED

Guangzhou NANFANG RIBAO in Chinese 5 Aug 85 p 2

[Article by Yang Xingfeng [2799 5281 6912] and Wen Zongkong [3306 1350 1313]: "Restructuring of S&T System in Guangdong Is In Full Swing, Integrated Bodies of Scientific Research and Production Spring Up Like Mushrooms; Over 300 Integrated Bodies of Scientific Research and Production Have Been Established, Spurring S&T to Gear to the Needs of Production and Strengthening the Capability of Enterprises to Develop"]

[Text] Along with restructuring of the S&T system in depth, integrated bodies of scientific research and production are springing up like mushrooms throughout the province. According to incomplete statistics, 359 of such integrated bodies have currently been established throughout Guangdong and quite a few are prepared to be set up. Development is most rapid in the Guangzhou area and the Zhujiang Delta area.

There are many types of integrated bodies of scientific research and production in Guangdong and primarily there are five. The first is the specialized technical cooperation type. Both parties of this type of integrated body has signed an agreement. The research institute provides the technical achievements and technology while the production unit is responsible for investment, production and management, and both share the profits or sales within a fixed period of time. They constitute approximately 40 percent of the total number of integrated bodies. For instance, the Guangdong Institute of Microbiology cooperated with the Gaozhou County in its mushroom wheat grain spawn formulation and manufacturing technique and established a mushroom wheat grain spawn production base in that county. In 1984 alone they produced over 10 million jin of mushroom with an output value of approximately 13 million yuan, making it the third key commodity of that county. The second is the scientific research and production management type. This type of integrated body clearly defines the responsibilities of both or all parties involved in a contract, forming a unified leading group to plan and coordinate development as well as the various services of production, supply and marketing, thereby binding the interests of both or all parties together. They currently constitute about 30 percent of the total number of integrated bodies. For instance, units of the South China Teachers University, Guangzhou Baiyunshan Pharmaceutical Plant and China Bee Corporation jointly funded and established the Lingnan Bee Development Corporation, which centrally carries out the

development, production, supply and marketing for the improvement of breeds, bee products and beekeeping equipment, and which practice profit sharing by all parties. The third is the S&T economic bodies, which is the integration of scientific research units and production units and which further leads to the incorporation of production units into scientific research units to become pilot test workshops (or plants) of scientific research units. For instance, after the integration of the Guangzhou No 9 Pharmaceutical Plant which had a deficit year after year and the Guangzhou Institute of Pharmaceutical Industry which relied on an annual allocation of 500,000 yuan in operating expenses, the two parties have formed a new S&T economic body which was able to achieve economic independence since last October and which made a net profit of more than 1 million yuan for the whole year. This type of integrated body constitutes about 11 percent of the total. The fourth is the engineering contract type. It is a contracting agency for certain specialized projects formed by one or more scientific research and design units. It contracts with enterprise units or public agencies and provides complete technical services. For instance, after the Guangzhou Construction Corporation accepted the work on the Shanghai Mechanical and Electrical Trade Building, it signed a design contract with the Guangdong Design Institute of Architecture and commissioned that institute to take up responsibility for the design plan of the project. This type of integrated body currently constitutes about 9 percent of the total. The fifth is the international cooperation and development type. They are integrated bodies formed by scientific research and design units in cooperation with certain companies abroad. The foreign firms are responsible for importing the technology, prototypes and equipment, and they jointly develop new products. They constitute about 10 percent of the total number of integrated bodies. For instance, in order to enable China to produce broadcast television antenna systems (including amplifiers and oscilloscopes) for which there is an urgent market demand, the Guangdong Institute of Electronic Technology has jointly established the Guangda Electronic Technology Development Corporation with the Hong Kong Yi Da Electronic Engineering Company which is relatively knowledgeable in broadcasting television technology.

Besides yielding notable economic results, integrated bodies of scientific research and production currently also shows numerous advantages. First, they give impetus to the implementation of the policy of gearing S&T to the needs of economic construction and speed up the transformation of technology and achievements into commodities. For instance, through integrated bodies, Jiangmen has established cooperative relations with 13 institutes of higher learning and 27 scientific research units throughout the country, and has popularized and applied more than 1,000 scientific research achievements. Moreover, the South China Agricultural College rapidly popularized its paddy rice soil formulation fertilizer technology in Gaoyao County through integrated bodies. Last year this county used an area of 700,000 mu with an average increased yield of 57.5 jin of paddy per mu, which increased the benefits for the peasants by more than 500,000 yuan. Second, they have strengthened the capability of economic independence of scientific research organs. For instance, since 1983 the Guangdong Institute of Machinery has established five integrated bodies of scientific research and production with concerned units. The income of this institute from these integrated bodies constitutes approximately 25 percent of its total income, thereby laying a

good foundation for its change from reliance on operating funds allocated by the higher level to economic independence.

9586
CSO: 4008/2028

NATIONAL DEVELOPMENTS

PROGRESS IN RESTRUCTURING HUNAN'S S&T SYSTEM REPORTED

Tianjin JISHU SHICHANG BAO [TECHNOLOGY MARKET WEEKLY] in Chinese 23 Jul 85 p 1

[Article: "Restructuring of Hunan's S&T System Yields Results: Multi-Level and Diverse Technology Market Begins to Take Shape; Scientific Research Is Undertaken by the State, Collective and Individual at the Same Time"]

[Text] Since the beginning of this year, heartening progress has been made in the restructuring of Hunan's S&T system. Restructuring of scientific research academies and institutes is developing in depth; a multi-level and diverse technology market has begun to take shape throughout the province; a good start has been made in the flow of talents; scientific research is undertaken by the state, collective and individual at the same time; S&T commissions at the prefectural and county levels are developing from the administrative and management type to the management and service type; and local policies are continually being perfected.

Currently, the number of independent scientific research organs subordinated to the province, prefectures and municipalities in Hunan undergoing experimental reform has already increased to 52, which constitutes 32.8 percent of the total. The Party Central Committee has 5 experimental reform scientific research units in Hunan, which constitute 41.7 percent of the total. The common features of their reform are: they are beginning to break through departmental, trade and regional boundaries, gearing to the needs of the society, linking factories and research institutes, engaging in joint development, joint technical management and integrated bodies for scientific research and production, transfering technical achievements through the technology market, providing technical services, using income from technology trade to enliven scientific research institutes and expand scientific research, and gradually realizing economic independence. According to the figures, experimental reform units have currently reduced their business expenses by varying degrees and 16 of them have achieved economic independence.

Hunan's technology market has developed from mere transference of technical achievements to diverse forms of joint technical management, technology shareholding, technology contracts, combining foreign trade enterprises with industrial and technological undertakings. Relations that cut across regions and trades as well as a professional and occupational technology market have

emerged. Some technical achievements which are "in short supply, cheap and effective" and which are highly practical and economically beneficial have been selling well. Some projects within the state scientific research plan have also begun to enter the technology market. Moreover, some items of technology and equipment which were at first planned to be imported from abroad and elsewhere in the country have been settled in Hunan's technology market. The provincial science and technology commission has decided to allocate a special annual fund of 1.5 million yuan to build the technology market during the period of the Seventh 5-year Plan.

A good momentum has also developed in the flow of talents. In the past 2 years, close to 10,000 scientists and technicians in Hunan have been mobilized through multiple channels. Approximately half of them are hired on a short-term or regular basis by small and medium-sized as well as rural and township enterprises along with technology transfer. An even larger number of scientists and technicians take part in the flow of knowledge and intelligence by taking concurrent sparetime jobs.

The number of civilian-operated scientific research and technical service organs founded with the approval of the various levels of S&T commissions throughout the province has reached 65. The state does not need to invest in these units or staff them. They are characterized by technical management as soon as they are founded and they achieve fairly good economic and social results within a relatively short period of time.

9586
CSO: 4008/2028

NATIONAL DEVELOPMENTS

NEW S&T INDUSTRIAL PARK IN SHENZHEN REPORTED

Beijing GUANGMING RIBAO in Chinese 3 Aug 85 p 1

[Report by Wu Xiaomin [0702 2556 3046]: "Import Advanced Technology and Foreign Capital; Develop High-Technology Products: Shenzhen Establishes S&T Industrial Park"]

[Text] In order to do a better job in developing technology-intensive and knowledge-intensive industry, the people's government of Shenzhen and the Chinese Academy of Sciences have jointly established the Shenzhen Science and Technology [S&T] Industrial Park. The inaugural ceremony was conducted in the afternoon of July 30. The municipal party committee secretary and mayor of Shenzhen Liang Xiang [2733 3276] and vice president of the Chinese Academy of Sciences Zhou Guangzhao [0719 0342 0664] attended the foundation ceremony.

The Shenzhen S&T Industrial Park is a comprehensive base that combines production and scientific research with education, with the goal of importing advanced technology from elsewhere in the country and abroad, importing foreign capital, and developing and producing high-technology products, and with emphasis on microelectronics, photoelectronics, precision machinery and new types of materials.

An administrative committee is set up above the Shenzhen S&T Industrial Park Corporation, with Liang Xiang as its chairman and Zhou Guangzhao and Shenzhen's vice mayor Zhou Xiwu [0719 3305 5294] as vice chairmen.

State Councilor Gu Mu [6253 3665] sent a congratulatory letter on the establishment of the Shenzhen S&T Industrial Park.

9586
CSO: 4008/2028

NATIONAL DEVELOPMENTS

JIUSAN SOCIETY OFFERS CONSULTING SERVICES

OW221135 Beijing XINHUA in English 1030 GMT 22 Oct 85

/Text/ Beijing, 22 Oct (XINHUA)--A group of scientific and technical experts has organized 78 teams to offer scientific and technical consulting services throughout the country.

The Jiusan (3 September) Society, one of China's 8 democratic parties, has offered consulting on 3,670 projects over the past 5 years.

Most of the Jiusan Society's members are scientists, engineers and professors, including one-fourth of the 400 division members of the Chinese Academy of Sciences.

In 1980, the Democratic Party began to organize its retired members to offer consulting services in urban areas designing new products and advanced equipment, developing new materials for enterprises, and designing small municipal works and buildings.

Since then, 70 percent of its local organizations have set up consulting offices. The office in Changchun, capital of northeast Jilin Province, designed the 21 rebuilt streets of the city. The team in Shanghai designed a compelte set of equipment for a new rubber production process. Those factories which adopted the new equipment have made large improvements in rubber productivity and quality.

The members also give lectures and classes to train other scientific and technical personnel. All of these services have won favorable comments, said an official from the Democratic Party's Central Committee in a revent interview with XINHUA.

The consulting services are now spreading to the countryside and the border areas populated by minority nationalities, the offical added. Forty local organizations of the society have established ties with nearby villages, helping them with new scientific farming and cultivation techniques. For example, the Beijing committee of the Jiusan society has helped Daxing county, just south of the capital. It has advised the county on cultivation, transferring embryos in milk cows, and irrigating sandy areas. The Jiusan members in Chongqing helped nearby Jianyang County improve its orange production, enabling the per capita annual income to increase 12 times.

There are eight noncommunist parties (generally called democratic parties) in China, which are composed of intellectuals from various circles, former industrialists and businessmen, or patriots of former Kuomintang. In addition to participating in political consultations on state affairs, they have offered their services to help the country's modernization and reunification program.

CSO: 4010/2002

NATIONAL DEVELOPMENTS

TIANJIN MAKES HEADWAY IN IMPORTED TECHNOLOGY USE

OW1709?8 Beijing XINHUA in English 0851 GMT 17 Oct 85

/Text/ Tianjin, 17 Oct (XINHUA)--One hundred and forty-five projects using imported technology are now operating in Tianjin, one of China's 14 open coastal cities.

Another 140 are being checked for acceptance, an official of the municipal economic committee said here today.

Tianjin is one of the pilot cities enpowered to retool old factories with advanced imported technology. The city has the use of a 200 million U.S. dollar state allocation annually between 1983 and 1986 for this purpose. To date 547 projects involving a total of 500 million U.S. dollars have been contracted.

The official said imports of technology have upgraded more than 100 major plants in industries which include engineering machinery, automobile manufacture, meter automation, radio and television sets, electronics, metallurgy, petroleum exploitation, rubber manufacture and woolen textiles.

Software imported in the form of patents and license accounts for over one-half of Tianjin's total imported projects, he added.

Imported technology for light industry and textiles generally begins to realize profits about 18 months from signing a contract to going on stream, according to the official. In machinery, electronics and chemicals, the time lag is about 2 years.

The city has organized television technicians to improve products by further study of the imported TV assembly lines. As a result, Tianjin's color TV production is up to 400,000 quality sets a year.

CSO: 4010/2002

PROGRESS IN CHINA'S PATENT WORK REPORTED

Tianjin JISHU SHICHANG BAO [TECHNOLOGY MARKET WEEKLY] in Chinese 9 Jul 85 p 1

[Article: "Inventors and Creators Are Enthusiastic, Patent Applicants Turn Up In Large Numbers: China's Patent Work Makes Heartening Progress; Patent Office Received 7,086 Applications In the First 3 Months"]

[Text] Since it took effect on April 1st, this year, China's Patent Law has received wide attention at home and abroad. Applicants have been very enthusiastic and patent work has made heartening progress. According to the figures of the Patent Office, from 1 April through 30 June, China received a total of 7,086 patent applications. Of this total, applications for invention patents constituted 63.4 percent, utility models 33.3 percent and designs 3.3 percent.

Starting in the month of May, the number of patent applications filed at the Patent Office stabilized from the peak in early April to an average of 40 to 50 per day. The number of applications this year is expected to top 12,000 and may increase further next year.

Of the domestic patent applications, service inventions made up about 60 percent, which mainly come from scientific research and education units; and individual applications made up about 40 percent. This shows that the patent system not only can encourage inventions and innovations by scientific research and education units but it can also mobilize and encourage the enthusiasm of the broad masses of people to invent and innovate.

The number of patent applications from abroad also makes up a considerable proportion of the patent applications in China, and there is a tendency to increase, which shows that China's Patent Law is welcome abroad.

However, currently the quality of the writing of some of China's patent application documents is not high enough and many of them need to be amended and corrected. The number of applications from industrial and mining enterprises is still low, which shows that our Patent Law has not yet been sufficiently popularized and that many industrial and mining enterprises have not yet been transformed from the production to the management and development types.

China's Patent Office is reported to be in the process of classifying and examining those applications which have already been accepted and it is preparing to announce one group of patents in late September and another group at the end of the year.

In the past 3 months, the implementation of the Patent Law has also effectively spurred the construction of a nationwide system in patent work. Patent service centers or offices are set up everywhere. There are already as many as 4,400 registered and licensed patent agents throughout the country and another 1,500 are being registered. This number is expected to rise to 7,500 by the end of this year.

In order to further do a good job in personnel training for patent work, China's Patent Office is preparing to organize a patent cadre training college in Shanghai and operate cadre training classes for patent administration in Chengdu; the State Education Commission is planning to set up patent departments at the Qinghua, Fudan, and Xi'an Jiaotong Universities; and the Ministry of Justice will also continue to train patent lawyers at colleges of political science and law.

PATENT APPLICATIONS RECEIVED, APRIL-JUNE 1985

Type:	Period:	First Day (April 1)	April (2-30)	May	June	Total
Domestic	Inventions	1,535	375	300	273	2,483
	Utility Models	884	515	424	484	2,307
	Designs	66	19	19	21	125
	Subtotal	2,485	909	743	778	4,915
Foreign	Inventions	929	239	381	458	2,007
	Utility Models	8	4	22	18	52
	Designs	33	29	33	17	112
	Subtotal	970	272	436	493	2,171
Total	Inventions	2,464	614	681	731	4,490
	Utility Models	892	519	446	502	2,359
	Designs	99	48	52	38	237
	Subtotal	3,455	1,181	1,179	1,271	7,086

PATENT APPLICATIONS RECEIVED BY VARIOUS PROVINCES, AUTONOMOUS REGIONS AND DIRECTLY-ADMINISTERED MUNICIPALITIES, APRIL-JUNE 1985

Area	Total	Inventions	Utility Models	Designs	Non-Service Inventions	Service Inventions
Beijing	915	502	378	35	358	557
Hebei	106	38	66	2	69	37
Nei Mongol	32	18	13	1	17	15
Shanxi	63	40	22	1	33	30
Liaoning	336	167	168	1	137	199
Jilin	193	107	85	1	81	112
Heilongjiang	144	59	83	2	103	41
Shanghai	420	237	172	11	186	234
Jiangsu	378	137	234	7	184	194
Zhejiang	163	82	81	0	93	70
Anhui	58	16	42	0	35	23
Jiangxi	91	33	54	4	59	32
Fujian	57	33	24	0	27	30
Shandong	166	79	84	3	73	93
Guangdong	122	61	56	5	58	64
Guangxi	81	27	54	0	59	22
Hubei	213	148	57	8	50	163
Hunan	335	133	196	6	180	155
Henan	137	76	60	1	75	62
Sichuan	222	125	92	5	97	125
Yunnan	61	32	29	0	21	40
Guizhou	37	24	11	2	15	22
Xizang	0	0	0	0	0	0
Shaanxi	169	91	77	1	63	106
Gansu	64	33	31	0	37	27
Qinghai	8	4	4	0	2	6
Xinjiang	15	11	4	0	9	6
Ningxia	12	4	8	0	2	10
Tianjin	317	166	122	29	186	131
Taiwan	0	0	0	0	0	0
Total	4,915	2,483	2,307	125	2,309	2,606

9586
CSO: 4008/2027

NATIONAL DEVELOPMENTS

SICHUAN GOVERNOR ON DEVELOPMENT OF S&T IN RURAL ENTERPRISES

Chengdu SICHUAN RIBAO in Chinese 29 Jul 85 p 1

[Report by Yao Min [1202 2404]: "Jiang Minkuan expects S&T Personnel to Vigorously Support the Development of Rural and Township Enteprises"]

[Text] Governor Jiang Minkuan [5592 3046 1401] of Sichuan Province recently stressed at the Sichuan municipal, prefectural, autonomous prefectural and county scientific and technical [S&T] cooperative work conference that organizing S&T personnel to go and work in the countryside and mountain areas and supporting the development of small and medium-sized as well as rural and township enterprises is a major strategic policy decision to make the people of Sichuan wealthy and improve the position of Sichuan, and it is an important step to implement the Party Central Committee's resolution concerning restructuring of the S&T system. It is even more necessary to rely on S&T to quadruple Sichuan's annual gross agricultural and industrial output by the year 2000.

Through learned societies, associations, research institutes, scientific popularization networks, S&T consulting agencies, S&T cooperation among factories and mines, and specialized S&T mass organizations and in accordance with the spirit of guidance by leading comrades of the provincial party committee and the provincial government, the provincial S&T cooperative system will mobilize 500,000 S&T staff members and 1,600,000 key technicians of the rural masses, further direct S&T into the broad rural areas and give impetus to the technical advancement of small and medium-sized as well as rural and township enterprises. The provincial S&T cooperative system hopes that four things will be undertaken throughout the province: (1) formulating programs and views supporting the development of small and medium-sized as well as rural and township enterprises; (2) selecting a number of applicable S&T achievements and popularizing them among these enterprises; (3) training a group of qualified rural technicians and managers; and (4) building a multi-level and diverse specialized S&T mass organization.

9586
CSO: 4008/2027

NATIONAL DEVELOPMENTS

BRIEFS

NATIONAL RECORDER QUALITY CONFERENCE--Nanjing, June 10 (XINHUA)--China is now able to produce all parts for all models of radio-recorders, it was stated at a recent national recorder quality test conference in Changzhou. The overwhelming majority of the parts and accessories of the 53 types of prize-winning radio-recorders are now produced in China. This marks the end of long dependence on imports of radio-recorder parts, officials at the conference said. China trial-produced its first cassette recorder in the early 1970s and mass production began in the 1980s. But most parts were imported through compensation trade and technical imports. China produced 1.52 million radio-recorders in 1981, 700,000 of which were assembled with foreign parts, accounting for 46 percent of the total. But only seven percent of the (76.04) million radio-recorders produced last year were assembled with foreign parts. Now Chinese-made radio-recorders are already dominant on the domestic market. [Text] [Beijing XINHUA in English 0658 GMT 10 Jun 85 OW]

CHINESE-CHARACTER COMPUTER CODING--Shanghai, June 28 (XINHUA)--Jin Yiping, a technician at the Shanghai Applied Electronics Research Institute, has succeeded in computer-coding 6,700 Chinese characters. The input unit can display 20 characters a minute on the screen, and has a wrong-code rate of below one percent. Previous attempts to computerize Chinese characters rarely managed to store more than about 1,000. According to institute sources, a beginner can learn to operate the unit in an hour, and the device is expected to appear on the market soon. [Text] [Beijing XINHUA in English 0846 GMT 28 Jun 85 OW]

COMMUNICATIONS COMPUTER SYSTEM DEVELOPED--Beijing, July 26 (XINHUA)--A small computer system, which can be used for long-distance communications and link up with foreign computer networks through geostationary communications satellites, passed the state certification test here Thursday. Developed by a research institute of the Astronautics Industry Ministry, it can be used to control and direct the launching of satellites and guided missiles. With a block structure, the computer may change its functions through increasing or reducing modules and software. The size of the main frame is similar to that of a household refrigerator. Experts said the system is up to the international level of the early 1980s. The computer will be put into small-quantity production soon. [Text] [Beijing XINHUA in English 0936 GMT 26 Jul 85 OW]

MICROCOMPUTERS USED TO UPDATE TECHNOLOGY--Beijing, September 4 (XINHUA)--Microcomputers have begun to be used to renovate outdated industrial equipment, today's "Economic Daily" reports, on the occasion of a seminar now being held on this subject in Chengdu, capital of southwest China's Sichuan Province. It was reported that attaching microcomputers to machine tools and industrial furnaces so far has proved successful. They are working more efficiently at a much lower cost. Applying microcomputers to renovate aging industrial sectors is included in the next five-year plan (1986 to 1990). [Text] [Beijing XINHUA in English 1535 GMT 4 Sep 85 OW]

NEW COMPUTER ARRAY PROCESSOR--Beijing, September 28 (XINHUA)--China's first array processor capable of highly-efficient digital and signal processing passed state certification here today. A key project in China's Sixth Five-Year Plan (1981-1985), the NCI-AP2701 was developed by the North China Institute of Computer Technology under the Ministry of Electronics Industry. Calling it important to China's computer industry, experts of the institute said that the array processor is capable of processing tens of millions of instructions per second. Once it is attached, it can enhance a computer's ability by several dozen times, officials said. A small or medium sized computer is capable of the work done by large computers if it has an array processor connected to it, the experts said. The new machine can be used widely in oil and mineral prospecting, meteorology, medical equipment, the power industry and national defense. The new development will be put into small-quantity production soon, the experts said. [Text] [Beijing XINHUA in English 1515 GMT 28 Sep 85 OW]

HEAVY ION CYCLOTRON--Lanzhou, 22 Sep (XINHUA)--The main magnet for China's first heavy ion cyclotron system is being installed in the Lanzhou Modern Physics Research Institute of the Chinese Academy of Science. The heavy ion cyclotron is a major project. Its principal components and parts, as well as the civil engineering construction, were designed and manufactured domestically. The total construction area is 18,000 square meters. The civil engineering project was completed in November 1984. Since then, bulky major equipment for the system has continually arrived at the construction site. The installation began in August this year. Now, the 6-meter 2,000-metric-ton principal magnet is in position. [Excerpts] [Beijing XINHUA Domestic Service in Chinese 0140 GMT 22 Sep 85 OW]

FIRST BIONIC COMPUTER DEVELOPED--After successfully developing the Galaxy 1 computer, the National Defense Science and Technology University has also successfully developed a digital bionic computer comparable to international advanced levels of the early 1980's. This digital bionic computer, called Galaxy Yx (Gang) 21, passed the State's examination in Changsha yesterday. This is the first time that China develops this kind of computer. Upon being assigned the task, the National Defense Science and Technology University, Institute for Computer Studies, worked day and night inspite of a manpower shortage because of the urgency of the task. It struggled hard and overcame problems. Within a period of two and a half years, it accomplished the work of readjusting and testing two sets of bionic languages. The features of this digital bionic computer are advanced, being supported by software, low cost, high accuracy, stable and reliable operation, is capable of making logical judgments and so on. This computer also has high military and economic values. [Text] [Changsha Hunan Provincial Service in Mandarin 2300 GMT 15 Oct 85]

S&T COMMON MARKET FORMED--The Forum of Presidents of Science Academies in the 10 provinces of Guangdong, Guangxi, Jiangxi, Gansu, Hebei, Shaanxi, Guizhou, Henan, Heilongjiang and Shandong was recently convened in Jinan. An agreement was reached at the conference on establishing a S&T common market for local science academies. The agreement specifies: all academies participating in the common market must exhibit, market and manage the S&T achievements and new products on behalf of the various academies in the S&T market run by their home province or region; each academy draws 1 percent of the business volume as administrative fee; each academy compiles a brief quarterly report with information on the S&T market of its home province for internal interchange, and the report should include information on the tendering of contracts to solve difficult problems, transference of achievements, new products introduced and market demands; each academy appoints an all-power representative to the common market who will exchange information with his counterparts in order to maintain contact and deal with problems in concern. [Text] [Beijing GUANGMING RIBAO in Chinese 5 Aug 85 p 2] 9586

CSO: 4008/2028

APPLIED SCIENCES

NATION'S FIRST WATERSIDE SOLAR OBSERVATORY OPERATIONAL

Beijing TIANTI WULI XUEBAO [ACTA ASTROPHYSICA SINICA] in Chinese Vol 5, No 4, Oct 85 p 254

[Text] The Beijing Observatory has built China's first waterside solar observation station at Huairou Reservoir north of the city. The solar magnetic field telescope has also been completed and is now operational. Construction of the Huairou solar observation station began in 1982. It is a relatively good site from which to carry out solar observations, having the following distinguishing features:

1. Excellent atmospheric conditions due to the fact that the solar magnetic field telescope is bordered on the east, south, and west by 1-2 kilometers of water;

2. The depth of the surrounding water is approximately 10 meters and the level is stable;

3. The telescope is 24 meters above the ground and 30 meters from the edge of the water. The observation room in the spherical dome may be rotated some 10 meters to face north.

The Huairou station is situated on the northern shore of the southern arm of Huairou Reservoir in Huairou County, Beijing Municipality.

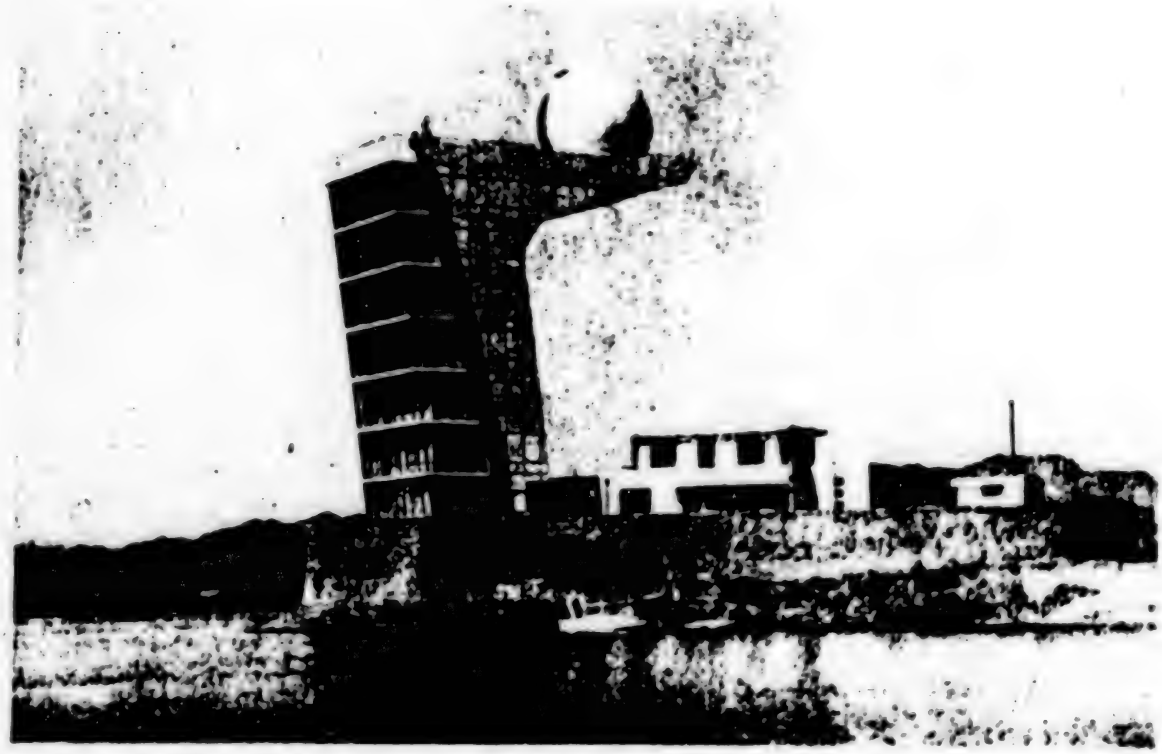

Plate I. Overall view of the Huairou observation station.

/8918
CSO: 4008/12

APPLIED SCIENCES

NATION'S FIRST HEAVY ION CYCLOTRON BEING ASSEMBLED IN LANZHOU

Shanghai JIEFANG RIBAO in Chinese 23 Sep 85 p 3

[Text] Recently, assembly began on the 2-meter-high, 2000-ton primary magnet of China's first heavy ion cyclotron at the Lanzhou Institute of Modern Physics, Chinese Academy of Sciences.

The heavy ion cyclotron system is a major national scientific project. Its major assembly and construction are entirely Chinese-designed and developed. Ground was broken on the project in November 1984 and the 18,000-square-meter facility has been inspected and accepted.

It has been reported that today there are [only] 20-odd heavy ion accelerators in the world and very few heavy ion cyclotrons of the type that China is now assembling. The completion of this accelerator will enhance China's basic theoretical research in nuclear physics and applied research in heavy ions; it will also promote the development of nuclear science and technology, new materials, favorable conditions for research on new technologies and new scientific research methods that may be applied in medicine, geology, astronomy, archaeology, and atmospheric monitoring.

/8918
CSO: 4008/11

APPLIED SCIENCES

DETERMINATION OF FISSION GASES IN IRRADIATED UO_2 FUEL ELEMENTS

Chengdu HE DONGLI GONGCHENG [NUCLEAR POWER ENGINEERING] in Chinese Vol 6 No 4, Aug 85 pp 54-59

[Article by Feng Mingquan [7458 2494 0356], Yuan Zhanglin [5913 2874 2651], Zhou Duoping [0719 1122 1627], Wang Yiru [3769 0034 1172], Yang Mingjin [2799 2494 6855], and Lu Xiangyu [7120 0078 3768]]

[Text] I. Introduction

The fission gases krypton and xenon produced by the UO_2 fuel elements during reactor operation not only will cause interaction between the fuel elements and the enclosure due to radiation swelling of the elements, but will also increase the internal pressure and thus degrade the thermal properties of the gases within the elements. As a result, the performance of the elements is greatly affected. In particular, in a nuclear power reactor using UO_2 elements, the safety of the reactor depends on whether the enclosure can withstand the increased pressure of the fission gases. For this reason, accurate determination of the amount of fission gases produced, and understanding of the release mechanism of fission gases as well as the relationship between the rate of release and the depth of burnup, the operating temperature, the power, and the production technique of raw UO_2 are of great importance to the improvement and development of new elements and to the theoretical study of irradiation effect.

The measurement of fission gas must be carried out in a vacuum system. First, a special piercing device is used to poke holes in the elements in a thermal chamber to release the gas inside. The gas is collected by a collection system outside the thermal chamber where its pressure, volume, and temperature are measured. A sample of the gas is analyzed by a chromatic spectral analyzer to determine its constituents. Finally, the total amount of He, Kr, and Xe is calculated according to the equation of state of an ideal gas.

II. Experimental Setup

The experimental setup consists of two parts: the gas collection system and the chromatic spectral analysis unit. On the basis of the properties of the elements, we have designed and built a fission gas collection system as shown in Figure 1. It includes the piercing device inside the thermal chamber and the gas collection unit outside the thermal chamber.

The piercing unit consists of a support bracket for the elements, a special table drill, and a piercing chamber. The special table drill and the piercing chamber are shown in Figure 2. In order to prevent the drill head from touching the UO_2 element which may lead to radioactive dust pollution, the piercing point is chosen to be located at the axial chamber 30 mm above the element. The interface between the element, the drill rod, and the piercing chamber are sealed using Wilson vacuum seal.

The glass collection system outside the thermal chamber consists of three parts: the gas capture unit, the pressure measuring unit, and the vacuum unit. The gas capture unit includes v_1, v_2, the diffusion pump 1, v_3, v_6 and the Toepler pump. v_1 is connected to a ϕ 10 mm standard ground opening, and is used for filling and monitoring the vacuum level. The diffusion pump 1 pumps the gas from the piercing chamber into the inner chamber of the Toepler pump. When the fission gas passed through v_3 into the Toepler pump, v_6 gradually opens into the atmosphere. The atmospheric pressure forces the mercury from the outer chamber into the inner chamber; as the mercury level rises, it pushes the float upward to shut off the gas inlet. When the mercury level reaches v_5, it closes v_5 and v_6, consequently the pressure in the outer chamber of the Toepler pump and the mercury level begin to drop, creating a high vacuum in the inner chamber, and the float is returned to its original position. Due to the pressure difference, the gas from v_3 again enters into the inner chamber. By repeating this process, gas is collected into the sampling ball. The pressure measuring unit includes the YG cursor bellows micro-pressure meter, the sampling ball, and the measuring chamber. The measuring chamber is located between v_4, v_5, the sampling ball piston, and the positive chamber of the micro-pressure meter. Its volume is determined according to Boyle's law. The vacuum unit includes the diffusion pump 2 and the 2x-2 mechanical pump; it provides the vacuum for the entire system prior to the piercing unit, and meets the evacuation requirement of the outer chamber of the Toepler pump.

In the chromatic spectral analysis unit, because of the small samples and low pressure (it is estimated that the total amount of each sample is 15-20 milliliters at a pressure of 50-80 mm Hg), we have designed and built a negative pressure sampling system which has a special four-way piston and an ordinary four-way piston (see Figure 3).

The circuit is evacuated using a mechanical pump and is connected to the 102G gas phase analyzer via a six-way valve. For precision measurement, the initial pressure of the sample is measured by the YG cursor micro-pressure meter. The peak of the spectrum is processed by a digital integration unit.

III. Method of Experiment

1. Collection of Gas Sample

(1) After being thoroughly cleaned, the element is inserted into the piercing chamber, which is then sealed; a thermocouple is inserted into the v_1 port, and the v_6 atmospheric inlet is closed. With all the other pistons connected, the entire system is evacuated.

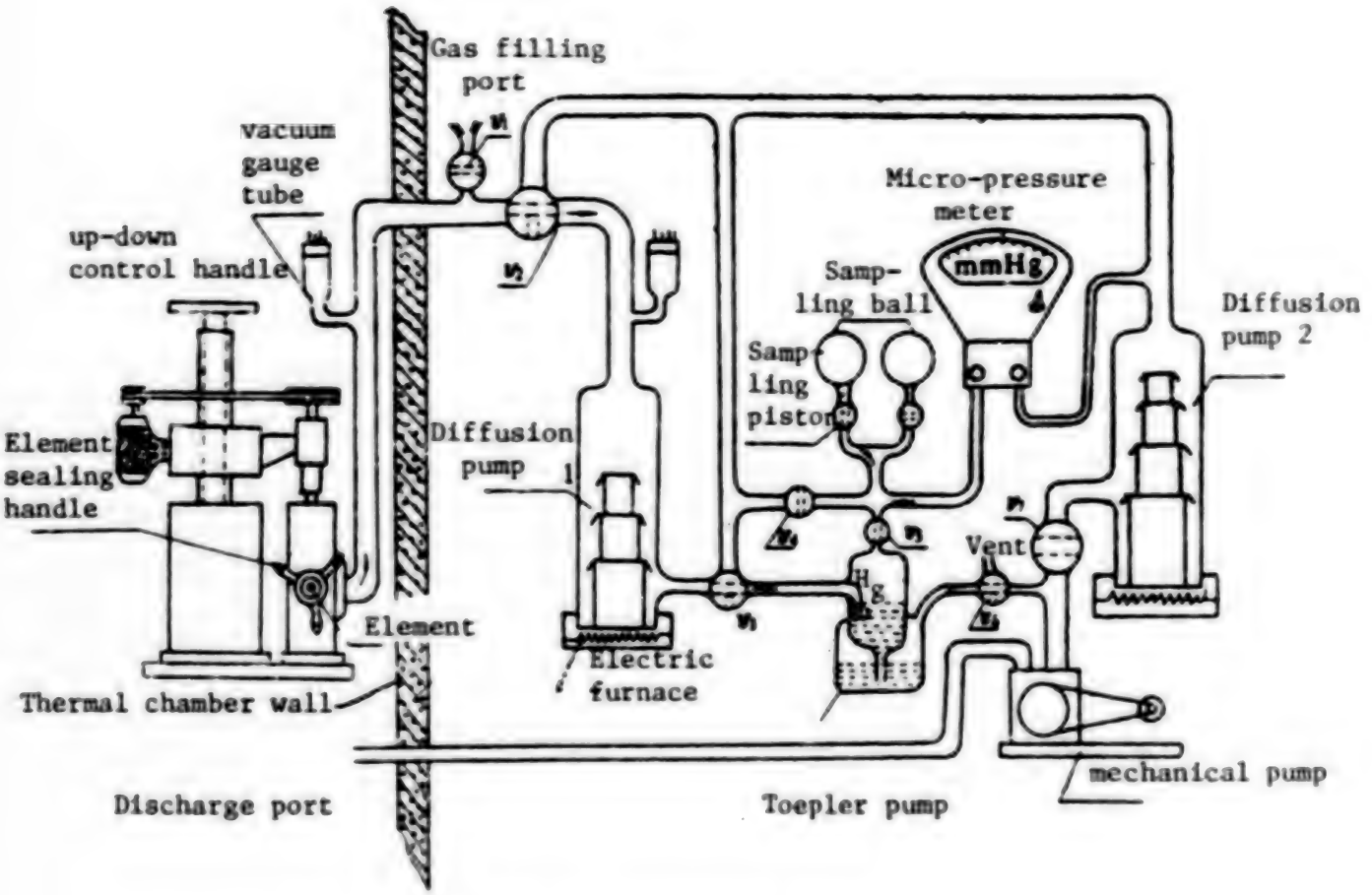

Fig. 1. Fission Gas Collection System

Note: v_1, v_4, v_5, v_7 are two-way valves: v_2, v_3, v_6 are three-way valves

(2) When the piercing chamber reaches a vacuum level of 1.5×10^{-2} mm Hg, the pistons of the system are rotated to the positions shown in Figure 1. The element enclosure is drilled through, and the Toepler pump is activated to begin collecting gas; at the same time, the amount of dosage is being monitored and pressure, temperature measurements are taken.

(3) The piston of the sampling ball is closed, and the gas in the measuring chamber is returned to the thermal chamber. The gas sample is then sent to the chromatic spectral analyzer.

2. Chromatic Spectral Analysis

(1) Selection of the chromatic spectral column. Because of the small volume of sample collected, a proper chromatic spectral column must be used so that each constituent of a sample can be completely separated. Having examined the separation properties of silica gel molecular sieve, active carbon and the mixed column under the conditions of 40 ml/min gas (He) rate, 200 mA heat conduction current, and different activation temperatures, we selected the silica gel molecular sieve as the chromatic spectral column.

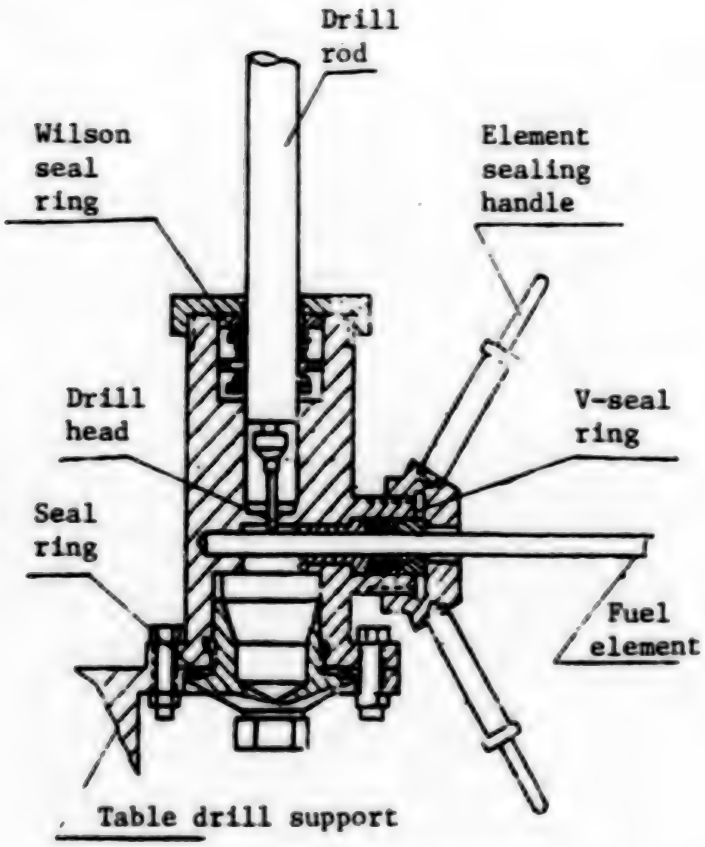

Fig. 2. Piercing Chamber

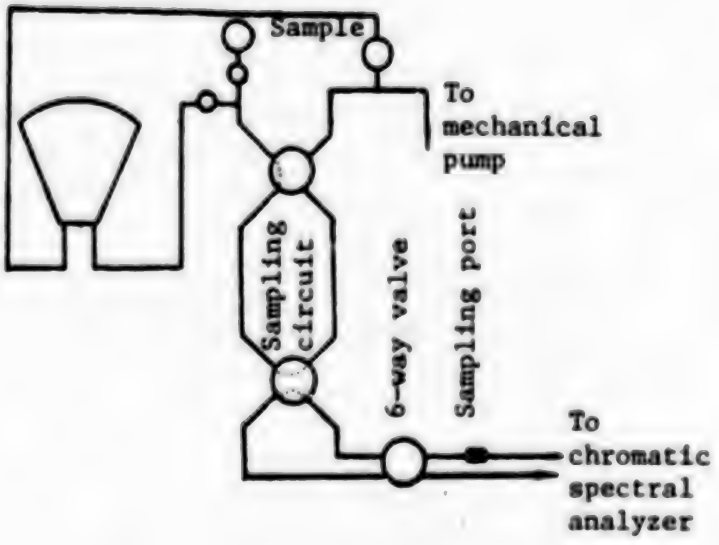

Fig. 3. Schematic Diagram of Sampling System

(2) Construction of Working Curves. By injecting test samples of air, Kr, Xe, CO (obtained from the reaction of sulfuric acid and formic acid and purified using silica gel molecular sieve) into the circuit and processing the data using both the peak height method and the area method, working curves for the five different gases have been constructed. (see Figures 4, 5).

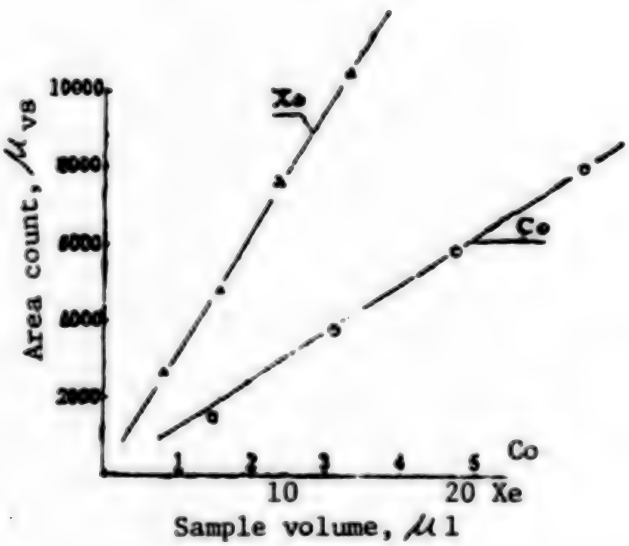

Fig. 4. Working Curves For Xe, CO

(3) Sample Analysis. After installing the sample bottle in the sampling circuit, the three-way tube and the sampling circuit are evacuated and tested. When the peaks of O_2, N_2 no longer register on the integration unit, the sampling circuit is evacuated, and the piston is rotated to let the sample inside; once equilibrium is reached, the sample is entered through the six-way valve into the chromatic spectral analyzer. The sampling pressure is calculated according to the following formula:

$$P_n = P_o \left(\frac{V_1 + V_2}{V_1 + V_2 + V_3} \right)^n$$

where P_o is the initial sample pressure, mm Hg; P_n is the sample pressure during the nth sampling process, mm Hg; V_1, V_2, V_3 are respectively the volumes of the sampling ball, the three-way tube and the sampling circuit. These volumes are mercury standardized prior to the experiment.

From the sample volume V_3, one can calculate the pressure from the above expression and the total volume of each sample from the gas equation of state (under standard condition).

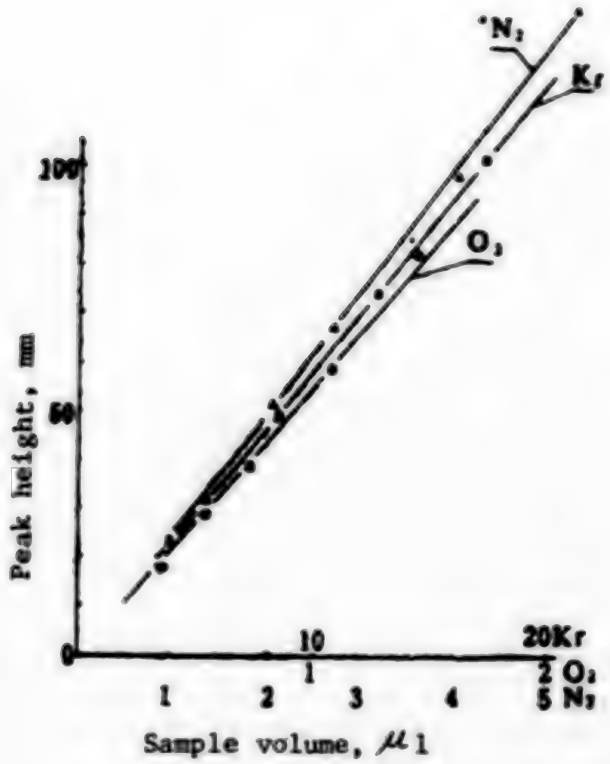

Fig. 5. Working Curves for Kr, O_2, N_2

Note: In constructing the curves, the peak height of Kr is scaled by 1/2, the peak height of O_2 is scaled by 2.

The spectral peak is processed by the digital integration unit to obtain the area count of Xe; the peak heights of O_2, N_2 and Kr are measured from the spectral diagram, and the absolute amount of each constituent in the analysis can be calculated from the working curves. Thus, the composition of the sample can be determined.

IV. Experimental Results and Errors

1. Experimental Results

Based on the results of relative burnup from γ scans, we selected three rods from the element containers E_{29}, G_{21}, and H_{24} for this experiment. The collected gas samples are spectral-analyzed to provide the spectral diagram shown in Figure 6. It shows good separation of the fission gases Kr, Xe, O_2 and N_2 as well as near-ideal peak shapes. Kr, O_2 and N_2 are processed using the peak height method, and Xe is processed using the area method. Calculations show that the Kr and Xe contents are respectively 0.13-2.03 percent and 1.25-9.17 percent. Based on the pressure, temperature and volume of the sample, one can calculate the volumes of Kr, Xe under standard conditions to be 10-59 μl and 93-520 μl respectively.

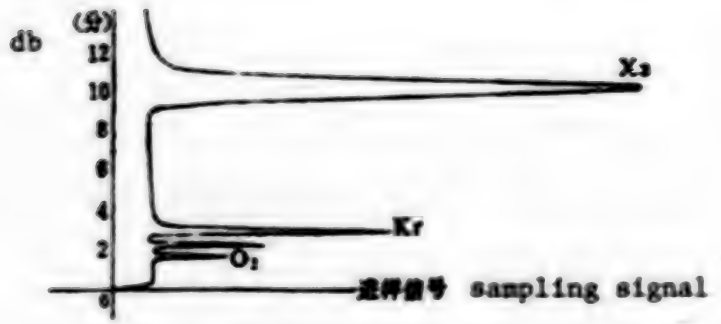

Fig. 6. Chromatic Spectrum of a Gas Sample

The release rate is a commonly used engineering index for measuring the amount of gas released. It is defined by the following expression:

$$K + \frac{V_{meas}}{V_{theo}} \cdot 100\%$$

where V_{meas} is the measured volume of the fission gas from the experiment, V_{theo} is the theoretically calculated volume of fission gas produced during reactor operation. V_{theo} is obtained from the following formula:

$$V_{theo} = \frac{MBCYV_o}{N_o}$$

where M is the single rod UO_2 capacity; B is the burnup value, MWd/T·U; $C=2.63\times10^{23}$ fissions/MWd, Y is the atomic yield of the fission gas, Y_{Kr} =0.0395 atoms/fission, Y_{Xe}=0.305 atoms/fission[1], V_o is the volume of 1 mol og gas under standard condition (22.4 liters); N_o is the Avogadro's Constant. From the above expressions, the release rates of Kr and Xe are calculated to be 0.10-0.34 percent and 0.12-0.38 percent respectively.

The internal pressure of the element is an issue that is of major concern to the designer. Based on the measured volume of the fission gas and the cold-state volume of the empty chamber, we have calculated the internal pressure to be 1.33-1.75 atmospheres. This increase in internal pressure is not attributed to the fission gases; it may be due to the pre-filling of He to a level higher than 1 atmosphere during the manufacturing process of the element. Figure 7 shows the relationship between the volume of Kr, Xe and burnup under standard conditions. Clearly, the amount of Kr, Xe released increases with the depth of burnup.

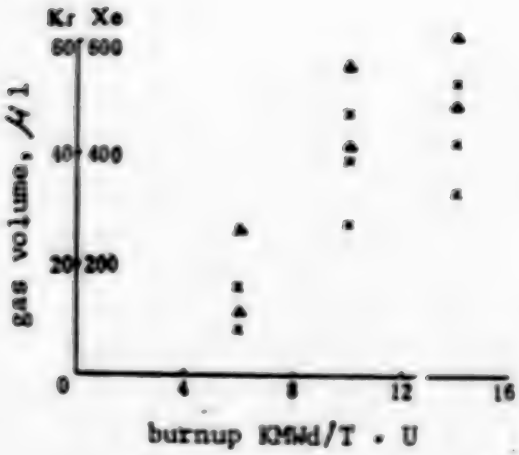

Fig. 7. Relationship Between the Volume of Fission Gas and Relative Burnup

2. Experimental Error

One difficult problem with this experiment is the large errors involved in measuring small quantities of fission gases. The main error sources are as follows:

(1) Error Due to the Collection Efficiency of the Gas Collection System. In order to test if this system can collect all the gases into the sampling ball, we performed a simulated experiment. By filling the system with a known quantity of Kr gas, and collecting the gas using the Toepler pump, we can calculate the volume of the captured gas, from which we can deduce the collection efficiency to be higher than 95 percent. After being analyzed by the chromatic spectral analyzer, the air content in the gas sample is less than 1 percent. The number of collections and the collection time depend on the volume of gases being collected. The collection process stops when the pressure reading and the monitored β dosages of the collected gas no longer increase. From this one can deduce that the error due to collection efficiency is 5 percent.

(2) Error Due to Leakage During the Collection Process. During the collection period, a small amount of air will leak into the system through the seal of the drill rod and through system aeration. By measuring the volume and vacuum level of the sections occupied by the fission gases both inside and outside the thermal chamber, we estimated the error from the ratio of air to gas sample in the system to be 0.4 percent. After analysis of the gas sample, the air content is 1 percent. The remaining error caused by drill rod rotation and system aeration is also 1 percent.

(3) Error Due to Measuring Instrument. It is known from the state equation of an ideal gas that the number of mols is a function of temperature, pressure and volume. The relative error due to measurement is

$$\frac{\Delta n}{n} = \frac{\partial T}{\partial n} + \frac{\partial P}{\partial n} + \frac{\partial V}{\partial n}$$

where $\frac{\partial T}{n}$ is error due to temperature measurement, $\frac{\partial T}{n} = \frac{\Delta T}{T} = 1\%$;

$\frac{\partial P}{\partial n}$ is error due to pressure measurement, $\frac{\partial P}{\partial n} = \frac{\Delta P}{P} = 1\%$;

$\frac{\partial V}{\partial n}$ is error due to volume measurement, $\frac{\partial V}{\partial n} = \frac{\Delta V}{V} = 1\%$.

(4) Error Due to Chromatic Spectral Analysis. In the absence of a gas sample, it is difficult to determine this error contribution. We only conducted an accuracy test in which five different gas mixtures were prepared using He as a base gas, and the experimental conditions for sample analysis were simulated. The standard deviation of the chromatic spectral analysis so obtained was less than 6 percent.

V. Conclusion and Discussion

Based on the measurements of fission gases from nine different fuel elements, we can draw the following conclusions:

1. It is feasible to use the above collection system to determine the amount of fission gases in the irradiated UO_2 fuel elements. By using this apparatus, we can pierce through the element enclosure within 10 seconds. The amount of fission gas collected is relatively small because the piercing device does not penetrate the UO_2 core. The β dosage 10 cm from the center of the sampling ball is approximately 30 mrad, and the γ dosage is close to the background level in the front part of the thermal chamber.

2. By using a silica gel-5A molecular sieve serial column, a mixture of Kr, Xe, O_2, N_2 and CO can be completely separated. Coupled with a vacuum sampling system, this unit provides an effective tool for analyzing small quantities of negative-pressure gas samples from irradiated fuel elements.

3. The element enclosure can withstand the increased pressure caused by the fission gases. Experimental results show that the internal pressure of the elements is greater than 1 atmosphere; however, the increased pressure due to He did not cause damages to the elements. This demonstrates that the enclosure design has sufficient margin of safety.

4. The elements can tolerate degradation of the thermal properties caused by the fission gases. Under the condition of moderate temperature and relatively low burnup, the amount of fission gases released is only one-tenth of the total volume of medium gases. Even though the thermal resistance of the fission gases is approximately 22 times that of He,[2] it will not cause catastrophic result.

The authors would like to express their thanks to comrades Zhang Zhaoyuan, Yao Shibing, Han Chuanbing for providing guidance in this work, and to comrades Gu Ziyou, Hu Xuehzheng for their assistance.

References

[1] Qinghua University Department of Engineering Physics, "Irradiation of Reactor Materials," Qinghua University Press, 108 (1975).

[2] Zhu Huannan, "Foreign Nuclear Technology," 4, 1 (1978).

3012
CSO: 4008/6

APPLIED SCIENCES

AUTOMATIC GATHERING, PROCESSING OF MULTIPOINT PRESSURE DATA ANALYZED

Tianjin TIANJIN DAXUE XUEBAO (ZHEN KAN) [JOURNAL OF TIANJIN UNIVERSITY (SUPPLEMENT) in Chinese No 2 (Mechanics), Dec 84 pp 115-120

[Article by Zhou Xinghua [0719 5281 5479]: "Equipment for Automatic Gathering and Processing of Multipoint Pressure Data by Means of the Microcomputer TP801"]

[Text] Abstract: This device uses a TP801 microcomputer as its main unit and the microtransducers CYG, A/D converter (Multichannel Voltmeter PF 3), I/O interface circuit and miniprinter TP 801 as its accessories. The automatic gathering and processing of multipoint pressure data can be made according to the software and the measurement result can be printed in real time. It can replace the manual calculation of measuring multipoint pressure data with a multitube manometer. As a result, the measuring speed and accuracy can be greatly enhanced. Fitted with different transducers and accompanied with appropriate software, this device can also measure other physical quantities and process their appropriate data.

I. Introduction

The measurement of pressure distribution on a solid surface submerged in a dynamic fluid is an important experimental subject in the field of fluid dynamics. If the pressure distribution curve is available, the loads at various parts of the object can be studied and thus can provide data in the design of strength. The lift and drag reacting on the object can also be calculated using the pressure distribution curve.

The traditional measuring method has been to measure multipoint pressure using a multitube manometer. The reading differential rate can only be achieved at around 0.5 mm H_2O due to the unevenness in the tube-diameter width and capillarity. Furthermore, it is relatively time-consuming in taking the reading of multipoint pressure individually. Some of the methods have been to take pictures of the fluid column heights of the multitube manometer. However, the processes of developing and printing the film, reading and calculation have to be taken in order to arrive at the final result, not to

mention the relatively substantial errors involved. It is the above situation which prompted us in the development of automatic gathering and processing of multipoint pressure data by means of the microcomputer TP 801.

II. Hardware

The equipment consists of a multichannel constant current supply, a solid microtransducer, a multichannel digital vol-meter, an I/O interface circuit, a microcomputer and a microprinter, as shown in Figure 1.

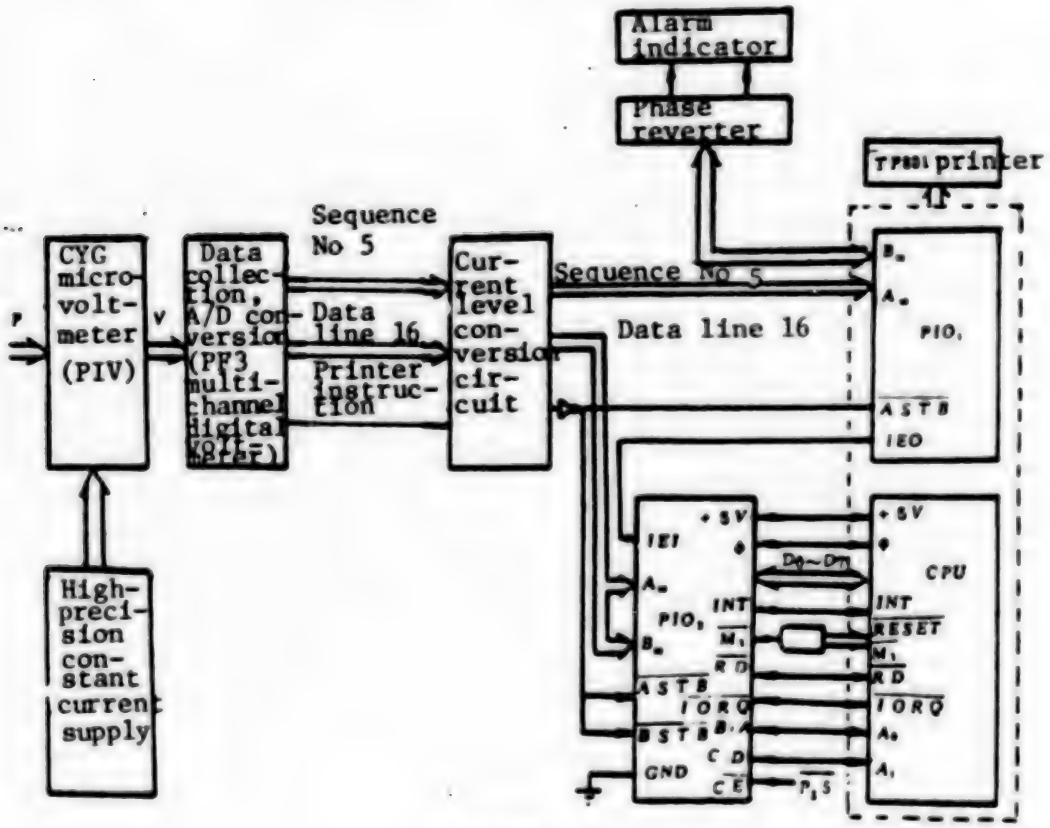

Figure 1.

1. Detection Section

This section is comprised of the microtransducer and the constant current supply. Pressures at tested points are detected by the transducer and are converted to voltage linearized with the pressure, i.e., $P(mmH_2O) = K(mmH_2O/mv)\ V\ (mv)$, where K is the conversion coefficient of P~V and is close to 1. Therefore, the requirement of the automatic gathering of data is satisfied. The CYG solid microtransducer we use has a measuring range of $+100mmH_2O$ ~ $-100mmH_2O$, with a differentiating capacity of $0.01mmH_2O$. It possesses excellent features such as high precision, good stability and high sensitivity. The constant-current supply which is the accessory current source for the transducer has a direct impact on the measurement precision of the transducer. Therefore, we have developed a 20-channel constant supply

which can simultaneously supply the working current to 20 transducers, with a working current of 8~12 mA for each transducer. The time drift of current: change in current $\Delta I \leqslant 2$ μA over 4 hours; the temperature drift of current: $\Delta I \leqslant 1$ μA under normal temperature; and the rate of loading change α: $\alpha = \frac{\Delta I}{I} < 0.5 \times 10^{-4}$ when loading changes ±100 percent. Hence it can be assured that the transducer can operate steadily within a technical range.

2. Automatic Gathering and Data Processing Section

Centering around the microcomputer TP 801, this equipment has such peripheral devices as the PF3 multichannel digital voltmeter, I/O interface circuit, TP 801P miniprinter and other auxiliary circuits.

a. Automatic Data Gathering and A/D Conversion

The transducer converts tested pressure into a simulated voltage signal and hence an A/D conversion link is needed. We employ the PF3 multichannel digital voltmeter which is already available in our laboratory to realize the A/D conversion for the automatic gathering of data. One round-trip detection can be performed in a given data collection time using the working format of single-scanning detection. This can indicate automatically the sequence number of the testing point, tested voltage and voltage polarity, unit and decimal point and so on. In addition, outputting a binary-coded decimal (BCD), it is connected to a TP 801 microcomputer via the I/O interface circuit to be used in data processing.

b. Current-level Conversion Circuit

The signal high-current level of a PF3 multichannel digital voltmeter is around 10 V while that of the I/O interface circuit is around 5 V. Therefore, we employ the method of voltage dispersion using impedance to realize a voltage conversion.

c. I/O Interface Circuit

We use parallel I/O interface chip Z80-PIO because the microcomputer cannot communicate directly with peripheral devices. It has two 8-bit I/O's and can be made into input or output interfaces using the I/O routine. Through this the microcomputer can be connected to the peripheral devices.

d. Alarm Display

The pressure-measuring limit of the transducer is ±100mmH_2O. The transducer could be damaged if such limit is exceeded. Our equipment is therefore equipped with two alarm displays (light-emitted diodes) as alarm indicators to warn the operator.

e. Automatic Processing of Data

Results are computed by a TP 801 microcomputer according to the software requirement and are transferred to a TP 801P miniprinter to be printed.

III. Software

We construct the following program with respect to software:

1. Monitor and Control Program (Figure 2)

The keyboard is managed using the key-scanning method to execute various operations and display functions to serve man-machine interaction. The design is based on the following requirement: When the machine is started, the interface PIO should be initialized, and the storage and various data space of the PIO has to be allocated, thus allowing the various data entry of the PIO to perform according to the required working format. The PIO is allowed to be interrupted only when the allocation is completed, and the various monitoring and controlling functions of the TP 801 microcomputer are to be kept. The monitor control program is a cycling routine. When data are input from the data collection section, the PIO temporarily interrupts the cycling of the monitor/control program using the interrupt format$_2$ to go into the computing procedure and the printing procedure, and then after the execution, it automatically returns to where the monitor/control procedure is interrupted to resume the processing.

2. Service Interrupt Program (Figure 3)

During the time the PF3 multichannel digital voltmeter performs single-scan data collecting on the 20 pressure points to be measured, each time when a set of data is gathered, the printing instruction signal sends a pulse signal to the PIO to cause interruption in the PIO to go into the service interrupt procedure.

3. Computation Procedure (Figure 4)

In order to enhance precision in computation and to avoid data overflow, floating-point computing is employed, and as many subroutines are used as can be found in the existing subroutine library. We elect to use the TP-SLIB-A subroutine library, and the entire computation procedure is carried out around the subroutines found in this library. The existing available subroutine library is also used in the conversion of codes. They are: DTOBF$_4$, FMULT$_2$, FADD$_4$, SINSUB, COSSUB, and so on. Figure 4 represents the computation procedure from the computing equations of pressure distribution, lift and drag for a dual wing. The equations are as follows:

$$F_x = \sum_{i=1}^{20} \frac{1}{2} \; (p_i + p_{i-1}) \times (y_i - Y_{i-1})$$

$$F_y = -\sum_{i=1}^{20} \frac{1}{2} \; (p_i + p_{i-1}) \times (x_i - x_{i-1})$$

$$L = F_y \cos\alpha - F_x \sin\alpha$$

$$D = F_y \sin\alpha + F_x \cos\alpha$$

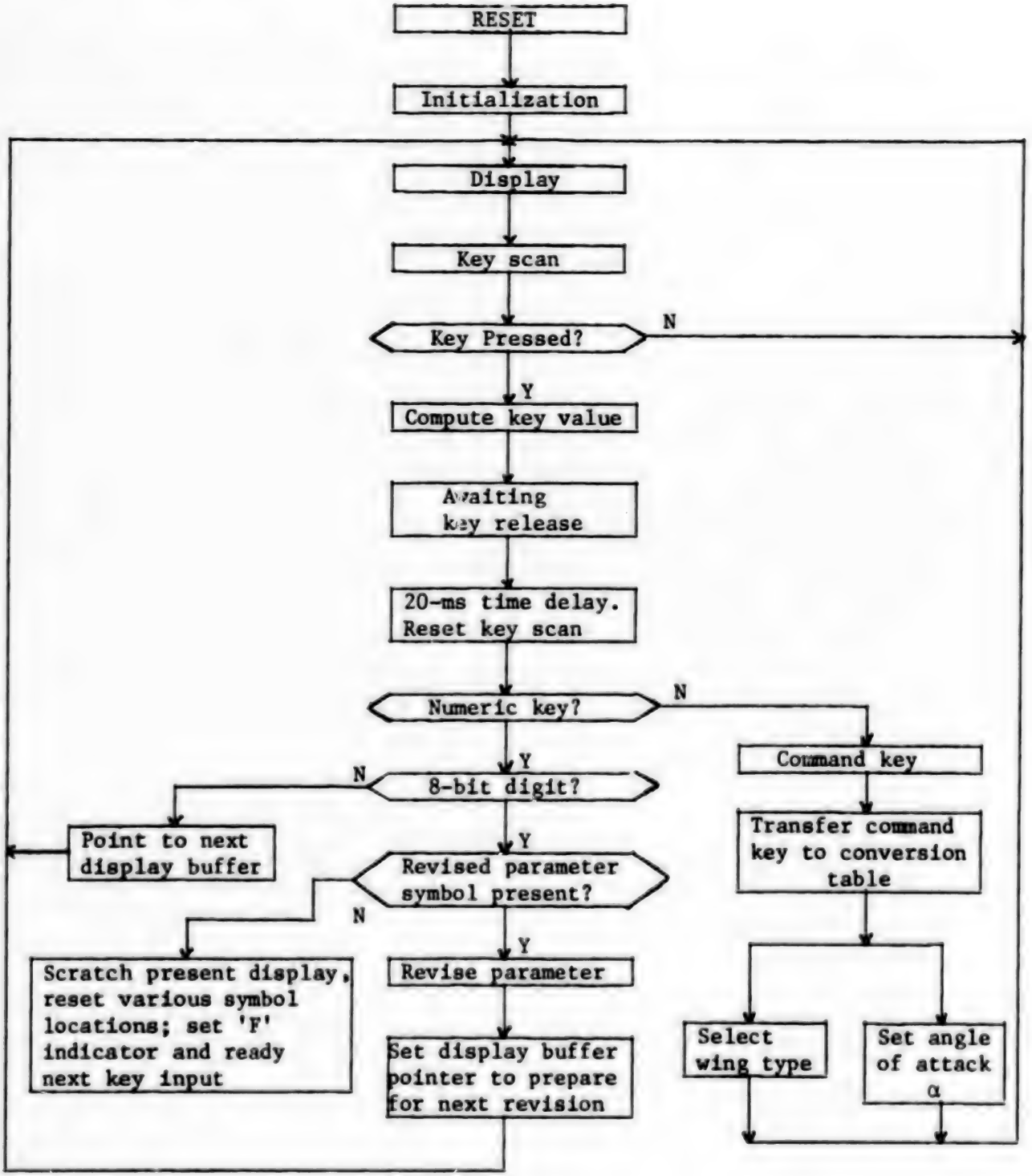
RESET
Initialization
Display
Key scan
Key Pressed?
N
Y
Compute key value
Awaiting key release
20-ms time delay. Reset key scan
Numeric key?
N
Y
Command key
8-bit digit?
N
Y
Point to next display buffer
Revised parameter symbol present?
Transfer command key to conversion table
N
Y
Scratch present display, reset various symbol locations; set 'F' indicator and ready next key input
Revise parameter
Set display buffer pointer to prepare for next revision
Select wing type
Set angle of attack α

Figure 2.

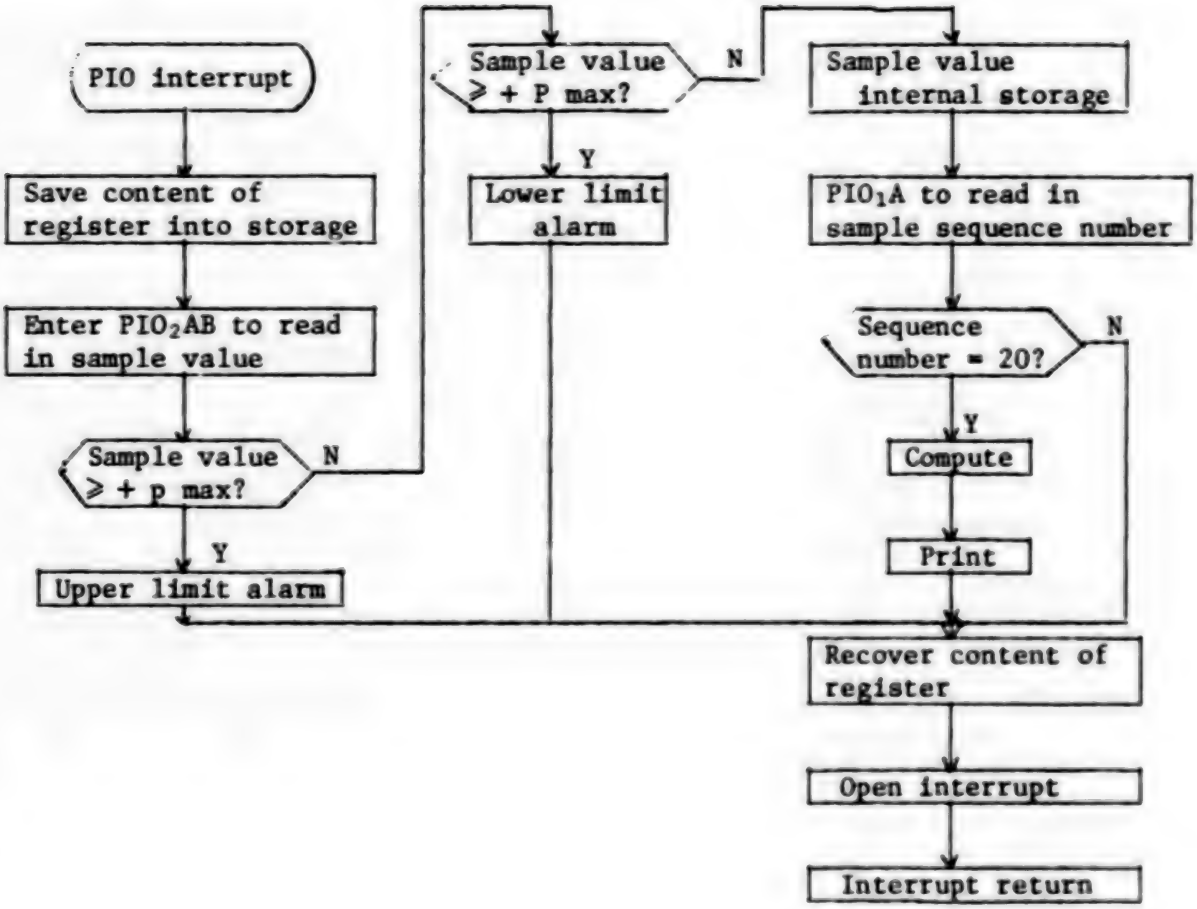
PIO interrupt
Save content of register into storage
Enter PIO2AB to read in sample value
Sample value ⩾ + p max?
N
Y
Upper limit alarm
Sample value ⩾ + P max?
N
Y
Lower limit alarm
Sample value internal storage
PIO1A to read in sample sequence number
Sequence number = 20?
N
Y
Compute
Print
Recover content of register
Open interrupt
Interrupt return

Figure 3.

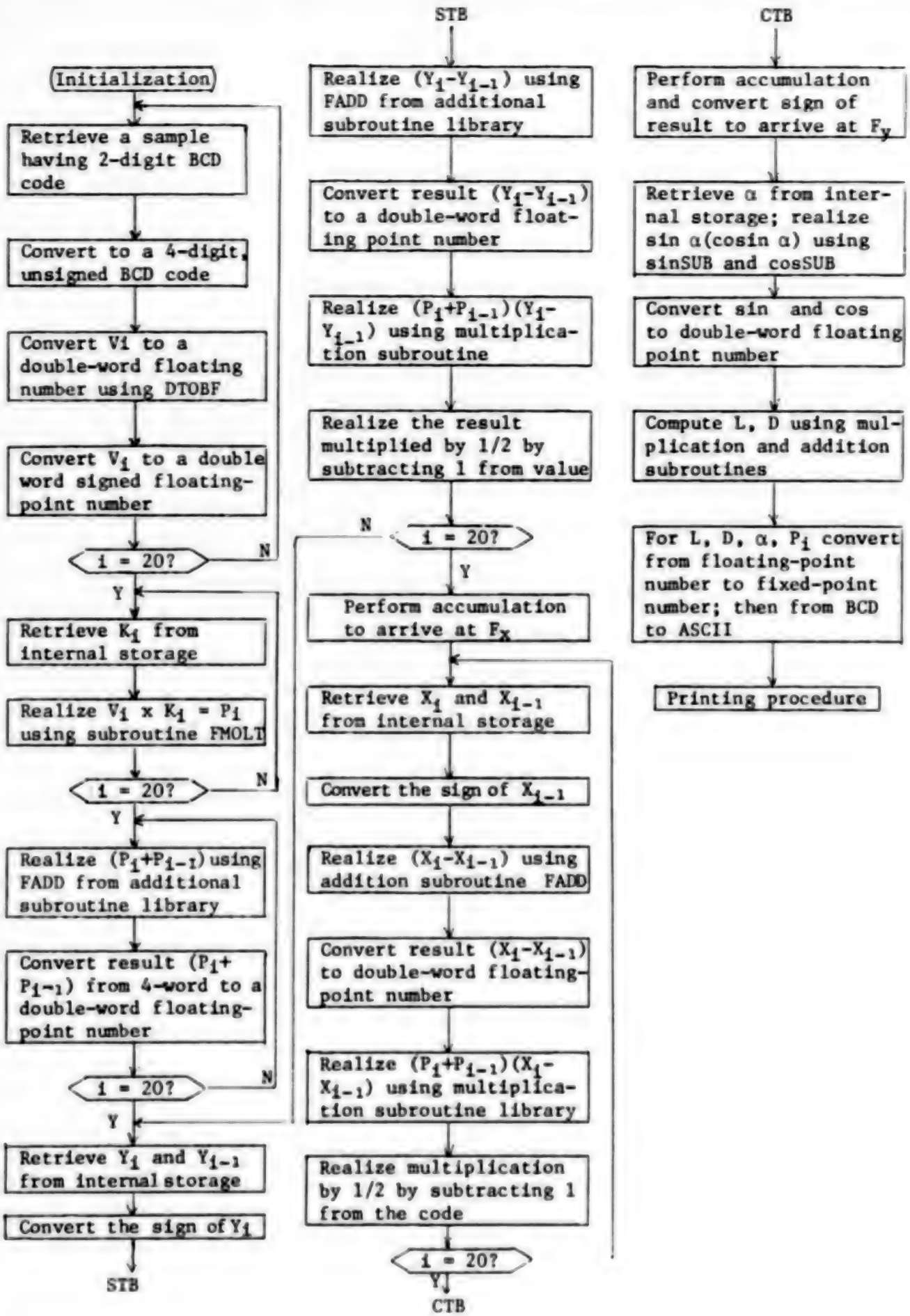
Initialization
Retrieve a sample having 2-digit BCD code
Convert to a 4-digit, unsigned BCD code
Convert Vi to a double-word floating number using DTOBF
Convert V_i to a double word signed floating-point number
i = 20?
N
Y
Retrieve K_i from internal storage
Realize $V_i \times K_i = P_i$ using subroutine FMOLT
i = 20?
N
Y
Realize (P_i+P_{i-1}) using FADD from additional subroutine library
Convert result (P_i+P_{i-1}) from 4-word to a double-word floating-point number
i = 20?
N
Y
Retrieve Y_i and Y_{i-1} from internal storage
Convert the sign of Y_i
STB
STB
Realize (Y_i-Y_{i-1}) using FADD from additional subroutine library
Convert result (Y_i-Y_{i-1}) to a double-word floating point number
Realize $(P_i+P_{i-1})(Y_i-Y_{i-1})$ using multiplication subroutine
Realize the result multiplied by 1/2 by subtracting 1 from value
N
i = 20?
Y
Perform accumulation to arrive at F_X
Retrieve X_i and X_{i-1} from internal storage
Convert the sign of X_{i-1}
Realize (X_i-X_{i-1}) using addition subroutine FADD
Convert result (X_i-X_{i-1}) to double-word floating-point number
Realize $(P_i+P_{i-1})(X_i-X_{i-1})$ using multiplication subroutine library
Realize multiplication by 1/2 by subtracting 1 from the code
i = 20?
Y
CTB
CTB
Perform accumulation and convert sign of result to arrive at F_y
Retrieve α from internal storage; realize sin α(cosin α) using sinSUB and cosSUB
Convert sin and cos to double-word floating point number
Compute L, D using multiplication and addition subroutines
For L, D, α, P_i convert from floating-point number to fixed-point number; then from BCD to ASCII
Printing procedure

Figure 4.

where P_i is the pressure of the i^{th} measuring point;
x_i and Y_i are the coordinates of the i^{th} measuring point; and
α is the angle of attack.

4. Printing Procedure

The printing procedure is carried out using a TP 801P miniprinter.

IV. Application Example

Figure 5 represents the relational curve of wing lift, drag and angle of attack graphed from the printed data. The curve can be printed directly if a TP 803 microcomputer and its associated full-width printer are used. With some modifications, this equipment can be utilized in experiment, which is to determine the velocity distribution in a fluid field.

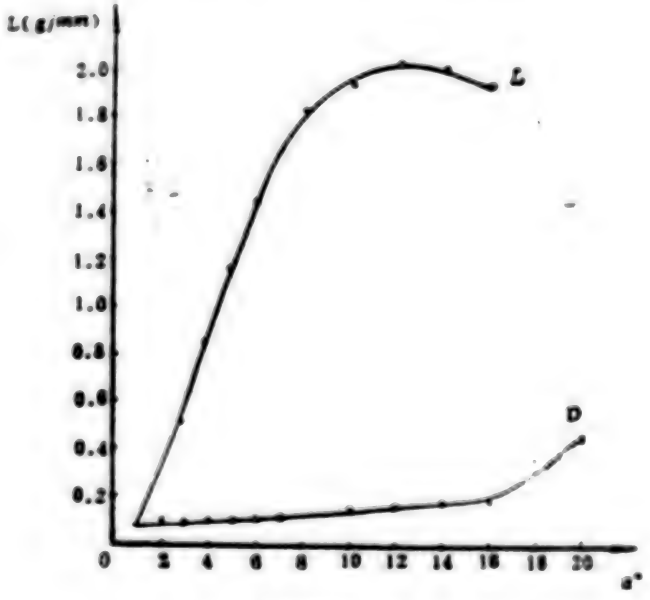

Figure 5.

Quality Comparison on Several Experimental Equipments

Name	Collection speed	Reading precision	Differentiating rate	Measure range	Measure speed
Photographics	1—3 minutes	approx. 2%	1mmH$_2$O	1~100 (mmH$_2$O)	Several days
Supersonic automatic gathering equipment	12—40 seconds	approx. 1%	0.1 (mmH$_2$O)	0.1~21500 -(mmH$_2$O)	Several tens of minutes
Transducer automatic gathering equipment and processing	2—10 seconds	approx. 0.8%	0.01 (mmH$_2$O)	-100~+100 (mmH$_2$O)	Several minutes

Appreciation is extended to Comrades Xue Fongwen and Hou Zhiyong, students at the Electronics University of Tianjin Automation Panel Company, who participated in this project.

BIBLIOGRAPHY

1. "Z80 Language Assembler Design," edited by the Chongqing Branch of the China Scientific and Technical Information Research Center and published by the Chongqing Branch of the Scientific and Technical Documents Press, August 1981.

2. Zhou Mingde, "Hardware and Software of Microcomputers and Their Applications," published by Qinghua University Press, October 1982.

3. "Microcomputers," edited by the Automation Panel Research Section of the Tianjin University Automation Department, 1982.

4. "TP 801-Z80 Microcomputer Operations Manual," edited by the Electronics Plant of Beijing Industrial University, June 1982.

5. "TP 804 Miniprinter Operating Instructions," edited by the Electronics Plant of Beijing Industrial University, June 1982.

13042
CSO: 4008/1076

APPLIED SCIENCES

THERMAL CONDUCTIVITY OF POLYURETHANE FOAM AT LOW TEMPERATURE

Beijing YUHANG XUEBAO [JOURNAL OF THE CHINESE SOCIETY OF ASTRONAUTICS] in Chinese No 2, 30 Apr 84 pp 54-65

[Article by Zhu Xian [2612 6343], Ji Yongfu [0370 0516 1133], Bai Pinxian [4101 0756 6343] and Han Yuanzhou [7281 3293 3166]]

[Text] Abstract: The heat-insulation mechanism of polyurethane foam is investigated. The relationship between the low-temperature thermal conductivity and certain parameters which can easily be measured at room temperature (such as density, fraction of closed cells, average cell diameter, and aging time, etc.) is determined. Calculations of the effective thermal conductivity based on room-temperature measurements and an analytical computational model yield results in agreement with experimental findings.

I. Introduction

The specific application to a great extent determines the choice of the insulation to be used. Although all porous insulating materials are clearly superior as heat insulators to materials without pores, other considerations, such as weight, resistance to shock and vibration, ease of protection, cost, etc., may militate against their selection. As a result, many low-temperature systems (particularly in large-scale equipment) do not employ vacuum thermal insulation. Polyurethane foam is a rigid plastic which is light-weight and has a high strength-to-mass ratio, a relatively low thermal conductivity at low temperatures, and other advantages. It is widely employed in ships for transporting liquefied natural gas, to insulate the hydroxide fuel chamber of rocket thrust engines, and in other large-scale equipment operating at low temperatures.

In general, the performance of foam plastics is closely related to the composition of the foam and the method of fabrication. Its effectiveness as a low-temperature insulator depends in a complicated way on several mutually interrelated parameters such as the density, fraction of closed cells, average cell diameter, etc. The latter parameters are readily measurable at room temperature, and if their relationship to the thermal conductivity can be

established experimentally and/or by theoretical analysis, it might be possible to find a reliable method for developing materials whose low-temperature. In addition to providing an easier method of quality control, this would also provide a foundation for developing industrial processes to manufacture better foam plastics. The present paper discusses more preliminary results of our research in this area.

II. Heat-insulation Mechanism of Polyurethane Foam

Virtually all of the foam plastics used as low-temperature insulators are rigid and contain closed cells--they are composed of gas-filled pores separated by solid resinous walls. The "closed cells" differ both from the gas-filled pores and from the external medium.

The following three factors limit the heat conduction through solid polyurethane foam to relatively low levels:

(1) The resinous walls in the polyurethane are highly disordered and amorphous (noncrystalline). This type of molecular structure insures that the thermal conductivity drops almost linearly with temperature (phonons also contribute to the heat conduction at very low temperatures).

(2) Low-density bubble foams expand laterally after fabrication, which greatly decreases the fraction of the total volume occupied by the solid heat-conducting (wall) material.

(3) In addition, the foaming process also introduces a "spatial exclusion factor" that further decreases the conductivity due to the solid component. As shown in Figure 1, the closed cells in polyurethane foam have a polygonal structure which causes them to conduct heat less effectively.

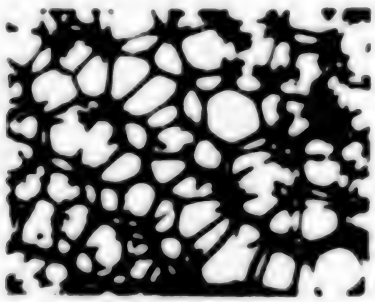

Figure 1a. Photomicrograph Taken Normal to the Direction of Bubble Formation

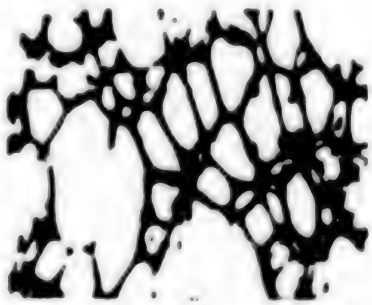

Figure 1b. Photomicrograph Taken Parallel to the Direction of Bubble Growth

The above discussion can be summarized by the equation

$$K_s = \phi V_s K_{resin} / V_{tot} \qquad (1)$$

for the thermal conductivity of the solid polyurethane foam material. Here K_{resin} is the thermal conductivity of the polyurethane resin; V_s is the volume of foam occupied by the cells, and V_{tot} is the total volume of the foam (the ratio V_s/V_{tot} is also equal to the ratio ρ_{foam}/ρ_{resin} where ρ_{foam} and ρ_{resin} are the densities of the foam and resin, respectively); ϕ is the spatial exclusion factor. Analysis of photomicrographs of the foams revealed that ϕ had the values $\phi_{\parallel} = 0.8$ and $\phi_{\perp} = 0.6$ along and transverse to the direction of bubble growth. The value of ϕ along other directions lies between these two extremes.

If we use the value $\rho_{resin} = 1{,}170$ kg/m^3 given by J. Navickas, et al.,[1] for the density of polyurethane resin, we find that $K_s = 0.8 \cdot (40/1{,}170) \cdot K_{resin} = 0.027\, K_{resin}$ if we take $\rho_{foam} = 40$ kg/m^3 and assume that heat conduction in the polyurethane foam occurs parallel to the direction of bubble growth. This result indicates that the bubble conductivity is just 2.7 percent of the value for the resin, so that the solid-state thermal conductivity of polyurethane foam is relatively low.

Although bubble formation substantially decreases both the thermal conductivity of the solid foam and the weight of the insulating foam layers, it also introduces heat-conducting gas inclusions and promotes radiative conduction. However, the following three factors insure that the gas conductivity K_g is very small compared to the conductivity K_{resin} of the excluded resin.

1. The gas conducts heat less efficiently because the pockets of gas phase trapped in the closed cells are not continuously distributed.
R.E. Skochdopole[2] has shown that convective heat transfer is negligible for cell diameters less than 3-4 mm. Since most insulating polyurethane foams have cell diameters of the order of 10^{-1}mm, convective heat transfer between the gas and the solid phases can be completely neglected, provided there are no cracks in the insulating foam layer and the volume fraction of closed cells is high.

2. The nonconvective heat transfer in the gas is to a great extent determined by the relative magnitudes of the mean free path λ of the gas molecules and the distance L between the cold and hot walls. As shown in Figure 2, if λ is much less than L the gas lies in the continuous conduction region in which the conductivity depends only on temperature, not on the pressure p. Indeed, according to molecular gasdynamic theory the conductivity in this region is given by the formula

$$K_g = \frac{1}{3} M\lambda n\bar{v}c_v \qquad (2)$$

where K_g is the thermal conductivity of the gas; M and λ are the molecular weight and mean free path of the gas; $\bar{v}$ is the average velocity of the gas molecules; c_v and n are the constant-volume specific heat of the gas and the number of gas molecules per 1 cm^3, respectively. Since n is proportional to the pressure p while the mean free path λ is proportional to 1/p, K_g is independent of p.

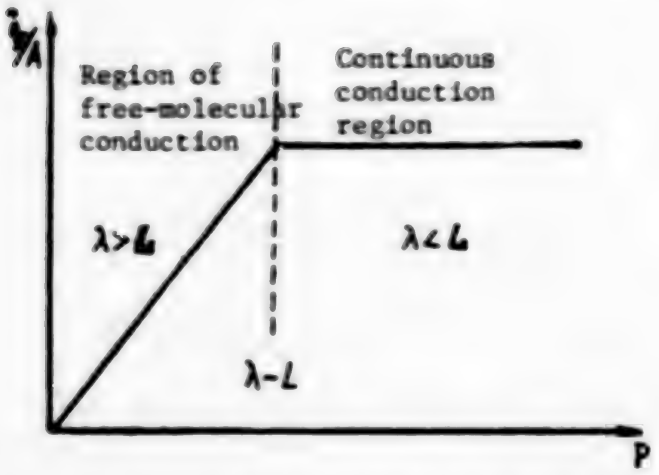

Figure 2. Thermal Conductivity of Gas Molecules

On the other hand, when λ is greater than the distance L between the cold and hot walls we have the free-molecular heat conduction regime, just as for the case of vacuum insulation, and K_g now drops linearly to very low values as p decreases. Since K_g can be neglected in practice under these conditions, in order to achieve good insulating properties one must clearly strive to insure that the free-molecular conduction regime holds in the gas. Since the mean free path of the gas molecules is given by

$$\lambda = 8.6 \times 10^{3} \frac{\eta}{p} \sqrt{\frac{T}{M}} \qquad (3)$$

it is completely determined for a specified temperature and pressure. (Here the viscosity coefficient η of the gas has been tabulated as a function of p and T for various gases.) Thus, the only way to force the gas into the free-molecular conduction regime is to decrease L. Small cells produced by pore formation are ideally suited for this purpose. If we assume an insulating layer thickness of 20 mm and a cell diameter of ~0.2 mm, we see by calculation that the cells can decrease the distance L from between the hot and cold walls by a factor of 100 or more. The effect of this is to insure free-molecular conduction even at relatively high pressures, so that K_g can be neglected. This neglect is particularly well justified when cryopumps evacuate th[illegible] from closed cells that lie within a certain distance from the cold s[illegible] (in this case the cells near the surface contain no gas at all).

3. Even close to the hot surface, the gas conductivity K_g is still much less than the conductivity K_{resin} of the solid polyurethane resin, which is equal to 1.32mW/cm·K at room temperature. By comparison, the room-temperature conductivity of Freon-11 is equal to 0.082 mW/cm·K, or just 6 percent of K_{resin} (Freon-11 can be used to fill the pores formed by the inflating agent). Even if the insulation ages and air (a relatively good conductor) seeps into the cells, the conductivity of air is still only 0.26 mW/cm·K, or just 20 percent of K_{resin}.

Finally, M.B. Hammond, Jr.,[3] has calculated the radiative heat transfer between the cell walls in the foam and found that it is also quite small; moreover, it drops very rapidly as T decreases. Polyurethane foam is thus well suited for use as a low-temperature insulator.

III. Experimental Results

1. Relation Between the Density and the Low-temperature Thermal Conductivity of Polyurethane Foam

In order to clarify the relationship between the low-temperature thermal conductivity and the density of polyurethane foam, we measured the conductivity of two series of foams, each consisting of eight samples of different densities. The measurements were made by using a flat-panel low-temperature conductometer which we built ourselves.[4] The temperature ranged from 20 to 320 K. Because the foam conductivity K_{foam} depends on several parameters simultaneously, in order to measure the effects of density on the thermal conductivity one must insure that the other parameters are kept as constant as possible. For this reason the experimental samples were very carefully controlled. The following five factors cannot be neglected.

(1) Directional and positional effects:

The foaming process generates different internal and external stresses on the pores parallel and transverse to the direction of growth. As a result, the foam cells are pulled along the direction of growth (see Figure 1), which gives rise to anomalous thermophysical and mechanical properties of the foam. In order to eliminate these directional effects one must generally sample the foams both parallel and normal to the growth direction and compare only results measured along the same direction. In practice, however, it is not enough to carefully control the direction of sampling. Figure 3 [Reference 5] shows that according to the narrow open-hole model, the growth direction often has the form of eddy current lines when the foaming agent is poured. Samples with longitudinal or transverse growth directions can be obtained only inside the dotted rectangle; elsewhere, the growth directions will deviate to varying degrees. The difference in the growth directions is one of the factors principally responsible for the divergence in the data on foam materials.

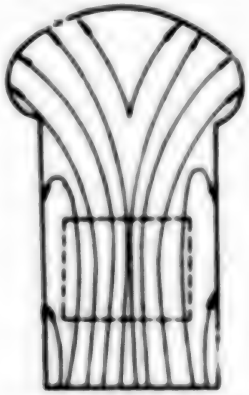

Figure 3. Pattern of Growth Directions in Different Portions of a Foam

(2) Aging effects:

The thermal conductivity of polyurethane foams varies with time. The conductivity is quite low for new foams but increases with time; this process is referred to as aging. The different degrees of aging of samples is another important factor behind the scatter in the thermal conductivity data.

(3) The relative number of closed cells N_{cc} has a decisive influence on K_{foam}. Figure 4 plots the dependence $K_{foam}(N_{cc})$ for polyurethane. The fraction N_{cc} influences K_{foam} by the following three mechanisms:

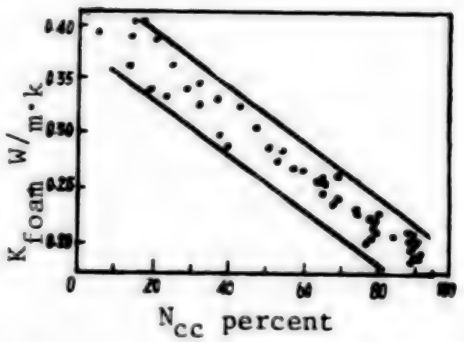

Figure 4. Thermal Conductivity at Room Temperature as a Function of the Relative Percentage N_{cc} of Closed Cells

(a) The closed cells are filled with Freon-11, which has a low thermal conductivity; by contrast, the open cells contain air, which conducts heat well.

(b) Because open cells tend to make the gaseous phase more continuous, they increase the distance L between the cold and hot wall surfaces, thereby taking the gas into the region of continuous conduction (Figure 2). In addition, they can also give rise to very large convective heat transfer.

(c) As the temperature drops, K_{foam} becomes much more sensitive to N_{cc}. If N_{cc} is large and a cryopump is used, the cells are evacuated and the thermal conductivity drops abruptly. By contrast, the opposite situation obtains if N_{cc} is small (so that most of the cells are open). Atmospheric air continually enters the foam, and the ongoing phase transitions (liquefaction, solidification) evolve a large amount of latent heat which is directly absorbed by the cold liquid in the storage chamber, so that a great deal of vapor is generated. These effects will obscure the dependence of the thermal conductivity on the density unless the samples are chosen so that the relative number of closed cells V_{cc} is the same.

In summary, the above discussion shows that in order to experimentally measure the thermal conductivity of poured foams as a function of foam density, one must insure that the cell growth directions are the same and that the samples tested are at the same locations in the foam. Moreover, the foaming time and subsequent storage conditions must be the same (identical temperatures

and ambient atmospheric compositions), and the foams must also be sampled at equal distances from the surface. Finally, we used the apparatus[7] developed in our work to measure the fraction of closed cells V_{cc} and selected only samples for which V_{cc} was the same to within 3 percent.

(4) In order to assess the influence of the experimental conditions, we successively measured the thermal conductivity of polyurethane foams of various densities at liquid hydrogen and nitrogen temperatures and at the freezing point of water (T = 280 K). Figure 5 shows the results. We see that the dependence of the thermal conductivity K_{foam} on the density ρ_{foam} is qualitatively different at the different temperatures. For liquid hydrogen, the dependence $K_{foam}(\rho_{foam})$ is very simple--K_{foam} increases monotonically and linearly with ρ_{foam}. By contrast, the dependence is nonmonotonic at 280 K--K_{foam} at first decreases as ρ_{foam} rises and reaches a very low value at ρ_{foam} $\approx$ 52 kg/m^3, after which K_{foam} starts to increase with ρ_{foam}. The behavior of $K_{foam}(\rho_{foam})$ in liquid nitrogen (T = 85 K) is intermediate beteen these two extremes--K_{foam} increases monotonically but nonlinearly with ρ_{foam}.

(5) The method used to analyze the experimental results is also important. The thermal conductivity in foams is a sum of three components: K_g, K_s and K_{rad} which correspond to the thermal conductivity of the gas and solid phases, and to radiative heat transfer, respectively. All three mechanisms act simultaneously, and the apparent thermal conductivity measured experimentally is given by

$$K_{eff} = K_g + K_s + K_{rad} \qquad (4)$$

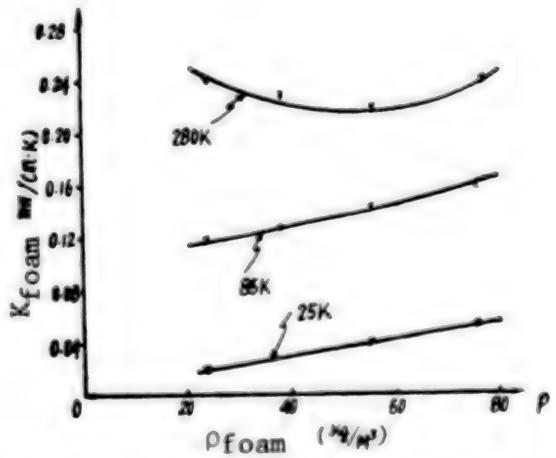

Figure 5. Foam Conductivity vs Foam Density at Three Different Temperatures

Calculations show that K_{rad} contributes appreciably to K_{foam} only at relatively high temperatures; as T drops, radiative heat transport in the foam falls off rapidly and generally becomes negligible even for T as large as $\simeq$ 230 K. In addition, K_g drops steadily as T decreases. Indeed, K_g actually vanishes because the cryopumps evacuate the gas from the cells. Consequently, the solid-state conductivity K_s dominates K_{eff} more as T decreases and this conduction

mechanism is effectively the only one for temperatures below 30 K. We thus have

$$K_{(LH_2)} = K_s = \phi \frac{\rho_{foam}}{\rho_{res}} K_{res} \propto \rho_{foam} \qquad (5)$$

where $K_{(LH_2)}$ is the thermal conductivity of the foam at liquid hydrogen temperature. Equation (5) shows that the thermal conductivity is directly proportional to the foam density at liquid hydrogen temperatures.

On the other hand, all three conduction mechanisms operate at 280 K, and the dependence $K_{foam}(\rho_{foam})$ becomes much more complicated. Although K_g continues to drop linearly with T just as before, the cell diameters increase, so that K_g and K_{rad} both increase. When the cell diameters reach a certain value, the increase in K_g and K_{rad} more than offsets the drop in K_g, so that there is a net increase in K_{eff} for polyurethane foam as T decreases. Thus, the density ρ_{foam} corresponding to a critical cell diameter will depend on the thickness of the cell walls, which in turn depends on how the foam is made.

The behavior at liquid nitrogen temperature is approximately intermediate between that observed at 280 K and at liquid hydrogen temperature.

Figure 6 shows how the thermal conductivity K_{foam} of polyurethane foam depends on temperature for two different foam densities. This type of representation yields information on the influence of density on K_{foam} for an entire range of temperatures and is more useful in practical applications.

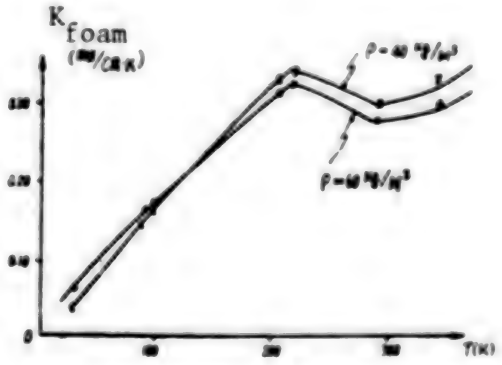

Figure 6. Temperature Curves of the Thermal Conductivity for Foams With Different Densities

2. Influence of Aging Time on the Thermal Conductivity of Polyurethane Foam

Gas occupies more than 95 percent of the total volume of the foam materials in common use. Since gas-phase conduction dominates the other mechanisms for a very wide range of temperatures, any change in the composition of the gas contained in the foam cells will appreciably alter the apparent thermal

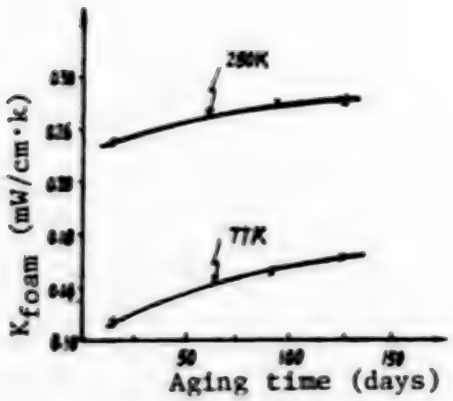

Figure 7. Effects of Aging on the Conductivity of a Polyurethane Foam

conductivity. The cells in freshly prepared foams are filled with Freon-11 or carbon dioxide, which have low thermal conductivities. If atmospheric air or some other ambient gas with high thermal conductivity diffuses into the cells, the apparent conductivity will tend to increase with time. Figure 7 shows our measurements on the effects of aging on a polyurethane foam (the sample was a poured foam of density 58 kg/m^3, the foaming agent was Freon-11, and the sample was 2.5 cm thick). The foam was aged by exposing it to air at room temperature.

Examination of Figure 7 leads to the following conclusions:

1) Aging appreciably increases the apparent thermal conductivity of the foam. The foams were aged for between 15 and 126 days, after which we measured the apparent conductivity K_{foam} at T = 77 K; K_{foam} was found to increase by more than 50 percent.

2) The amount by which aging increases K_{foam} is related to the temperature. If the aging period is relatively short, K_{foam} does not significantly increase at room temperature; however, it rises very substantially for low temperatures (below 77 K). It is therefore particularly important to ascertain how aging degrades the performance of foams in low-temperature applications.

3) Aging also gives rise to breaks in the dependence $K_{foam}(T)$ for polyurethane foam of the type shown in Figure 6. Because of the aging, the heat-conducting gas in the cells actually consists of a mixture of Freon-11 and atmospheric air. The thermal conductivity $K_{mixture}$ of the mixture can be calculated by the formula[8]

$$K_{mixture} = 0.5\,(K_\alpha + K_\beta)$$

$$K_\alpha = \sum_{i=1}^{n} m_i K_i \qquad (6)$$

$$\frac{1}{K_\beta} = \sum_{i=1}^{n} \frac{m_i}{K_i}$$

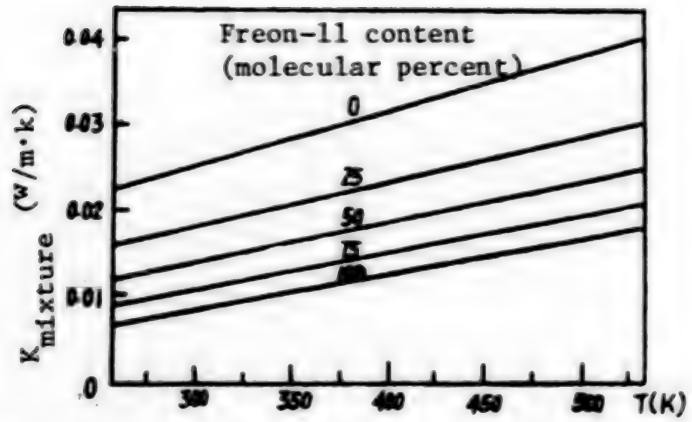

Figure 8. Themal Conductivity as a Function of Temperature for Several Air + Freon-11 Mixtures

where K_i is the thermal conductivity of each gas component present in the mixture; m_i is the gram-molecular weight of the i-th gas component in the mixture; n is the total number of components. The thermal conductivity of the gas mixture is very sensitive to the relative composition of the mixture. Figure 8 shows curves $K_{foam}(T)$ calculated using Equation (6) for several Freon-11 + air mixtures of different relative compositions. If we assume a 1:1 mixture by molecular weight, we see that $K_{mixture}$ drops with decreasing T as shown by the curve in Figure 8 labeled by 50, the constant relative Freon-11 content in percent; the decrease continues down to the condensation point of Freon-11. For lower Freon-11 contents, more air is present and the conductivity of the mixture is higher, as shown in Figure 8, even though the number of molecules in the gas also decreases with the Freon content. This is responsible for the breaks in the curves in Figure 6. As the temperature drops and the Freon-11 condenses, the thermal conductivity increases until air is the only gaseous component remaining in the cells, and only then does K decrease as T drops further.

The above analysis also explains why the effects of low-temperature aging are more pronounced than at room temperature. Indeed, Freon-11 condenses at relatively high temperatures, so that air is the only remaining gaseous component contributing the thermal conductivity; the thermal conductivity of the mixture is therefore described by the top curve in Figure 8 [Reference 8] and is much higher than if no air had mixed with the Freon-11. By contrast, at room temperature none of the Freon has condensed and the conductivity is therefore described by one of the lower curves corresponding to the actual Freon content. If the aging period is short, so that relatively little air has leaked in, the thermal conductivity is essentially given by the lowest (100 percent Freon) curve in Figure 8, and the relative increase is very small.

IV. Analytical Model

1. Brief Description

Because of difficulties caused by the evolution of latent heat of phase transition when large quantities of air are present at low temperatures, it is quite difficult to develop a model for analyzing the thermal conductivity of foams that contain open cells in contact with atmospheric air. Fortunately, in actual experiments the foams are contained in hermetically sealed layers which protect them from atmospheric air (for example, thin-film air-tight seals may be used). The analytical model described below is valid only for hermetically sealed foams.

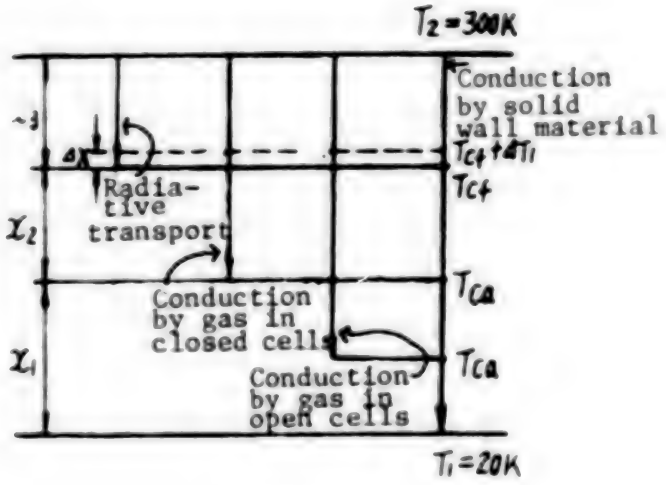

Figure 9.

Figure 9 schematically shows the insulating layers used in a vessel containing liquid hydrogen. All of the heat conduction mechanisms occur simultaneously on the face at room temperature--that is, it is not possible to neglect either the radiative heat transfer or heat conduction across the solid cell walls, through the gas in the open cells, or in the air + Freon-11 mixture in the closed cells. We will refer to this conduction region as region I. Region I continues until $T = T_{cf}$, at which Freon-11 "condenses." Region II begins for $T < T_{cf}$; here only the solid wall material and the air in the closed and open cells contribute to the heat transfer, and this situation persists until T reaches $T_{ca\ closed}$, at which the air in the closed cells "condenses." Region III begins for $T < T_{ca\ closed}$; here the air is in the free-molecular region (Figure 1) and its thermal conductivity is negligible. The heat conduction is due entirely to the air in the open cells and to the thermal conductivity of the solid cell walls. Region III continues until T reaches $T_{ca\ open}$, at which the air in the open cells "condenses" and region IV begins. Thereafter, heat transfer is due entirely to conduction in the solid walls. Here by the "condensation" temperature we mean the temperature at which the mean free path λ of the gas molecules becomes greater than the distance L between the cold and the hot walls. For this reason, the "condensation" temperatures for

the air inside the open and closed cells are not the same, because L is much greater for the open cells.

In order to find the average total effective thermal conductivity $\bar{K}_{eff}$ we need only calculate the contributions from each conduction mechanism and take the sum, i.e.,

$$K_{eff} = K_s + K_g + K_{rad} \tag{7}$$

In what follows we will calculate the contribution from each heat conduction mechanism.

2. Contribution From Solid Wall Material

As we have described above, the conductivity of the solid wall material is given by $K_s = \phi V_s/V_{tot} \cdot K_{resin}$; the average thermal conductivity for temperature between T_1 and T_2 is therefore equal to

$$K_s = \frac{\phi V_s/V_{tot} \int_{T_1}^{T_2} K_{resin}\, dT}{T_2 - T_1} \tag{8}$$

3. Radiative Contribution

It is an extremely complicated matter to calculate radiative heat transfer within the solid material because transmission, absorption, and radiation all occur simultaneously. Essenhigh[9] has proposed a method for calculating radiative heat transfer in solids which is based on measuring the "relative absorptivity" E. Using his method, we get the expression

$$K_{rad} = \frac{\int_{T_{cf}}^{T_2} 4\sigma T^3 dT}{(T_2 - T_1)\, E} \tag{9}$$

for calculating the radiative contribution to the effective thermal conductivity of foam materials. Here σ is the Stefan-Boltzmann constant and E is the experimental value of the relative absorptivity. For polyurethane foams of density 32, 48 and 59 kg/m^3 and cells of diameter ~0.2 mm, E is approximately equal to 9.6, 14.4 and 17.7/cm, respectively.

4. Gas Contribution

The average thermal conductivity can be deduced from Figure 9:

$$K_g = \frac{\int_{T_{ca\,open}}^{T^2} V_{open}/V_{tot} K_{air}\, dT}{T_2 - T_1} + \frac{\int_{T_{ca\,closed}}^{T_{cf}} V_{closed}/V_{tot} K_{air}\, dT}{T_2 - T_1} + \frac{\int_{T_{cf}}^{T^2} V_{closed}/V_{tot} K_{mixture}\, dT}{T_2 - T_1} \tag{10}$$

where V_{open}/V_{tot} and V_{closed}/V_{tot} are the volume ratios of the open and closed cells relative to the total volume, respectively; they can be calculated from experimental measurements of the relative number of closed cells and the average cell volume.[7] The first two integrals in (10) can be calculated without difficulty, and data have been published[10] of the thermal conductivity K_{air} of air as a function of temperature within the continuous conduction region (Figure 1). The limits of integration are as follows: T_2 is the temperature of the warm surface of the thermal insulation and may be taken equal to 300 K; T_{cf} and $T_{ca\ closed}$ are the "condensation" temperatures of the Freon-11 and the air inside the closed cells, respectively; $T_{ca\ open}$ is the "condensation" temperature of air in the open cells. These temperatures can be determined by the following method:

T_{cf}: The Freon-11 pressure in the closed cells immediately after formation is approximately equal to 600 torr at room temperature. Because Freon-11 permeates the polyurethane cell walls only very slowly, the Freon pressure in the closed cells remains constant over long times. As the temperature decreases, the partial pressure of the Freon-11 varies as described by the ideal gas law until the condensation point is reached; this occurs when the constant-volume curve for the ideal gas intersects the saturated vapor pressure curve for Freon-11. For T below the condensation point, the decreasing pressure follows the saturated vapor pressure curve; at T = 230 K, $P_f \simeq 30$ torr. Because the partial pressure of the air at this temperature is generally very high, the contribution from the Freon pressure p_f is negligible by comparison, so that we may take the lower limit T_{cf} equal to 230 K.

$T_{ca\ closed}$: We can find $T_{ca\ closed}$ by following the vapor saturation pressure curve in air, measuring the temperature T and pressure p at the corresponding points, and using the tables in [10] to find the viscosity η corresponding to these T, p. Equation (3) can then be used to calculate the corresponding molecular mean free path λ. We find the temperature at which $\lambda \sim L$ by comparing λ with the distance L between the cold and hot walls of the foam cell (we have $L \simeq 2 \times 10^{-2}$ cm for closed cells in polyurethane foam). This temperature is equal to $T_{ca\ closed}$, the "condensation" point of the air inside the closed cells. Using the above procedure, we found the values $T_{ca\ closed} = 50$ K, $p \simeq 0.7$ torr, $\lambda \simeq 2 \times 10^{-2}$cm. These values are such that the air in the closed cells lies in the free-molecular conduction regime, so that the thermal conductivity is negligible.

$T_{ca\ open}$: The procedure here is the same as for $T_{ca\ closed}$, except that we take L to be equal to one-half the full thickness of the thermally insulating layer rather than the average cell diameter of the foam. Thus, $L \simeq 1.25$ cm. The calculated results indicate that the gas in the open pores enters the region of free-molecular conduction only when T = 28 K, $p \simeq 10^{-5}$ torr.

It is rather difficult to evaluate the third integral $\int_{T_{cf}}^{T_2} V_{closed}/V_{tot} \cdot K_{mixture}\, dT$ in Equation (10), partly because both air and Freon-11 are present in the closed cells for T between T_{cf} and T_2, and partly because their relative density distribution varies with storage time and distance from the surface of the foam. It is therefore necessary to express the

thermal conductivity $K_{mixture}$ of the Freon + air mixture directly as a function of temperature. The following complicated sequence of steps is required in order to do this:

(a) The data provided by R.A. Stengard in "New Information About Urethane Foam" can be used to find D_{film}, the diffusion coefficient for air across a polyurethane film.

(b) Following the method developed by J. Navickas, et al.,[1] and using the formula

$$D_{foam}/D_{film} = \rho_{film}/F\rho_{foam} \tag{11}$$

one can deduce the diffusion coefficient D_{film} in the interior of the polyurethane foam from the diffusion coefficient D_{film} for the air inside the cell wall material. Here ρ_{film} and ρ_{foam} are the densities of the polyurethane resin and foam, respectively. The effective mass component F is equal to the mass resistance to the diffusion of air normal to the direction of diffusion. In general we may set F = 1/2.

(c) We next regard the foam material as a homogeneous medium and use Fick's law[12] for gas diffusion in homogeneous materials to calculate the partial pressure p_{air} of the air inside the insulating foam layer as a function of the time t and the distance x from the wall of the container.[3] We get the result

$$p_{air} = 1 - \frac{4}{\pi}\sum_{n=0}^{\infty}\frac{(-1)^n}{2n+1}e^{-D_{foam}(2n+1)^2\pi^2 t/\Delta l^2}\cos\frac{(2n+1)\pi x}{2l} \tag{12}$$

where ℓ is the thickness of the foam. Figure 10 (Reference 10) shows the results calculated using Equation (12) for a foam with ℓ = 2.55 cm and density ρ_{foam} = 52.8 kg/m^3.

(d) The rate of Freon-11 diffusion toward the outside of the cells is extremely slow compared to the rate of air diffusion into the cells. We therefore assume in the calculations that the Freon-11 partial pressure is essentially equal to the pressure just after foam formation (roughly 600 torr) for aging times that are not too long (e.g., between 2 and 3 years).

(e) The next step is to find the coordinate $x_1 + x_2$ corresponding to the lower limit T_{cf} of the integral. The point of departure is the formula[13]

$$Q = \bar{K}\frac{T_2 - T_1}{l} = \frac{1}{l}\int_{T_1}^{T_2} K_{(T)}dT \tag{13}$$

which describes the heat flux through a coarse-fine homogeneous rod of length ℓ whose two ends are at temperatures T_1 and T_2, respectively. Here $K_{(T)}$ and $\bar{K}$ are the differential thermal conductivity and the value of the conductivity averaged over T between T_1 and T_2, respectively. The equations

$$\dot{Q} = \bar{K}_{eff} \cdot \frac{T_2 - T_1}{\ell} \tag{14}$$

and

$$Q = \frac{1}{x_1 + x_2}\left[\int_{T_1}^{T_{cf}} \phi V_s/V_{tot} K_{resin} d_T + \int_{T_{ca\ open}}^{T_{cf}} V_{open}/V_{tot} K_{air} d_T + \right.$$

$$\left. \int_{T_{ca\ closed}}^{T_{cf}} V_{closed}/V_{tot} K_{air} d_T \right] \tag{15}$$

follow by applying Equation (13) to the entire heat-insulation layer and to the part with T between T_1 and T_{cf}. The requirement that the heat flux be continuous leads to the equation

$$x_1 + x_2 = \frac{\ell}{\bar{K}_{eff}(T_2 - T_1)} \left[\int_{T_1}^{T_{cf}} \phi V_s/V_{tot} K_{resin} d_T + \right.$$

$$\left. \int_{T_{ca\ open}}^{T_{cf}} V_{open}/V_{tot} K_{air} d_T + \int_{T_{ca\ closed}}^{T_{cf}} V_{closed}/V_{tot} K_{air} d_T \right] \tag{16}$$

Here $\bar{K}_{eff}$ may be taken equal to $\bar{K}_{eff0}$, the previously measured experimental value.

(f) Assume that the remaining length $x_3 = \ell - (x_1 + x_2)$ contains 10 insulating sublayers, each of width Δx. We can then use Equation (12) or Figure 10 to calculate the air pressure $P_{air}(x)$ in each sublayer corresponding to a specified aging time.

(g) The equation

$$m_{air}(x) = \frac{P_{air(x)}}{P_{air}(x) + P_{freon}}, \quad m_{freon}(x) = 1 - m_{air}(x) \tag{17}$$

can now be used to calculate m_{air} and m_{freon}, the gram-molecular fractions of air and Freon-11 in the gas mixture inside the cells in each insulating sublayer, provided the layer temperatures $X = X_{(T)}$ can be calculated, i.e., T is known as a function of the depth x in the foam. The integral can then be evaluated easily by the formula

$$\int_{T_{cf}}^{T_2} K_{mixture}(m_{(x)}, T)\, d_T = \sum_{i=1}^{10} K_{mixture}(m_{(T_i)}, T_i)\Delta T_i \tag{18}$$

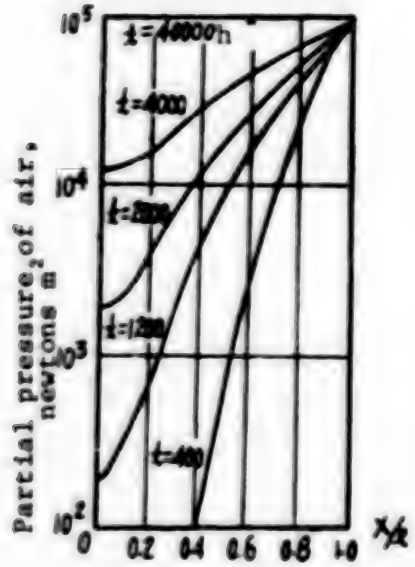

Figure 10. Air Pressure in Foam Cells for Five Different Aging Times (in hours)

(h) The details of the procedure for finding the spatial distribution $X = X_{(T)}$ of the temperature are the same as for part (e) above. One applies Equation (13) successively to the entire insulating layer or just to the part for $X = 0$ to $X = X_1 + X_2 + \Delta X$. Invoking the continuity of the heat flux once again, we obtain

$$X_1 + X_2 + \Delta X = \frac{\ell}{K_{eff0}(T_2 - T_1)} \left[\int_{T_1}^{T_{cf}+\Delta T_1} \phi V_s / V_{tot} K_{resin} d_T + \right.$$

$$\int_{T_{ca\ open}}^{T_{cf}+\Delta T_1} V_{open} / V_{tot} K_{air} d_T + \int_{T_{ca\ closed}}^{T_{cf}} V / _{closed} / V_{tot} K_{air} d_T +$$

$$\left. \int_{T_{cf}}^{T_{cf}+\Delta T_1} V_{closed} / V_{tot} K_{mixture} d_T + \int_{T_{cf}}^{T_{cf}+\Delta T_1} \frac{4\sigma}{E} T^3 dT \right] \qquad (19)$$

Since ΔX is very small, we can replace K_{resin}, K_{air}, $K_{mixture}$, and T by their values at $X = X_1 + X_2$, $T = T_{cf}$. We thus calculate the temperature $T = T_{cf} + \Delta T_1$ corresponding to $X_1 + X_2 + \Delta X$ and use $X_1 + X_2 + \Delta X$ and $T_{cf} + \Delta T_1$ (which are now known) in Equation(19) to calculate the temperature $T = T_{cf} + \Delta T_1 + \Delta T_2$ corresponding to $X_1 + X_2 + 2\Delta X$. We obtain in this way until $x = X_3$ is reached and the temperatures of all 10 sublayers have been calculated.

(i) In this final step we use (18) to evaluate the integral; all three integrals in Equation (10) have now been calculated.

5. Total Average Effective Thermal Conductivity

The total effective conductivity is given by

$$\bar{K}_{eff} = \bar{K}_s + \bar{K}_g + \bar{K}_{rad}$$

Proceeding in accordance with the above steps, we calculate the average conductivity $\bar{K}_{eff1}$, substitute this value into Equation (16) in step (e), then recalculate a new value $\bar{K}_{eff2}$, substitute back again, and iterate. The process stops when $\bar{K}_{eff\ \eta+1} = \bar{K}_{eff\eta}$.

V. Comparison With Experiment

We tested a polyurethane foam of density 59 kg/m^3, thickness ℓ = 2.55 cm, closed cell fraction 91 percent, and average cell volume 4 x 10^{-6} mℓ which had been aged in air for 300 hours at room temperature. The cold surface of the foam was at liquid hydrogen temperature, while the warm surface was at 300 K. The average effective thermal conductivity $\bar{K}_{eff}$ = 1.28 x 10^{-1} mW/cm·K was calculated by carrying out three iterations using the analytical model, as described in the previous paragraph. The conductivity $\bar{K}_s$ = 1.9 x 10^{-2} mW/cm·K along the solid walls of the cells accounted for 15 percent of the total value $\bar{K}_{eff}$, $\bar{K}_{air}$ = 10.6 x 10^{-2} mW/cm·K accounted for 80 percent, and the remaining 5 percent was due to radiative heat conduction, $\bar{K}_{rad}$ = 0.6 x 10^{-2} mW/cm·K.

The experimentally measured average effective thermal conductivity $\bar{K}_{eff}$ = 1.22 x 10^{-1} mW/cm·K agrees very closely with the calculated value. Because only a flat-panel conductometer[9] is currently available, the experimental values $\bar{K}_{exp}$ were determined in the following three steps:

(a) We first used the conductometer to measure the differential effective thermal conductivity $K_{eff(T)}$ for cold-surface temperatures between 20 and 300 K (this corresponded to various thermal loads across the polyurethane foam insulation);

(b) The curve $K_{eff(T)} \sim T$ was then constructed;

(c) Graphical methods were employed to find the average effective thermal conductivity, i.e., the integral

$$\bar{K}_{eff} = \frac{\int_{T_1}^{T_2} K_{eff(T)}\,dT}{T_2 - T_1} = \frac{\sum_i K_{eff(T_i)}\,\Delta T_i}{T_2 - T_1} \qquad (20)$$

was evaluated graphically.

VI. Summary

1. The experimental results on the relation between density and thermal conductivity indicate that there is an optimum density ρ_{opt} corresponding to maximum heat-insulating effectiveness, and that ρ_{opt} depends on how the

foam is made. For a given solid-state foaming process, one can find ρ_{opt} by measuring the average effective thermal conductivities $\bar{K}_{eff}$ of a series of foams with different densities.

2. In addition, because of the radiative heat transfer and conduction in the gas, convective and other types of conduction mechanisms occur when the cell diameters increase beyond a certain point. These mechanisms all become more important as the foam cells grow in size. In terms of the insulating properties, therefore, the best process is the one that produces foams with the smallest cell diameters for a given foam density. For a specified foam density, the insulating efficiency improves as the cells become smaller and their walls thinner; however, the mechanical properties of the foam deteriorate under these conditions.

3. If suitable measures are taken to isolate the layer of insulating foam from air, so that the evolution of latent heat of phase transition associated with extensive air infiltration is avoided, the above analytical model can be used to estimate the average effective thermal conductivity of foams containing open cells with acceptable accuracy. We have thus achieved our objective of determining the low-temperature thermal insulation properties of polyurethane foam in terms of easily measured quantities (density, fraction of closed cells, mean cell diameter, diffusion coefficients, aging time, etc.).

On the other hand, since our analytical model completely neglects convective transfer, which also increases with cell size, it predicts values that may be somewhat too high for low-density foams with very large cells. In addition, suppose that instead of using our relatively small flat-panel conductometer we used a larger circular tub or spherical apparatus to measure the average effective thermal conductivities. Because the cooling process can crack large foam blocks, the resulting convective heat transfer in this case may cause the experimental results to deviate considerably from the values found using the analytical model.

4. In contrast to what might be expected intuitively, it is the gas in the cells rather than the solid cell walls that gives the dominant contribution to the thermal conductivity of foam plastics. The relative importance of the three heat-conduction mechanisms depends on the density, fraction of closed cells, aging time, and other foam parameters. Assume for example that we have a polyurethane foam with $\rho_{foam} = 59$ kg/m^3 and $V_{cc} = 91$ percent which has been aged for 300 hours at room temperature, and assume that the cold side is at liquid hydrogen temperature, while the warm side is at room temperature. Then the gas, solid-wall, and radiative contributions to the total average effective thermal conductivity are equal to 80 percent, ≈ 15 percent, and ≈ 5 percent, respectively (although small, the latter contribution is by no means negligible).

We are grateful to Wang Hongkui [3769 7703 1145] and Huang Qian [7806 3383] for providing the foam samples.

REFERENCES

1. Navickas, J. and Madsen, R.A., ADVANCES IN CRYOGENIC ENGINEERING, Vol 22, 1975 p 233.

2. Skochdopole, R.E., CHEM. ENG. PROG., Vol 57, 1961.

3. Hammond, M.B., Jr., ADVANCES IN CRYOGENIC ENGINEERING, Vol 15, 1969 p 332.

4. Zhu Xian, et al., DIWEN WULI [LOW TEMPERATURE PHYSICS], Vol 3 No 4, 1981.

5. Doherty, D.J., Hurd, R. and Lester, G.R., CHEM. IND., (London) 1340 (1962).

6. Kmax, R.E., ASHRAE J., Vol 4, 1962 p 43.

7. Zhu Xian., et al., DIWEN WULI [LOW TEMPERATURE PHYSICS], Vol 3 No 2, 1981.

8. Reid, R.C. and Sherwood, T.K., "The Properties of Gases and Liquids," McGraw-Hill, New York (1958).

9. Essenhigh, R.A., "On Radiative Heat Transfer in Solids," AIAA Paper 67-287, and AIAA Thermophysics Specialists Conf., New Orleans, April 1967.

10. Sparks, L.L., "Nonmetallic Materials and Composites at Low Temperatures," Plenum Press, New York (1979).

11. "Handbook of Ultra-low Temperatures, Part I," Ranliao Huaxue Gonye Chubanshe, 1973.

12. White, "Experimental Techniques in Low-temperature Physics," [Chinese translation by Hong Hansheng, et al.,]

12617
CSO: 4008/381

TABLE OF CONTENTS OF WEIXING JISUANJI NO 3, 14 MAY 1985

Chongqing WEIXING JISUANJI [MICROCOMPUTERS] in Chinese No 3, 14 May 85

[Text]

CSO: 4008/1009

AUTHOR: FENG Guiyun [7458 2710 0061]
QU Wenxiao [2575 2429 1321]

ORG: Southwestern Institute of Physics, Leshan, Sichuan

TITLE: "A Numerical Method for Solving a Two-point Boundary Value Problem By Directly Integrating Nonlinear Ordinary Differential Equations"

SOURCE: Beijing SHUZHI JISUAN YU JISUANJI YINGYONG [JOURNAL ON NUMERICAL METHODS AND COMPUTER APPLICATIONS] in Chinese Vol 6, No 3, Sep 85 pp 135-142

TEXT OF ENGLISH ABSTRACT: Starting from the problem of the steady radial plasma transport in tokamak devices with divertor, we discuss a numerical method for solving a two-point boundary value problem by directly integrating nonlinear ordinary differential equations. The problem in question is reduced to one of solving a set of nonlinear equations by expanding their integral formal solution in terms of a set of orthogonal functions. When the cosine functions are taken to be orthogonal functions, special techniques are presented for numerical calculations of the multiple integrals with single variable limit and for solving transcendental equations whose root covers a wide range and for numerically solving systems of nonlinear equations. These techniques make our method more economical in computation. The method offered can, at least in principle, be extended to solve other two-point boundary value problems of the same class. (Paper received on 24 November 1982)

AUTHOR: MA Yanwen [7456 1693 2429]
FU Dexun [0102 1795 5651]

ORG: Beijing Institute of Aerodynamics

TITLE: "Difference Schemes in Computation of Viscous Flow"

SOURCE: Beijing SHUZHI JISUAN YU JISUANJI YINGYONG [JOURNAL ON NUMERICAL METHODS AND COMPUTER APPLICATIONS] in Chinese Vol 6, No 3, Sep 85 pp 143-153

TEXT OF ENGLISH ABSTRACT: A one-step difference scheme for solving the Navier-Stokes equations is discussed. Three improvements on this scheme are given: scheme with control factor, scheme with upwind computation and implicit factored scheme. Numerical experiments for the nonlinear Burgers equation are made and the results are compared with the solutions of explicit and implicit MacCormack scheme. This implicit factored scheme is shown to be most effective. (Paper received on 20 December 1982)

REFERENCES:

[1] И. Ю. Боаиловская, доклады АН СССР, 160:5 (1965).
[2] J. S. Allen, S. I. Cheng, The Physics of Fluids, Vol. 13, No. 1 (1970).
[3] R. W. MacCormack, AIAA Paper 69—354 (1969).
[4] R. M. Beam, R. F. Warming, AIAA Journal, Vol. 6, No. 4 (1978).
[5] R. W. MacCormack, AIAA Paper 81—0110 (1981).
[6] S. I. Cheng, Y. W. Ma, MAE Report No. 1558-MAE, Princeton University (1982).
[7] 马延文,计算数学 No. 2(1978).
[8] 马延文,待发表.

AUTHOR: WANG Rishuang [3769 2480 3642]

ORG: Beijing Institute of Aeronautics and Astronautics

TITLE: "The Convexity Discriminants of a Bicubic Spline Surface"

SOURCE: Beijing SHUZHI JISUAN YU JISUANJI YINGYONG [JOURNAL ON NUMERICAL METHODS AND COMPUTER APPLICATIONS] in Chinese Vol 6, No 3, Sep 85 pp 154-160

TEXT OF ENGLISH ABSTRACT:

This paper is a continuation of [9], in which a sufficient condition of strict convexity $CB\tilde{C} > 0$ is given for the surface block where

$$C = \begin{bmatrix} 1 & 1 & 1 & 1 & 1 \\ 4 & 3 & 2 & 1 & 0 \\ 6 & 3 & 1 & 0 & 0 \\ 4 & 1 & 0 & 0 & 0 \\ 1 & 0 & 0 & 0 & 0 \end{bmatrix}, \quad \tilde{C} = \begin{bmatrix} 1 & 0 & 0 & 0 & 0 \\ 1 & 1 & 0 & 0 & 0 \\ 1 & 2 & 1 & 0 & 0 \\ 1 & 3 & 3 & 1 & 0 \\ 1 & 4 & 6 & 4 & 1 \end{bmatrix},$$

$$B = [b_{ij}]_{1 \le i,j \le 4}$$

with b_{ij} depending on the coefficients a_{ij} of the surface block

$$z = [x^3\ x^2\ x\ 1][a_{ij}]_{1 \le i,j \le 4} \begin{bmatrix} y^3 \\ y^2 \\ y \\ 1 \end{bmatrix}, \quad 0 \le x,\ y \le 1.$$

In this paper, discriminants are given by means of network lines and vertexes:

$$C_1 B_1 \tilde{C} \le 0$$

and

$$C_1 \begin{bmatrix} b_{11} \\ b_{12} \\ b_{13} \end{bmatrix} \le 0, \quad C_1 \begin{bmatrix} \sum_{i=1}^{3} b_{i1} \\ \sum_{i=1}^{3} b_{i2} \\ \sum_{i=1}^{3} b_{i3} \end{bmatrix} \le 0$$

respectively, where

$$C_1 = \begin{bmatrix} 1 & 3 & 6 \\ 2 & 3 & 0 \\ 1 & 0 & 0 \end{bmatrix}, \quad B_1 = [b_{ij}]_{1 \le i,j \le 3}.$$

They are useful in computer geometry.

AUTHOR: LI Zhengxiu [2621 2973 4423]
FENG Zhenxing [7458 2182 5281]

ORG: LI of Huazhong Institute of Technology, Wuhan, Hubei and FENG of Wuhan University of Wuhan, Hubei

TITLE: "The Numerical Design and Automatic Plotting of Non-symmetric Joukowski Airfoils"

SOURCE: Beijing SHUZHI JISUAN YU JISUANJI YINGYONG [JOURNAL ON NUMERICAL METHODS AND COMPUTER APPLICATIONS] in Chinese Vol 6, No 3, Sep 85 pp 169-175

TEXT OF ENGLISH ABSTRACT: The alogrithm of an iterative method for designing symmetric Joukowski airfoils is generalized to arbitrary non-symmetric Joukowski airfoils with specified chord, maximum thickness and bentness of the camber line. A numerical example is given using this algorithm. The corresponding FORTRAN program includes an automatic plotting scheme. (Paper received on 29 December 1982) (This work was done in collaboration with Prof T.G. Huang of Wisconsin Univeristy)

12949
CSO: 4009/1009

ERRATUM: This abstract is republished from JPRS-CST-85-034 of 1 October 1985 to correct source name.

AUTHORS: HUANG Guifang [7806 2710 5364]
YU Ximao [0151 1598 5399]
DING Mingyu [0002 2494 3768]

ORG: HUANG and DING of Department of Chemical Analysis, Wuhan College of Geology; YU of Department of Chemistry, Wuhan University

TITLE: "A New Highly Sensitive Reagent, p-Acetylcarboxylazo-p, for Determining Thorium"

SOURCE: Beijing HUAXUE SHIJI [CHEMICAL REAGENTS] in Chinese Vol 7 No 2, 28 Apr 85 pp 109-110

ABSTRACT: A developer, p-acetylcarboxylazo-p, has been synthesized for the first time by the Wuhan University; the agent is used in the luminescence analysis of rare earth elements. The optical conditions of the development reaction between the developer and thorium are presented. In the 0.1 N hydrochloric acid, a blue complex is formed and will remain stable for 12 hours. In a 25 ml volume, the range of 1 to 18 Ug of ThO_2 obeys Beer's Law. At present, this is a highly sensitive method for determining trace amounts of thorium. Satisfactory results can be obtained in analyzing ore specimens by using the method. Two figures show the absorption (spectrum) curves and working curve. Two tables list data for the recovery experiment and sample analysis results.

REFERENCES

1. Pan Jiaomai [3382 2403 7796], Chen Yasen [7115 0068 2773] and Yan Hengtai [0917 1854 1132], XIANSEJI JIQI ZAI YEJIN ZHONGDI YINGYONG [DEVELOPER AND ITS APPLICATIONS IN METALLURGICAL ANALYSIS], Shanghai Science and Technology Publishing House, 416 (1981).

2. Hubei Geology Laboratory, GONGWU YANSHI FENXI [ANALYSIS OF MINERALS], 284 (1972).

10424/9365
CSO: 4009/1113

Computers

AUTHORS: JIN Dexuan [6855 1795 1357]
JIN Xuexin [6855 1331 2450]

ORG: JIN Dexuan of Jiangsu Provincial School of Posts and Telecommunications; JIN Xuexin of Second Changzhou Radio Plant

TITLE: "Computer System Design in Telephone Service Management"

SOURCE: Shenyang XIAOXING WEIXING JISUANJI XITONG [MINI-MICROCOMPUTER SYSTEMS] in Chinese No 5, 8 May 85 pp 43-49, 64

ABSTRACT: This article reports on the design of a telephone service management system controlled by a model DJS-112 microcomputer for an HJ-921A (model) crossbar automatic exchange with a capacity of 10,000 telephone numbers of the Wuxi Bureau of Posts and Telecommunications. The design includes the structure, function and operational plan. The system's economic benefits and advantages in widescale acceptance are evaluated. The central processing unit (CPU) is a DJS-112 digital computer with 16-bit words, 32 K internal memory and a computing speed of 150,000 operations per second; the CPU controls (and computes) the telephone service system. The peripheral equipment includes model HZD-5 eight-unit control panel printers, a model CDZ-2 punched tape machine, a model RDG-12 photoelectric input terminal, and a model 55 teletype (for man-machine dialog and supplementary output printing-punching). TMS-2 application software has been developed. The computer system can perform the following functions: automatically recording of the number of calls for subscribers, billing for subscribers' telephone numbers or addresses, tariff analysis, and automatic time keeping and tariff recording for long-distance calls. The system was placed in service at Wuxi in April 1983; certification was awarded on 19 December 1983. The accuracy in counting the number of calls is as high as 99.86 percent. Ten figures show a block diagram of the telephone service management system; telephone wire connections for the crossbar automatic exchange; the interface for counting the number of calls; formats of service line, subscriber and address billing charts; logic block diagrams for tariff analysis and automatic time keeping (and tariff recording) for long-distance calls; and long-distance call charts for input and interruption as well as authorized subscribers.

10424/9365
CSO: 4009/1100

Computers

AUTHOR: KANG Huaguang [1660 5478 0342]
LIN An [2651 1344]
WU Hongxiu [0702 7703 0208]

ORG: None

TITLE: "On Real-time Processing of Cardiac Blood Flow"

SOURCE: Wuhan HUAZHONG KONGXUEYUAN XUEBAO [JOURNAL OF HUAZHONG UNIVERSITY OF SCIENCE AND TECHNOLOGY] in Chinese Vol 13, No 3, Jun 85 pp 1-8

TEXT OF ENGLISH ABSTRACT: A microcomputer [CF-I]-based automatic real-time processing system developed by the authors is reported. Some special techniques for processing the cardiac blood flow are presented and excellent performance of the system is obtained from clinical tests for various cases of illness. Typical test data are discussed. (Paper received on 8 February 1985)

REFERENCES:

[1] Kubicek, W. G. et al., *Ann N. Y. Acand Sci*, 170, p. 724(1970).
[2] Miyamoto, Y. et al., *Proceedings of the Vth ICEBI TOKYO*, Aug. pp. 46～48(1981).
[3] Yoshimi Miyamoto et al., *Biotelemetry patient Monitoring*, 8. pp. 189～203(1981).
[4] Bleicher, W. et al., *Proceedings of the Vth ICEBI TOKYO*, Aug. pp. 87～80(1981).
[5] 况明星等，医疗器械，第4期，第23～27页(1983).
[6] Kubicek, W. G. et al., *Aerospace Med.*, 37, pp. 1208～1212(1966).
[7] A. V. 奥本海姆等，数字信号处理，科学出版社(1983).
[8] D. A. 麦克唐纳，动脉中的血液流，科学出版社，第184页(1982).

AUTHOR: QU Anlian [4234 1344 6647]
CUI Jianmin [1508 0256 3046]
JIANG Genghe [3068 1649 0735]

ORG: None

TITLE: "Display Technique and Intelligent Control of Vectorcardiograph"

SOURCE: Wuhan HUAZHONG KONGXUEYUAN XUEBAO [JOURNAL OF HUAZHONG UNIVERSITY OF SCIENCE AND TECHNOLOGY] in Chinese Vol 13, No 3, Jun 85 pp 43-48

TEXT OF ENGLISH ABSTRACT: A new vectorcardiograph consisting of a specific system with a Z80A microprocessor is described, which is capable of automatically examining a vectorcardiogram (VCG). The VCG in three planes F, S and H and the ECG in three axes X, Y and Z can be displayed in either moving or freezing form. The device is also capable of displaying its working conditions, the scale factors and the required results in the form of characters. (Paper received on 13 January 1985)

REFERENCES:

[1] W.J. Tompkins and J.G. Webster eds., *Design of Microcomputer-Based Medical Instrumentation* (1981).

[2] 林绍芳、宋供发、曹钧编，心电向量图学，人民卫生出版社(1983).

[3] J.B. Peatman, *Microcomputer-Based Design* (1977).

AUTHOR: LI Feixia [2621 7378 7209]

ORG: None

TITLE: "The Temperature Transmitter Circuit for a Temperature Control System Using Microcomputer"

SOURCE: Wuhan HUAZHONG KONGXUEYUAN XUEBAO [JOURNAL OF HUAZHONG UNIVERSITY OF SCIENCE AND TECHNOLOGY] in Chinese Vol 13, No 3, Jun 85 pp 81-86

TEXT OF ENGLISH ABSTRACT: The transmitter circuit design for temperature control by microcomputer is described. The constant current supply for the input circuit is adopted, improving the linear relation between the signal voltage V_t, and temperature T. The compensation method for enhancing the linearity of the transmitter characteristics and the method for automatic calibration are also suggested. (Paper received on 5 February 1985)

REFERENCES:

[1] 石油化工部编，电动单元组合仪表，石油化工出版社(1977)。

[2] 李清泉、黄昌宁编著，集成运算放大器的原理与应用，科学出版社(1980)。

[3] 张郑弘、庄灿涛编著，晶体管放大器及其应用，国防工业出版社(1978)。

[4] P. Horowitz and W. Hill, *The Art of Electronics*, Cambridge University Press, New York (1980).

12949
CSO: 4009/1014

JPRS-CST-85-039
13 November 1985

AUTHOR: ZHAO Zhaoyi [6392 0340 7328]
ZANG Xinian [5258 1585 1628]
ZHOU Quanfu [0719 0356 4395]
ZHAO Huimin [6392 1979 2404]

ORG: ZHAO Zhaoyi and ZANG of Qinghua University; ZHOU and ZHAO Huimin of Research and Design Institute No 728

TITLE: "Single-Pass Mixed Lattice Method and CHAN-2 Code for Subchannel Analysis of Reactor"

SOURCE: Beijing HE KEXUE YU GONGCHENG [CHINESE JOURNAL OF NUCLEAR SCIENCE AND ENGINEERING] in Chinese Vol 5 No 2, Jun 85 pp 113-119

TEXT OF ENGLISH ABSTRACT: In this paper the reliability and advancement of the single-pass mixed lattice method is demonstrated. It is also shown why the CHAN-2 code is more efficient than the COBRA-III C/MIT-2 code. By means of the calculation for the exit water temperature in hot assembly of the Maine Yankee core the computational results, calculated using the CHAN-2 code, agree well with the measured values in the reactor. Comparison of the computational results for the Qinshan Nuclear Plant's reactor core, using subchannel analysis, with those using single-channel analysis are also presented.

AUTHOR: ZHANG Jingcai [1728 2417 2088]

ORG: Southwest Institute of Nuclear Reactor Engineering

TITLE: "The Operating Limit of Water Reactor Pressure Vessel"

SOURCE: Beijing HE KEXUE YU GONGCHENG [CHINESE JOURNAL OF NUCLEAR SCIENCE AND ENGINEERING] in Chinese Vol 5 No 2, Jun 85 pp 120-131

TEXT OF ENGLISH ABSTRACT: The operating control principle and method for the water reactor pressure vessel, as an approach to prevent the brittle fracture of the reactor coolant pressure boundary, is described based on the requirements of ANSI N18.2 and 10CFR 50App. A. Calculations have been made in accordance with both the transition temperature approach and the linear elastic fracture mechanics approach. The operation limit diagram for the cylindrical shell of the pressure vessel of a 900MWe nuclear power plant is obtained.

The results obtained by different methods are analyzes and compared, and comments are given.

AUTHOR: SHENG Weilan [4141 4850 5695]

ORG: Southwest Institute of Nuclear Reactor Engineering

TITLE: "The Calculation of Neutron Fluence on Pressure Vessel for Nuclear Power Station"

SOURCE: Beijing HE KEXUE YU GONGCHENG [CHINESE JOURNAL OF NUCLEAR SCIENCE AND ENGINEERING] in Chinese Vol 5 No 2, Jun 85 pp 132-138

TEXT OF ENGLISH ABSTRACT: The neutron fluence on the pressure vessel for a nuclear power station is calculated using two-dimensional discrete ordinates radiation transport code DOT3.5. The results are consistent with the measurement within +20 percent. The calculation sensitivity and deviation are analyzed, including various uncertainties. The total standard deviation of the calculated neutron fluence is +20 percent. This is consistent with the comparison between the calculation and measurement.

AUTHOR: YI Min [0122 2404]
CHEN Dingfang [7115 1353 5364]
HA Hongfei [0761 7703 7378]
WU Jilan [0702 1323 5695]

ORG: Department of Technical Physics, Beijing University

TITLE: "The Gamma Radiation Effect of the Systems TBP-Ketone, TBP-DMSO and Their Energy Transfer Kinetics"

SOURCE: Beijing HE KEXUE YU GONGCHENG [CHINESE JOURNAL OF NUCLEAR SCIENCE AND ENGINEERING] in Chinese Vol 5 No 2, Jun 85 pp 139-146

TEXT OF ENGLISH ABSTRACT: Work at this laboratory has proved that under γ-radiation TBP may form at least three kinds of active species or states in TBP-DBBP, TBP-DBPP and TBP-DBBP-C_6H_6 systems.

In order to spread these studies, experiments were performed in TBP-Ketone and TBP-DMSO systems. $\rangle C = O$ and $\rangle S = O$ have similar bonds as $\rangle P = O$. The displaced groups on carbon and sulphur atoms and the different polarities of those molecules will give rise to different effects on the energy transfer. The systems used are convenient for distinguishing the different active species of irradiated TBP and make the observation of the sensitized process of additives easy.

The results show that both $CH_3\overset{O}{\overset{\|}{C}}CH_3$ and $CH_3\overset{O}{\overset{\|}{S}}CH_3$ have a double effect of energy transfer for two kinds of excited states of TBP. Therefore, the range in energy transfer systems with TBP and the applicability of the sensitized equation derived in this laboratory have been extended.

A kinetic study has also been done in this work. The inhibition equation $G_i = G_0(1-nx)$ for the second excited state of irradiated TBP is derived. Here n represents the efficiencies of energy transfers and is different for different inhibitors.

A new explanation for the inhibition equation for the second excited state of TBP* is provided. The aggregations (or domains) formed by one molecule of an inhibitor with several molecules of TBP should be considered to be more reasonable. In these aggregations (or domains) the energy of excited TBP* can be transferred to the molecule of the inhibitor.

AUTHOR: ZHENG Hualing [6774 5478 6875]
ZHOU Shunli [0719 7311 0448]
CHEN Shuming [7115 2885 6900]
JIAO Rongzhou [3542 2837 3166]
WANG Shouzhong [3769 1343 1813]
et al.

ORG: ZHENG, ZHOU and CHEN of Beijing Institute of Nuclear Engineering; JIAO, WANG, et al., of the Institute of Nuclear Energy, Qinghua University

TITLE: "A Study of the Process of Extracting Actinides by Trialkyl (Mixed) Phosphine Oxide (TRPO)"

SOURCE: Beijing HE KEXUE YU GONGCHENG [CHINESE JOURNAL OF NUCLEAR SCIENCE AND ENGINEERING] in Chinese Vol 5 No 2, Jun 85 pp 147-153

TEXT OF ENGLISH ABSTRACT: This paper presents results from a study that has been completed with cascade experiments and a multistage miniature counter-current centrifugal extractor on the process and separation conditions of cleaning up α-nuclides by 30 percent TROP-OK from simulated high level liquid waste arising from power reactor fuel reprocessing. The results show that the proposed process could simultaneously extract U, Np, Pu, Am, Cm, Tc and RE α-nuclides with transuranium clean-up rates of more than 99.9 percent. The process steps are simple and hold promise for industrial utilization.

AUTHOR: ZHU Huannan [2612 3562 0589]
YUAN Luzheng [5913 1462 2973]
HUANG Daoli [7806 6670 4539]
et al.

ORG: Institute of Atomic Energy, Chinese Academy of Sciences

TITLE: "Physical Start-up of Heavy Water Research Reactor with UO_2 Fuel Core"

SOURCE: Beijing HE KEXUE YU GONGCHENG [CHINESE JOURNAL OF NUCLEAR SCIENCE AND ENGINEERING] in Chinese Vol 5 No 2, Jun 85 pp 174-180

TEXT OF ENGLISH ABSTRACT: Physical start-up has been performed with the UO_2 fuel core in HWRR. An on-line computer is used during the experiments. The experimental results have verified the theoretical design, and the main physical characteristics necessary for operators and users are provided. The relationship between the height of the control rod bank and excess reactivity was studied and is explained. A practical and convenient method for the excess reactivity measurement during the core life-time is given.

9717
CSO: 4009/291

Engineering

AUTHORS: WU Yanqing [0702 1750 0615]
CAI Jingyin [5591 2417 7299]

ORG: WU, an engineer with the Shanghai Electrical Apparatus Research Institute; CAI, an engineer with the Shanghai Electrical Welding Machine Factory

TITLE: "Type DH_2-1 Chromium-Zirconium-Copper Alloy for Resistance Welding Electrode Tips"

SOURCE: Harbin HANJIE XUEBAO [TRANSACTIONS OF THE CHINA WELDING INSTITUTION] in Chinese Vol 6 No 3, 25 Sep 85 pp 143-148

ABSTRACT: This paper chiefly deals with the manufacturing technique and the application of a new type welding electrode tip made of DH_2-1 chromium-zirconium-copper alloy. With the purpose of obtaining the longest possible service life, the optimum composition range of the alloy and the technical specifications for each step of alloy production process are studied. The results of study are as follows: optimum composition range of DH_2-1 alloy, Cr0.25 ~ 0.40 percent, Zr0.08 ~ 0.15 percent; solution heat treatment, 950 ~ 970°C for 1.5 ~ 2 hrs; cold deformation rate, 40 ~ 50 percent; aging treatment, 450 ~ 500°C for 2 ~ 3 hrs. For electrode tips made according to the above technology, the following superior properties can be assured: conductivity ≥75 percent IACS, Rockwell Hardness HRB ≥80, softening temperature ≥600°C. Through a lot of practice and application in both ferrous and nonferrous alloy welding, the quality of welds proved excellent. As compared with the chromium-aluminum-magnesium alloy (M_{II}-4) zirconium-copper alloy (Zr-Cu) and silver-chromium-copper alloy (AC_2), which have been widely used in China, the service life of DH_2-1 alloy electrode tips is increased generally by 3 ~ 10 times, in addition to the greatly improved welding quality and productivity. (Paper received 8 May 1985)

REFERENCES

〔1〕铃木寿，川勝一郎，北野均，村瀬昭次：《日本金属学会誌》，31(1967)，№1，P14--19。
〔2〕駒井俊雄，手島光一，待鳥晴香：《东芝評論》，28(1973)，P613—616。
〔3〕川勝一郎，铃木寿，北野均：《日本金属学会誌》，31(1967)，№11，P1253—1257。
〔4〕铃木寿，川勝一郎，北野均：《日本金属学会誌》，31(1967)，№4，P342—346。
〔5〕浜崎正信：《搭接电阻焊》，国防工业出版社，北京，(1977)。

/9365
CSO: 4009/1010

AUTHORS: YU Shangzhi [0205 1424 4249]
ZHU Liansheng [2612 6647 3932]
LI Yan [2621 3543]
WU Yixiong [0702 3015 7160]
ZHAO Ying [6392 4481]

ORG: Shanghai Jiao Tong University

TITLE: "The Development of a New Transistor Power Source--Exploring the Mechanism of Arc-Ignition With Low Open Circuit Voltage"

SOURCE: Harbin HANJIE XUEBAO [TRANSACTIONS OF THE CHINA WELDING INSTITUTION] in Chinese Vol 6 No 3, 25 Sep 85 pp 149-156

ABSTRACT: This paper puts forward the technical and economic significance of developing a low open circuit voltage transistor power source after analyzing the GTA welding condition when using transistor power sources. The mechanism of no-touch arc-ignition with low open circuit voltage power source has been explored in order to find a theoretical basis for developing the new power source. By mathematical analysis of the welding circuit system, the authors investigated the influence of feedback units upon the process of arc stabilizing in the arc igniting period, thus making the optimal design of the circuit system for the welding power source possible. The paper gives also the technical parameters of the designed power source. The arc ignition has been proved to be very reliable in welding production. (Paper received 21 March 1985)

REFERENCES

〔1〕 Birchbield J.R., 〈Welding Design & Fabrication〉, 56(1983),№6,P39.
〔2〕 Эсибян Э.М, 〈Автоматическая сварка〉,(1975),№.2,P54.
〔3〕 董文军等，〈小直径 TIG 全位置自动焊晶体管电源〉，(1979)。
〔4〕 上海电焊机厂，〈50A大功率三极管脉冲氩弧焊电源〉，(1979)。
〔5〕 丁凤姣等，〈JHD-05-Z 型晶体管式高频脉冲钨极气体保护焊电源及其应用〉，(1979)。
〔6〕 刘成武等，〈开关型晶体管钨极脉冲氩弧焊机的研究〉，(1982)。
〔7〕 江剑平等，〈阴极电子学与气体放电〉，国防工业出版社，(1980)。

/9365
CSO: 4009/1010

Fluid Dynamics

AUTHORS: FU Weibiao [0265 4850 2871]
WANG Qiang [3769 1730]

ORG: Department of Engineering Mechanics, Qinghua University, Beijing

TITLE: "Research on the Law of Ignition of Monogranular Water-coal Slurry Under Forced Convective Conditions"

SOURCE: Beijing ZHONGGUO KEXUE(A JI) [SCIENTIA SINICA (SERIES A)] in Chinese No 7, Jul 85 pp 602-603

ABSTRACT: This article discusses the experiments on and makes a theoretical analysis of the ignition problem of monogranular water-coal slurry under forced convective conditions. The experiments indicate that under the condition in which the Reynolds numbers are greater, the flame appears in axial symmetry, and ignition occurs in the boundary layer of the front hemisphere. The article builds a simplified model of the flame on the boundary layer of the two-dimensional axial symmetric laminar flow and makes numerical value calculations. The results of computation and experimentation are fairly in accord and can be used as methods for estimating the ignition temperature and ignition time of water-coal slurry under forced convective conditions.

12949/9365
CSO: 4009/1134

Lasers

AUTHORS: LI Yulin [2621 7183 2651]
LU Jianhua [0712 1696 5478]
JIANG Jialin [5592 1367 7792]
CHENG Guanchang [4453 7070 9480]

ORG: Shanghai Institute of Laser Technology

TITLE: "Generation and Analysis of Wideband Optical Quasi-continuum in a Multimode Optical Fiber"

SOURCE: Shanghai YINGYONG JIGUANG [APPLIED LASER] in Chinese Vol 5 No 4, Aug 85 pp 145-148

ABSTRACT: A wideband nonlinear scattering spectrum (1.1-1.9 μm) was obtained in a multimode optical fiber pumped with an A-O (acoustic-optical) Q-switched Nd-YAG laser at 1.06 μm. The spectrum forms a good quasi-continuum at the zero-material-dispersion range of the fiber. The generation mechanism of the continuum is discussed. The continuum is shown to be generated by combined interaction of stimulated Raman scattering (SRS) and four-photon mixing. The study uses a multimode optical fiber with GeO_2-SiO_2 as its core cladded with SiO_2. Three figures show the experimental set-up, wideband scattering spectrum of the multimode optical fiber, and the procedures in determining the scattering spectrum. The paper was received for publication on 11 April 1985.

AUTHORS: YIN Daren [1438 6671 0086]
XU Shenlong [6079 3932 7893]

ORG: Kunming Institute of Physics

TITLE: "Spectral Analysis for Measuring Laser Spots"

SOURCE: Shanghai YINGYONG JIGUANG [APPLIED LASER] in Chinese Vol 5 No 4, Aug 85 pp 149-152

ABSTRACT: A spectral analysis method for rapid and accurate measurement of gaussian spot parameters is reported. The method may also serve in the measurement of distortion parameters of non-gaussian spots. This simple and easy method imposes very high requirements on equal-width accuracy of the sector modulation disk, stability of the rotational speed, concentricity of the tracing circle, frequency resolving power of the frequency spectrograph, and properties of the antecedent magnifier, among other factors. These requirements are higher for the less intense energy due to the smaller laser spot. The authors are grateful to Ni Mutao [0242 2606 2711] for his assistance. One figure shows a sector modulation disk and its scanning method. One table lists measured data of the frequency spectrum of a He-Ne laser beam. The paper was received for publication on 31 December 1984.

AUTHORS: LIN Yingyi [2651 5391 0308]
WU Zhengliang [0702 2973 0081]
SHANGGUAN Cheng [0006 1351 6134]
WANG Yiman [3769 1837 2581]
SHU Juping [5289 5468 0988]
DOU Airong [4535 1947 2837]
YANG Guang [2799 0342]

ORG: Shanghai Institute of Optics and Fine Mechanics, Chinese Academy of Sciences

TITLE: "Research on Properties of R 560 Dye Laser Pumped by an XeCl Laser"

SOURCE: Shanghai YINGYONG JIGUANG [APPLIED LASER] in Chinese Vol 5 No 4, Aug 85 pp 153-154, 152

ABSTRACT: The quasimolecular laser has the advantages of operational simplicity, low cost, high repetition rate equal to that for the N_2 molecular laser; and a sufficiently long pulse persistence time and the high power output advantages of the Nd-YAG laser. Compared with other quasimolecular lasers, the XeCl laser, in particular, has attractive advantages such as long service life and the great majority of dyes pumped in addition to its low cost. An experimental study of an R 560 dye pumped by an XeCl laser is reported. The tunable range of the dye laser is 5617 Å to 5886 Å. The line width of the tunable laser is 0.08 Å. Experimental results for six dyes are presented concisely. Three figures show the experimental set-up, the ultraviolet absorption spectrum of the R 560 dye, and a curve of energy conversion efficiency. Two photographs show the tuning spectrum and interference rings of an R 560 laser. One table lists data of experimental results for other dyes pumped by the XeCl laser. The authors express their gratitude to Huang Danhong [7806 2481 3163] and Ye Lin [5509 3829] for taking part in some experiments; and to the Tianjin Municipal Chemical Reagent Research Institute for supplying several dyes for the experiment. The paper was received for publication on 29 January 1985.

10424/9365
CSO: 4009/295

Lasers

AUTHORS: LUO Shiyu [5012 6108 5940]
YU Chaofan [0151 6389 0416]

ORG: LUO of Chongqing Communications College; YU of the Institute of Modern Physics, Chinese Academy of Sciences

TITLE: "Quantum-mechanical Description of Plane Channeling Radiation Characteristics"

SOURCE: Shanghai ZHONGGUO JIGUANG [CHINESE JOURNAL OF LASERS] in Chinese Vol 12 No 8, 20 Aug 85 pp 449-454, 464

ABSTRACT: The radiation characteristics of plane channeling particles are described in terms of quantum mechanics. In the inharmonic approximation (of Lindhard potential), the spectral distribution of the channeling radiation is calculated; comparison with the experimental data shows good agreement. Five figures show the geometric relationship between the particle motion and channeling radiation direction in a laboratory coordinate system; the frequency spectrum distribution of channeling radiation in (110) plane channel of a silicon monocrystal; the relationship between the occupancy probability on the one hand, and the particle energy in the transverse and longitudinal directions, on the other; and the relationship between occupancy probability and the particle incident angle. The paper was received for publication on 8 March 1984.

AUTHORS: CHENG Zhaogu [4453 0340 6253]
WANG Zhe'en [3769 0772 1869]
ZHA Hongkui [2686 7703 6652]
SHEN Junquan [3088 0193 3123]
CHEN Kexin [7115 0668 1800]
XI Quanxin [1151 0356 2450]
WANG Runwen [3769 3387 2429]

ORG: Shanghai Institute of Optics and Fine Mechanics, Chinese Academy of Sciences

TITLE: "Choice of the Optical Axis Position for a Transverse Flow CO_2 Laser Resonator"

SOURCE: Shanghai ZHONGGUO JIGUANG [CHINESE JOURNAL OF LASERS] in Chinese Vol 12 No 8, 20 Aug 85 pp 455-458

ABSTRACT: The paper discusses the selection of the optimal optical axis position of a transverse flow CO_2 laser resonator in a setting in which the resonator and the electric discharge are at the same position. The role played by the discharge current in the optimal position of the optical axis is disregarded in the study. Given the condition of a reasonable approximation, an approximation formula is given for the choice of the optical axis position for a transverse flow CO_2 laser resonator. The theory coincides closely with the experimental results. Four figures show the distribution (along the flow) of the small-signal gain of the transverse flow CO_2 laser; relationship curves between the optimal position of the optical axis on the one hand, and atmospheric pressure and wind velocity, on the other; a transverse flow CO_2 laser resonator; and curves showing the variation in the atmospheric pressure to wind velocity ratio and the optimal position of the optical axis. One photograph shows the output patterns of a 1 kw transverse flow CO_2 laser. One table lists theoretical and experimental data of the optimal positions of the optical axis of four transverse flow CO_2 lasers with different parameters. The authors express their gratitude to Wu Donglai [0702 2639 0171], Zhang Baofu [1728 1405 1381], Chen Ping [7115 1627], Jiang Miao [3068 8693] and Xi Wenlong [1151 2429 7893] of transverse flow CO_2 laser group of Shanghai Institute of Optics and Fine Mechanics. The paper was received for publication on 6 August 1984.

AUTHORS: LI Ziaguang [2621 0375 0342]
CHENG Zuhai [4453 4371 3189]
HE Xuhui [0149 3563 6540]

ORG: Institute of Lasers, Huazhong Engineering College

TITLE: "Output Beam Quality of Positive-branch Confocal Unstable Resonator"

SOURCE: Shanghai ZHONGGUO JIGUANG [CHINESE JOURNAL OF LASERS] in Chinese Vol 12 No 8, 20 Aug 85 pp 459-464

ABSTRACT: Currently in China, the stable resonator multimode output is usually adopted for transverse flow electrically excited continuous wave (CW) CO_2 lasers. This kind of multimode output laser beam is generally difficult in being made to conform to the requirements of laser cutting and welding. The authors adopted a positive branch confocal unstable resonator in the HGL-84 model, 5 kw transverse flow, electrically excited CO_2 laser. A laser output (fundamental model) of 3.82 kw was achieved with the maximum electro-photo conversion efficiency of 9.6 percent. The theoretical and experimental studies were conducted on a transverse-flow electrically excited CW CO_2 laser as to the intensity and the near-field and far-field patterns of an unstable confocal resonator. Results of both studies are in good agreement. Eight figures show the structural diagram and output properties of the above-mentioned CO_2 laser; the measurement set-up of the exposure display of thermo-sensitive paper for the laser spot diffraction pattern; the measurement set-up for the energy distribution; a comparison between theoretical and experimental data; diffraction patterns of far-field laser spots; the relative distribution of near-field intensities of output laser spots; and a theoretically calculated curve of the far-field intensity of a single fundamental mode. Four photographs show burn-corrosion patterns of far- and near-field plexiglass by an annular output laser beam; burn corrosion of a plexiglass rod showing the energy distribution in the far-field diffraction pattern; and a comparison of properties in cutting stainless steel specimens of output laser beams from the stable resonator multimode and unstable resonator annular fundamental mode. One table lists the measured geometric parameters of plexiglass burn corrosion. The paper was received for publication on 2 July 1984.

AUTHORS: YU Gang [5713 6921]
CAO Yuli [2580 0151 7812]
QI Guiyun [7871 2710 0061]
YU Shipeng [0060 0013 1756]
HAN Yong [7281 3196]

ORG: Beijing Vacuum Electron Devices Research Institute (Research Institute No 12), Ministry of Electronics Industry

TITLE: "Tunability of CO_2 Waveguide Lasers"

SOURCE: Shanghai ZHONGGUO JIGUANG [CHINESE JOURNAL OF LASERS] in Chinese Vol 12 No 8, 20 Aug 85 pp 471-475

ABSTRACT: CO_2 waveguide lasers have a number of advantages: small dimensions, compact structure, high gain, and good selection and control of the transverse mode. In addition, the capability of high gas pressure filling can strongly enhance output frequency tunability. Therefore, these lasers have a good prospect in heterodyne applications such as lidar, doppler ranging and optical guidance (among other areas), and analysis (with high resolving power) in infrared spectra. In the application of these systems, in addition to requirements on device mode and power, higher requirements are imposed on the tunability of the output frequency from these devices. The paper analyzes, theoretically and experimentally, the tunability of CO_2 waveguide lasers. It has been shown that the frequency tuning on one line can only be realized under given conditions. The tuning range is a function of laser gain, total loss, gas pressure and gas mixture, as well as the discharge current. Seven figures show the Littrow auto-quasi-structure; transition spectral line of the CO_2 molecule; the structure of CO_2 waveguide laser; the layout of a testing system; tunability properties of the waveguide laser before and after improvements; and the relationship between tuning width and gas pressure filling. One table lists vacuum measurement data for the CO_2 laser wavelengths. The paper was received for publication on 3 September 1984.

AUTHORS: WANG Songyue [3769 2646 1471]
JIN Juguang [6855 1565 1684]
WANG Xiulan [3769 4423 5695]
SUN Xiaozhong [1327 1321 1813]

ORG: Changchun Institute of Applied Chemistry, Chinese Academy of Sciences

TITLE: "Indirect Observation of High-resolution Spectra of Neon by Means of Laser-excited Atomic Fluorescence Spectrometry in a Low-resolution Detection System"

SOURCE: Shanghai ZHONGGUO JIGUANG [CHINESE JOURNAL OF LASERS] in Chinese Vol 12 No 8, 20 Aug 85 pp 478-481

ABSTRACT: Because a wealth of information inside matter can be exposed by the atomic fluorescence method, early in this century many physicists applied this method in a great number of studies on certain atomic systems. With the advent of the laser, laser-excited atomic fluorescence spectrometry has attracted growing attention. Through calculations and analyses, the authors applied, for the first time, laser-excited atomic fluorescence spectrometry to observe indirectly the high-resolution spectra of the atomic neon transitions of $2p_3 \rightarrow 4s_1'$ and $2p_7 \rightarrow 4d_3$ in a low-resolution detector system. This achievement further confirms the correctness of the conclusion that the neon spectral line at 5919.037 Å is identified to the transition of $2p_7 \rightarrow 4d_3$. Six figures show the emission spectrum of the neon atom; the laser-excited neon atom transition and the related energy level diagram; an illustrative diagram of laser-excited atomic fluorescence spectrometry and synchronous detection photoelectric effect; and the fluorescence signal and photoelectric signal at 5961.628 Å, 5987.911 Å and 5113.677 Å of the neon atom. The authors express their gratitude to associate researcher Wang Wenyun [3769 2429 7301] for revising the paper. The paper was received for publication on 22 September 1984.

AUTHORS: CAI Yingshi [5591 5391 2514]
YI Jingrong [0122 2529 2837]
NIU Wanqing [3662 5502 7230]

ORG: Shanghai Institute of Optics and Fine Mechanics, Chinese Academy of Sciences

TITLE: "Fabrication and Performances of Double Pockels Cells at 10.6 μm"

SOURCE: Shanghai ZHONGGUO JIGUANG [CHINESE JOURNAL OF LASERS] in Chinese Vol 12 No 8, 20 Aug 85 pp 485-487

ABSTRACT: One method for generating short single laser pulses is the use of a light switch. Currently, Pockels cells are commonly used. The authors developed a single Pockels cell for experiments. In order to increase the (light) extinction rate, the authors are working on the fabrication of double Pockels cells (described in the paper) with an aperture of 11 x 12 mm^2; performances are measured. The double Pockels cells were used in selecting short single laser pulses from a mode-locked TEA CO_2 laser. The rise time of a laser pulse switched-out from the smooth long pulse of a single longitudinal mode hybrid TEA CO_2 laser is less than 1 ns. One figure shows the experimental set-up. Five photographs show the voltage waveform, mode locking laser pulse, and laser pulse waveforms. The paper was received for publication on 23 August 1984.

10424/9365
CSO: 4009/290

AUTHOR: GUTU, M.V.
UDREA, D.
DUMITRAS, V. Draganescu
WANG Zheen [3769 0772 1869]
ZHA Hongkui [2686 7703 6652]
CHENG Zhaogu [4453 0340 6253]

ORG: GUTU, UDREA and DUMITRAS of the Central Institute of Physics, Bucharest, Romania; WANG, ZHA and CHENG of the Shanghai Institute of Optics and Fine Mechanics, CAS

TITLE: "Construction and Operation of a Gas Transport CO_2 Laser"

SOURCE: Shanghai ZHONGGUO JIGUANG [CHINESE JOURNAL OF LASERS] in Chinese Vol 12, No 9, 20 Sep 85 pp 518-520

TEXT OF ENGLISH ABSTRACT: The construction and the operation of a Co_2 gas transport laser with cylindrical geometry is presented. This work aims at developing a small size and light weight gas transport laser at high output level. This has been accomplished by using a single metallic cylinder for electric discharge, recirculation and the cooling of the gas mixture. More than 1kW laser power was obtained from a laser of the length of 1.45 m, diameter 0.54 m and cca weight 180 kg. Typical parameters were: pressure [illegible] Torr, CO_2:N_2: He=1:8:11, discharge current 8 A, efficiency 12 percent and laser spot 28x22 mm^2.

AUTHOR: FEI Lin [6216 2651]
WANG Kejun [3769 0344 0193]
ZHU Xuhui [6175 2485 6540]

ORG: None

TITLE: "A $^{14}CO_2$-$^{12}CO_2$ Isotope Laser"

SOURCE: Shanghai ZHONGGUO JIGUANG [CHINESE JOURNAL OF LASERS] in Chinese Vol 12, No 9, 20 Sep 85 pp 524-527

TEXT OF ENGLISH ABSTRACT: A $^{14}CO_2$-$^{12}CO_2$ isotope laser has been developed and 80 laser lines were measured. Forty lines originated from lasing transition of $00^{\circ}1$-$(10^{\circ}0, 02^{\circ}0)_1$ band of $^{14}CO_2$ and the strongest line output power was over 4.0 W. The competition effect between isotopes were experimentally observed and domination of lasing radiation of $^{14}CO_2$ were found even if the content of $^{14}CO_2$ was less than $^{12}CO_2$.

AUTHOR: LI Guohua [2621 0948 5478]
ZHANG Huaihuai [1728 2037 2037]
GUO Yanqiu [6753 7159 4428]

ORG: Institute of Lasers, Academy of Sciences of Hebei Province

TITLE: "A Long Life-time Sealed-off TEA CO_2 Laser With Higher Average Power"

SOURCE: Shanghai ZHONGGUO JIGUANG [CHINESE JOURNAL OF LASERS] in Chinese Vol 12, No 9, 20 Sep 85 pp 528-531

TEXT OF ENGLISH ABSTRACT: A sealed-off TEA CO_2 laser with higher average output power and longer operation is reported. The performances are: the continuous operating time--up to 7 hours at 40 pps; the higher average output power--above 70 W; the life-time--longer than 10^6 shots (FWHM).

AUTHOR: LOU Qihong [2869 4388 3163]

ORG: Shanghai Institute of Optics and Fine Mechanics, CAS

TITLE: "Gain Measurement of Pulsed Avalanche Discharge XeCl Laser By Means of Amplified Spontaneous Emission"

SOURCE: Shanghai ZHONGGUO JIGUANG [CHINESE JOURNAL OF LASERS] in Chinese Vol 12, No 9, 20 Sep 85 pp 532-534

TEXT OF ENGLISH ABSTRACT: The small signal gain of pulsed avalanche discharge XeCl laser was measured by means of amplified spontaneous emission (ASE). In comparison with the gain obtained by oscillator-amplifier method, the obtained effective saturation pump power density of X-ray preionized XeCl laser was I_{ps}=0.8 MW/cm^3.

AUTHOR: SUN Linghong [1327 0109 5725]
CAI Zhonghou [5591 0022 0624]
et al.

ORG: Laser Chemistry Laboratory, Fudan University"

TITLE: "Single-pulse CO_2 Laser Initiated Deflagration of C_2H_4-O_2 mixtures"

SOURCE: Shanghai ZHONGGUO JIGUANG [CHINESE JOURNAL OF LASERS] in Chinese Vol 12, No 9, 20 Sep 85 pp 555-559

TEXT OF ENGLISH ABSTRACT: The deflagration of C_2H_4-O_2 mixtures initiated by a single pulse from TEA CO_2 laser has been studied. It was found that the laser power threshold for initiating deflagration was a function of the laser frequency, the composition and total pressure of the gas mixture. The minimum laser power threshold was observed at the laser frequency of 947 cm^{-1}. In the presence of Pt-Rh or Ag surface, the power threshold was obviously decreased. The main product analyzed were C_2H_2, CO, CO_2 and H_2O. Their relative quantities were dependent on total pressure and the ratio of C_2H_4 to O_2 in the gas mixtures.

12949
CSO: 4009/8

AUTHOR: WANG Yuzheng [3769 5940 2398]
WU Guodong [0702 0948 2767]
JIANG Liren [3068 4539 0086]
et al.

ORG: Shanghai Institute of Nuclear Research, Academia Sinica

TITLE: "A Two-dimensional Multiwire Proportional Chamber Imaging Device With Delay Line Readout"

SOURCE: Shanghai HE JISHU [NUCLEAR TECHNIQUES] in Chinese No 5, Aug 85 pp 5-8

TEXT OF ENGLISH ABSTRACT: A two-dimensional multiwire proportional chamber (MWPC) imaging device with delay line readout is described. It consists of a multiwire proportional chamber, a delay line, a main amplifier, a timing single channel amplitude analyser and a time to amplitude converter. The MWPC is based on the gas flow of Ar-CO_2. Its sensitive area is 20x20cm^2. Spatial resolution is 2.06mm. A phase-compensated distributive parameter electromagnetic delay line is used. Its delay rate is 6.3ns/mm, the rise-time is 100ns. The time shift of the timer is 1 ns (for dynamic range 13:1). The radioactive distribution of the ^{14}C labelled compounds on the paper chromatogram and photograph of the special ring model imaging are given.

AUTHOR: AN Jigang [1344 4949 0474]
HE Tianqing [0149 1131 7230]
WANG Shouzhong [3769 1343 1813]

ORG: Nuclear Energy Technology Institute, Qinghua University

TITLE: "Investigation of Vacuum Fission Chamber"

SOURCE: Shanghai HE JISHU [NUCLEAR TECHNIQUES] in Chinese No 5, Aug 85 pp 9-13

TEXT OF ENGLISH ABSTRACT: This paper summarizes the investigation and construction of a vacuum fission chamber and gives the measurement results of the primary characteristics of the detector. The experimental data are analyzed and discussed. It is shown from the experimental results that vacuum fission chamber is another type of applicable reactor detectors and is much better than the usual boron ion chamber or self-powered detector on some characteristics and should be paid great attention to.

AUTHOR: DU Kangsen [2629 1660 2773]
YAO Zewu [1202 0463 2745]
JI Huaxiang [1323 5478 4382]

ORG: Shanghai Institute of Nuclear Research, CAS

TITLE: "The On-line Relative Measurement of Neutron Flux Distribution in the Light Water Zero-power Reactor"

SOURCE: Shanghai HE JISHU [NUCLEAR TECHNIQUES] in Chinese No 5, Aug 85 pp 32-33, 35

TEXT OF ENGLISH ABSTRACT: Classical activation method is often used in the reactor physical experiment for relative measurements of neutron flux distribution in a reactor, this method takes much time and cannot produce results quickly. By using a kind of micro-neutron detector with conventional electronic equipment and mechanical device, we measured the axis relative distribution of neutron flux on-line in the light water zero-power reactor. The deviation of the results obtained by using microdetector on-line from off-line is less than 3 percent.

12949
CSO: 4009/12

Optics

AUTHORS: LIU Jiyuan [0491 4764 6678]
TENG Xuyan [3326 0650 0350]
XIAO Jinkai [5618 6855 0418]

ORG: LIU of the Institute of Remote Sensing Applications, CAS; TENG of Changchun Microwave Remote Sensing Laboratory, CAS; and XIAO of Geophysics Institute (Guiyang), CAS

TITLE: "Imaging Radar Graphs of the Space Shuttle in Land Use Investigation"

SOURCE: Beijing KEXUE TONGBAO [SCIENCE BULLETIN] in Chinese Vol 30 No 10, [May] 85 pp 775-778

ABSTRACT: A feasibility study of land utilization in the Tangguantun area of Jinghai County was conducted as part of the Tianjin Municipality land resource investigation project by using SIR-A graphs obtained from the SIR-A imaging radar in the space shuttle Columbia during its November flight in 1981. The I S101 graphic (computer) processing system was employed in equal-density sectional processing; emphasis centered on match-processing with the Landsat MSS graphs. Visual interpretations were made of land uses. Apparently, it is difficult to distinguish fruit orchards, ponds and populated locations from MSS conventionally combined graphs, as shown in one of three photographs. It is also difficult to distinguish fruit orchards, ponds and truck farms from the SIR-A equal-density sectional graph as shown in another photograph. However, in the lone remaining photograph showing the standardized combination graph of SIR-A and MSS, interpretation accuracy was better (to 81.7 percent of land classification accuracy). This is because this kind of graph retains the spectral characteristics of visible light and near infrared reflected waves of ground objects (shown on MSS graphs), and also the back-scattering characteristics of microwaves (for ground objects) with high resolution and different observation angles of the SIR-A graph. Thus, digital graphic processing such as graph matching and standardized combination can enhance SIR-A graphs in land use investigation. Two tables list data for land use interpretation and discrimination accuracy of land uses. The paper was received for publication on 4 October 1984.

10424/9365
CSO: 4009/1005

JPRS-CST-85-039
13 November 1985

AUTHOR: LI Shifang [2621 0013 5364]
YIN Lifeng [3009 4539 1496]
HU Qiquan [5170 0120 6898]
et al.

ORG: Shanghai Institute of Optics and Fine Mechanics, Chinese Academy of Sciences

TITLE: "Optogalvanic Effect of ArII in HCD"

SOURCE: Shanghai GUANGXUE XUEBAO [ACTA OPTICA SINICA] in Chinese Vol 5 No 8, Aug 85 pp 679-684

TEXT OF ENGLISH ABSTRACT: An experimental investigation of the optogalvanic effect of ArII in an HCD lamp by using an Ar^+ laser, with its lasing line at 514.5 nm, 496.5 nm and 476.5 nm separately, is reported. By considering various effects, such as ionization, recombination and other mechanisms of excited ions, we propose a simplified model which can be used to explain experimental results satisfactorily. The possibility of measuring some parameters of discharge plasmas in the low-possibility of measuring the optogalvanic effect is also suggested.

AUTHOR: SONG Yaozu [1345 5069 4371]
XIA Xuejiang [1115 1331 3068]

ORG: SONG of the Institute of Engineering Thermophysics, Chinese Academy of Sciences; XIA of the Department of Physics, Qinghua University

TITLE: "Evaluation of Isotope Shifts in Atomic Spectral Profiles from Profiles of Fabry-Perot Interferograms"

SOURCE: Shanghai GUANGXUE XUEBAO [ACTA OPTICA SINICA] in Chinese Vol 5 No 8, Aug 85 pp 685-690

TEXT OF ENGLISH ABSTRACT: In this paper a convolution form of atomic spectral profiles having isotope shifts transformed by a scanning planar Fabry-Perot interferometer (SFPI) is presented. The method and corresponding code of deconvolution of the spectral line profile obtained by SFPI are proposed and are characterized by using the nine-parameter Gauss iteration of the least squares fitting for the first time. By this method the magnitude of isotope shift, isotope abundance ratio, Lorentz width and Doppler width of the spectral profile can be deduced.

AUTHOR: HOU Meiying [0624 5019 5391]
ZHANG Zuren [1728 4371 0088]
FENG Baohua [7458 1405 5478]
et al.

ORG: Institute of Physics, Chinese Academy of Sciences

TITLE: "Saturated Three-photon Ionization of Na Atoms"

SOURCE: Shanghai GUANGXUE XUEBAO [ACTA OPTICA SINICA] in Chinese Vol 5 No 8, Aug 85 pp 691-696

TEXT OF ENGLISH ABSTRACT: Synchronized by being triggered with the same spark gap, two independently tunable flashlamp-pumped dye lasers with compound cavity structure were used to obtain saturated doubly resonant (3S-3P-4D) three-photon ionization of sodium. Rate equations of such a system under the condition of saturated transitions were analytically solved. Comparison of the calculated ionization curve with experimental results gave good correspondence. The ionization cross section of sodium 4D state has been measured from the curve at laser wavelength 5890Å, $\sigma_{4D}(5890Å) = (1.2 \pm 0.4) \times 10^{-18}$ cm^2. It is in good agreement with the theoretical calculation, which is also given in this article.

AUTHOR: WANG Zhijiang [3769 0037 3068]
YANG Benqi [2799 2609 4389]

ORG: Shanghai Institute of Optics and Fine Mechanics, Chinese Academy of Sciences

TITLE: "Ultrashort Pulses and Intracavity Dispersion"

SOURCE: Shanghai GUANGXUE XUEBAO [ACTA OPTICA SINICA] in Chinese Vol 5 No 8, Aug 85 pp 697-701

TEXT OF ENGLISH ABSTRACT: It is necessary to compensate for the dispersion completely within the demanded wavelength range in a mode-locked laser cavity to obtain ultrashort pulses. Operation with no dispersion can be achieved by appropriating the design of films coated on mirrors to match the medium inside the cavity. In this way, ultra-pulses can be obtained.

AUTHOR: WANG Dening [3769 1795 1337]
PAN Huizhen [3382 1979 3791]

ORG: Shanghai Institute of Metallurgy, Chinese Academy of Sciences

TITLE: "Analysis of Dynamic Characteristics of 'Crescent' GaAs/(GaAl)As Lasers Integrated with Buried Passive Waveguide"

SOURCE: Shanghai GUANGXUE XUEBAO [ACTA OPTICA SINICA] in Chinese Vol 5 No 8, Aug 85 pp 702-708

TEXT OF ENGLISH ABSTRACT: Based on the injection carrier diffusion equation, dynamic characteristics of the 'crescent' GaAs/(GaAs)As lasers integrated with buried passive waveguide have been analyzed by using the Runge-Kutta and Simpson's numerical methods. Effects of structure parameters (such as central thickness d_0 of the active layer, stripe width S, channel width W, and carrier diffusion length L_D) on the threshold current I_{th} or threshold current density J_{th} are analyzed. According to the analysis, in order to reduce the threshold current or threshold density, the channel width W must be reduced to 2-4 μm and the stripe width S must be less than 5 μm. A cavity length L=350 and a thickness d_0=0.17 μm are reasonably recommended. Centers of non-radiative recombination should be reduced, the more the better. In this way, optimum results can be reached. We also discuss ways to improve device quality and device structure.

AUTHOR: ZHANG Xiaojie [1728 1420 3381]
DONG Xiaoyi [5516 1321 5030]
SHEN Shouchun [3088 1108 2504]

ORG: Department of Physics, Nankai University

TITLE: "Two-dimensional Intensity Modification of a Gaussian Laser Beam by Acousto-optic Effect"

SOURCE: Shanghai GUANGXUE XUEBAO [ACTA OPTICA SINICA] in Chinese Vol 5 No 8, Aug 85 pp 709-716

TEXT OF ENGLISH ABSTRACT: Theoretical and experimental results of the intensity profile modification of a Gaussian laser beam by 2-D ultrasonic standing waves are reported. The results indicate that the Gaussian intensity profile of a focused laser beam can be modified by a 2-D ultrasonic standing wave when the spot size of the Gaussian laser beam on the input face of the acoustic cell is smaller than the ultrasonic wavelength. The intensity of a focused laser beam can be made nearly flat in the central region if the acoustic pressure is properly controlled. The flatness and the flat region can be changed continuously by varying the acoustic pressure.

AUTHOR: ZHU Qingshi [2612 3237 2514]
LI Mingguang [2621 2494 0392]
ZHANG Yi [1728 0001]
et al.

ORG: ZHU of Dalian Institute of Chemical Physics, Chinese Academy of Sciences; LI, ZHANG, et al., of Qinghai Salt Lake Institute, Chinese Academy of Sciences

TITLE: "Laser Excitation Fluorescence Spectroscopy of A-X(100)-(000) Transitions of CaOH Radicals and Measurement of Their Rotational Temperature"

SOURCE: Shanghai GUANGXUE XUEBAO [ACTA OPTICA SINICA] in Chinese Vol 5 No 8, Aug 85 pp 765-768

TEXT OF ENGLISH ABSTRACT: The laser excitation fluorescence spectra of CaOH A-X(100)-(000) transitions were investigated. The assignments were made, and the molecular constants of $A^2\Pi_{1/2}(100)$ state were derived by least-squares fitting to be $B' = 0.337097(10)$, $D' = 0.377(5) \times 10^{-6}$, and $P = -0.04039(2)$ cm^{-1}. The rotational temperature of CaOH was also derived from the relative intensities of the rotational lines to be $T_R = 308$ K.

9717
CSO: 4009/294

Physical Chemistry

AUTHOR: XIAO Gongwei [5618 0581 0251]

ORG: Jiangxi Provincial Academy of Sciences, Nanchang

TITLE: "Relationship Between Crystal Structure and Crystal-State Electron Density"

SOURCE: Beijing KEXUE TONGBAO [SCIENCE BULLETIN] in Chinese Vol 30 No 10, [May] 85 pp 747-752

ABSTRACT: For many years, a number of researchers attempted to resolve the problem of crystal structure of metals. If all metals in the periodic table are considered as a system, up to now there has not been an effective method of explaining the types of metal crystal structure by generally considering the entire metal system with results consistent with observations. Drawing on another paper by the author in this journal, KEXUE TONGBAO, 23 (1978), 11, pp 653-657, this paper attempts to theoretically explain the causes underlying the formation of different crystal structures by metals (and nonmetals) with application of the electron state concept within the metal (and nonmetal) crystals, while referring to Hume-Rothery and Jones' theory of electron density but using different fundamental concepts. One figure shows the relationship between the calculated electron density, and its critical values in fundamental metal crystal structural types based on element groups in the periodic table. Two tables list compactness data of fundamental crystal types, the critical values of electron density in calculations, and electron density values of metals (and nonmetals other than gases). The paper was received for publication on 13 June 1984.

10424/9365
CSO: 4009/1005

JPRS-CST-85-039
13 November 1985

AUTHOR: WU Huasheng [0702 5478 3932]
WU Zhongchi [0702 0112 1062]
QIAN Youhua [6929 0147 5478]

ORG: Department of Physics, Fudan University

TITLE: "A Study of Determination of Optical Absorption Coefficient of Sample with Rough Surface. I. Theory"

SOURCE: Shanghai HONGWAI YANJIU [CHINESE JOURNAL OF INFRARED RESEARCH] in Chinese Vol 4 No 4, Aug 85 pp 249-254

TEXT OF ENGLISH ABSTRACT: An idea for measuring the optical absorption coefficient for semiconductor wafers with rough surfaces, using a method of combining transmittance and reflectance measurements, is presented. Factors related to diffusive light reflection diffraction, along with a parameter termed characteristic roughness, are introduced to describe the surface roughness of samples. The dependence of reflectivity and transmittance on the characteristic roughness and absorption is given from a statistical point of view. The problem of data analysis in absorption coefficient measurement on rough surface samples is theoretically solved.

AUTHOR: CHU Junhao [5969 0689 3185]
XU Shiqiu [1776 0013 4428]
JI Huamei [1323 5478 5019]
et al.

ORG: Shanghai Institute of Technical Physics, Chinese Academy of Sciences

TITLE: "Determination of Composition of $Hg_{1-x}Cd_xTe$ with the Infrared Absorption Method"

SOURCE: Shanghai HONGWAI YANJIU [CHINESE JOURNAL OF INFRARED RESEARCH] in Chinese Vol 4 No 4, Aug 85 pp 255-260

TEXT OF ENGLISH ABSTRACT: The intrinsic absorption spectra for $Hg_{1-x}Cd_xTe$ thin samples with compositions of $x = 0.17 \sim 0.443$ at 300 K are measured, and the energy positions of the band gaps for all the samples are determined with the method presented by the authors in 1982 and 1983. It is found that $\alpha(E_g, 300\ K) = 500 + 5600x$, where $\alpha(E_g, 300\ K)$ is the absorption coefficient at the energy of the band gap at 300 K. This is the operating curve for determining composition x by the infrared absorption method. For a thick sample of $Hg_{1-x}Cd_xTe$ with unknown composition, the absorption edge can first be measured at 300 K, and then the $E_g(300\ K)$ can be obtained by extending the edge to $\alpha(E_x, 300\ K)$. The composition to be measured will be $x = 3.8158 - \sqrt{13.9547 - 5.263E_g(300\ K)}$.

AUTHOR: LU Jiachang [7120 1367 2490]
LI Zhengzhi [2621 2973 4160]

ORG: Department of Physics, Suzhou University

TITLE: "Deconvolution Processing of Image in Infrared Remote Sensing"

SOURCE: Shanghai HONGWAI YANJIU [CHINESE JOURNAL OF INFRARED RESEARCH] in Chinese Vol 4 No 4, Aug 85 pp 271-276

TEXT OF ENGLISH ABSTRACT: It is shown that in infrared remote sensing the radiation distribution of ground targets can be well retrieved by the FFT deconvolution techniques. The computer-calculated results with various window functions are given and discussed.

AUTHOR: WU Baoye [0702 1405 2814]

ORG: Kunming Institute of Physics

TITLE: "Calculation of Detection Distance of a Passive Night Vision System"

SOURCE: Shanghai HONGWAI YANJIU [CHINESE JOURNAL OF INFRARED RESEARCH] in Chinese Vol 4 No 4, Aug 85 pp 283-288

TEXT OF ENGLISH ABSTRACT: A new method for calculating the detection distance of a passive night vision system is described from the application viewpoint. A calculative formula and a practical example are presented. This method can be used either for designing a new system or for estimating performances of an old one.

AUTHOR: XU Huaifang [1776 2037 2455]

ORG: Department of Physics, Shanghai Teachers University

TITLE: "A New Phenomenon in $LiNbO_3$ Crystal--Conjecturing the Existence of 90° Domain Wall in $LiNbO_3$ Crystal"

SOURCE: Shanghai HONGWAI YANJIU [CHINESE JOURNAL OF INFRARED RESEARCH] in Chinese Vol 4 No 4, Aug 85 pp 319-322

TEXT OF ENGLISH ABSTRACT: When $LiNbO_3$ crystals are observed carefully with a spectrometer, a conjugate image of the reticle in the telescope of the spectrometer is found. The author conjectures that 90° domain walls may exist in the $LiNbO_3$ crystal. At room temperature and without an extra electric field, the angle between the domain walls is found to deviate from 90° about 21'~26'.

9717
CSO: 4009/292

AUTHOR: YANG Jinwei [2799 6651 5588]
ZHANG Jinling [1728 6855 1545]
GUO Gancheng [6753 1626 1004]

ORG: Southwestern Institute of Physics, Leshan, Sichuan

TITLE: "Absolute Measurement of Hard X-ray Radiation Intensity in Non-circular Cross Section Tokamak"

SOURCE: Chongqing HEJUBIAN YU DENGLITIZI WULI [NUCLEAR FUSION AND PLASMA PHYSICS] in Chinese Vol 5, No 3, 15 Sep 85 pp 145-150

TEXT OF ENGLISH ABSTRACT: This paper describes the measurement of bremsstrahlung spectrum and radiation of hard X-ray produced by the bombardment of runaway electrons on limiter and inner shell. The method of deducing the scintillation spectrum to energy spectrum and the measurement of photo-peak efficiency are presented.

AUTHOR: ZHANG Guangqiun [1728 1639 4428]
SHAO Chongming [6730 6850 2494]
YANG Sinian [2799 0943 1819]

ORG: Institute of Plasma Physics of CAS, Hefei

TITLE: "The Design and Experimental Result of a Detection System of Multichannel Light Guide Fiber"

SOURCE: Chongqing HEJUBIAN YU DENGLITIZI WULI [NUCLEAR FUSION AND PLASMA PHYSICS] in Chinese Vol 5, No 3, 15 Sep 85 pp 157-160

TEXT OF ENGLISH ABSTRACT: The principle and preliminary experimental result of a detection system of multichannel light guide fiber are presented. The space resolving power of this system is 1.2mm, the time resolving power is determined according to the sampling rate. The time-space evolution of volume emission coefficients for HeI 5875.6Å in He lamp is measured using this system. The result agrees with theoretical analyses.

AUTHOR: ZHANG Yanzhen [1728 3601 3791]
XU Huihua [1776 1920 5478]

ORG: Shanghai Institute of Optics and Fine Mechanics, CAS

TITLE: "A Small Ion Charge Collector"

SOURCE: Chongqing HEJUBIAN YU DENGLITIZI WULI [NUCLEAR FUSION AND PLASMA PHYSICS] in Chinese Vol 5, No 3, 15 Sep 85 pp 161-164

TEXT OF ENGLISH ABSTRACT: In this paper, the design of a small ion charge collector is presented. This collector has been used in the measurement of ions from laser-produced plasma. It can be used for measuring the ion drift velocity, the ion kinetic energy and the ratio of ion energy to the laser energy.

AUTHOR: GE Yuanjing [5514 5913 7234]

ORG: Institute of Plasma Physics, CAS, Hefei, Anhui

TITLE: "Experiment of Equilibrium System on HT-6A Tokamak"

SOURCE: Chongqing HEJUBIAN YU DENGLITIZI WULI [NUCLEAR FUSION AND PLASMA PHYSICS] in Chinese Vol 5, No 3, 15 Sep 85 pp 165-169

TEXT OF ENGLISH ABSTRACT: The equilibrium system of HT-6A as well as the experiments on this tokamak are described. The contribution of the brass shell to plasma equilibrium is presented. The horizontal and vertical displacement instability under different index factors n of the vertical field are observed. The plasma displacement is found to be closely related to the MHD disturbance. Appropriate values of the vertical field for different plasma current were calculated using shell theory. The results are in good agreement with the experiments.

AUTHOR: HU Wenjing [5170 2429 7231]
ZHANG Wenlan [1728 2429 3482]
CHEN Dingguo [7115 1353 0948]
et al.

ORG: Southwestern Institute of Physics, Leshan, Sichuan

TITLE: "Microcomputer Based Data Acquisition and Processing System on MM3 Experiment"

SOURCE: Chongqing HEJUBIAN YU DENGLITIZI WULI [NUCLEAR FUSION AND PLASMA PHYSICS] in Chinese Vol 5, No 3, 15 Sep 85 pp 170-173

TEXT OF ENGLISH ABSTRACT: This paper describes an Apple-II plus microcomputer based data acquisition and processing system and also its application to the MM3 device. Some electrostatic probes were used to diagnose plasma parameters. The data of electron temperature and density and the plasma electric potential were obtained with this system.

AUTHOR: SHI Bingren [4258 4426 0088]

ORG: Southwestern Institute of Physics, Leshan, Sichuan

TITLE: "Optimization of Tokamak Plasma Pressure Profile Against Ideal MHD Ballooning Modes"

SOURCE: Chongqing HEJUBIAN YU DENGLITIZI WULI [NUCLEAR FUSION AND PLASMA PHYSICS] in Chinese Vol 5, No 3, 15 Sep 85 pp 179-181

TEXT OF ENGLISH ABSTRACT: The ballooning-mode eigen equation for circular tokamak is solved analytically to obtain the dependence of the critical pressure gradients on q-profiles. It is found that considerably high-β stable equilibria can be obtained by current tailoring to produce proper q-profiles in which q value decreases from the center towards the edge of confined plasmas.

AUTHOR: ZHANG Shouyun [1728 1108 0061]
ZHANG Enguan [1728 1869 1351]
DAI Guangsen [2071 0342 2773]
et al.

ORG: None

TITLE: "A Miniature Pulsed Electron Beam Accelerator"

SOURCE: Chongqing HEJUBIAN YU DENGLITIZI WULI [NUCLEAR FUSION AND PLASMA PHYSICS] in Chinese Vol 5, No 3, 15 Sep 85 pp 174-178

TEXT OF ENGLISH ABSTRACT: A miniature pulsed electron beam accelerator for studying the electron beam pumped laser is described. The main output parameters are 500kV, 50kA and 60ns (FWHM). It is a movable accelerator with high reliability. The construction and test results of the accelerator are presented in this paper.

AUTHOR: YANG Shikun [2799 1709 0981]

ORG: Southwestern Institute of Physics, Leshan, Sichuan

TITLE: "Measurement of the Plasma Potential in Mini-Torus"

SOURCE: Chongqing HEJUBIAN YU DENGLITIZI WULI [NUCLEAR FUSION AND PLASMA PHYSICS] in Chinese Vol 5, No 3, 15 Sep 85 pp 186-188

TEXT OF ENGLISH ABSTRACT: The Mini-Torus plasma potential has been measured using Langmuir probes and a "SDP" probe system which is formed of these probes. The measurement shows that the plasma edge in Mini-Torus is potentially positive relative to the vessel wall, and under the present operating condition, the radial electric field strength is about 15 V/cm. The rotation of the plasma column in this device is analyzed. The result is in accord with high-speed photograph measurements.

12949
CSO: 4009/11

- END -

END OF FICHE DATE FILMED

12 DEC 85